Identifying Inflammatory Mechanisms in Calcific Aortic Valve Disease

By

Michael Aston Raddatz

Dissertation

Submitted to the Faculty of the

Graduate School of Vanderbilt University

in partial fulfillment of the requirements

for the degree of

DOCTOR OF PHILOSOPHY

in

Biomedical Engineering

June 30, 2020

Nashville, Tennessee

Approved:

W. David Merryman, Ph.D.

Brian Lindman, M.D.

Meena Madhur, M.D., Ph.D.

Marjan Rafat, Ph.D.

Cynthia Reinhart-King, Ph.D.

Dedication

This work is dedicated to my mother, who taught me to dream big, and my partner,

Demetra Hufnagel, who dreams with me each day.

Acknowledgements

  I would like to first thank my advisor, Dave Merryman, who has believed in my ideas and abilities when there has been no reason to, often turning an initially depressing dataset into an optimistic look towards next steps. There are many lows in science; shared excitement about the highs is what keeps you coming in at 8 am on Saturdays to run the next experiment. Second, I thank my co-sponsors and collaborators who have pursued my ideas with me and encouraged me when necessary with gentle redirection: Meena Madhur and Brian Lindman. I would also like to thank my thesis committee members Cynthia Reinhart-King and Marjan Rafat who have had open doors, ears, and calendars through the entirety of this project.

  I take particular joy in acknowledging the colleagues, co-authors, and labmates who have spent time alongside me with the cells, mice, data, ideas, and or grants: Maggie Axelrod, Matt Bersi, Erin Booton, Meghan Bowler, Cyndi Clark, Steph Dudzinski, Caleb Ford, Tessa Huffstater, Cami Johnson, Ethan Joll, Joe Luchsinger, Matt Madden, Kelsey McNew, Natalie Noll, Brad Reinfeld, Duncan Smart, Caleb Snider, Christi Scott, Cody Stothers, Lance Riley, Mark Vander Roest, and many others. Many are cited throughout the text as collaborators on published work, but whether our collaborations succeeded (never as planned) or failed spectacularly, I learned from each of them. Similarly, I must acknowledge both the leadership and all the incredible trainees of the Vanderbilt Medical Scientist Training Program. None of the cells, mice, or ideas likely would have survived without these communities of scientists and mentors around me. I also owe gratitude to my undergraduate mentor, John Kim: his mantra of "camaraderie" and time spent on an undergraduate's questions about Western blots first instilled in me the principles of "team science," without which none of this work would have been possible. I would also like to thank the National Institutes of Health, and by extension the American people, for supporting my training. While investment in science is often debated and rarely lauded in the public arena, the advocates and legislators who believe in the next

generation of scientists in fact make our development possible. Their work, like ours in pursuing human health, is never over, but it is always appreciated.

I am also so thankful for my family—Robin, Dave, Andy, and Chris. Thank you for always being there, and for your support of my crazy aspirations for my training, for my life, and for the world. And finally, to Demetra, my partner in the truest sense: thank you for keeping me going. You inspire me every single day to do the best work I can and be the best person I can: for my friends, family, and colleagues; for my patients; and for you. I could never have done this work without you.

Table of Contents

List of Tables

List of Figures

Glossary of Terms and Abbreviations

Abbreviation	Term
APC	antigen-presenting cell
AS	aortic stenosis
AV	aortic valve
AVA	aortic valve area
AVAi	indexed aortic valve area
AVEC	aortic valve endothelial cell
AVIC	aortic valve interstitial cell
AVR	aortic valve replacement
BMDC	bone marrow-derived dendritic cell
BMI	bone marrow index
BMM	bone marrow-derived macrophage
CAVD	calcific aortic valve disease
CD	cluster of differentiation
CDH11	cadherin-11
CN	calcific nodule
COX	cyclooxygenase
CTL	cytotoxic T lymphocyte
DAMP	damage-associated molecular pattern
DI	dimensionless index
EF	ejection fraction
EMR	electronic medical record
HG	high gradient
HLA	human leukocyte antigen
ICD	international classification of diseases
IFN	interferon
IL	interleukin

IL-1Ra	IL-1 receptor antagonist
JAK	just another kinase
LDL	low density lipoprotein
LF	low flow
LG	low gradient
LPS	lipopolysaccharide
LVOT	left ventricle outflow tract
MACS	magnetic-assisted cell sorting
MHCII	major histocompatibility complex II
MI	myocardial infarction
N1$^{+/-}$	*Notch1*$^{+/-}$
NF-κB	nuclear factor kappa-light-chain-enhancer of activated B cells
OR	odds ratio
PAMP	pathogen-associated molecular pattern
pLF, LG	paradoxical low flow, low gradient
RANK	receptor activator of nuclear factor kappa-B
RT-qPCR	quantitative real time-polymerase chain reaction
SAVR	surgical aortic valve replacement
SEM	standard error of the mean
SNP	single nucleotide polymorphism
STAT3	signal transducer and activator of transcription 3
SV	stroke volume
SVi	indexed stroke volume
TAVR	transcatheter aortic valve replacement
TGF-β1	transforming growth factor beta 1
Th (cells)	T helper (cells)
TLR	Toll-like receptor
TNFα	tumor necrosis factor alpha
VEGF	vascular endothelial growth factor

V_{max}	peak jet velocity
VTI	velocity-time integral
VUMC	Vanderbilt University Medical Center
WT	wild-type
αSMA	alpha-smooth muscle actin

Clinical Trials

Abbreviation	Full Name
APC	Adenoma Prevention with Celecoxib Trial
APPROVe	Adenomatous Polyp Prevention on Vioxx
PARTNER	Placement of Aortic Transcatheter Valve Trial
PARTNER 2	Placement of Aortic Transcatheter Valves – PII A
PARTNER 3	The Safety and Effectiveness of the SAPIEN 3 Transcatheter Heart Valve in Low Risk Patients with Aortic Stenosis (P3)
PRECISION	Prospective Randomized Evaluation of Celecoxib Integrated Safety vs Ibuprofen or Naproxen
SALTIRE II	Study Investigating the Effect of Drugs Used to Treat Osteoporosis on the Progression of Calcific Aortic Stenosis

Chapter 1: Introduction and Motivation

Aortic stenosis (AS) affects 2-5% of all people over 75 years of age, with treatment commonly required as early as 50, especially for patients born with a congenital aortic valve (AV) malformation.[1–3] Approximately 15,000 deaths each year are attributed to AV disease or associated complications in the United States, and an additional 50,000 to 100,000 undergo life-saving surgery, altogether forming a sizable healthcare burden.[2,4,5] Calcific aortic valve disease (CAVD) is both the primary cause of AS, and the pathophysiology through which patients with valve abnormalities progress to AS. AS involves hemodynamic obstruction of blood flow to the body, and increased pressures in the left ventricle, leaving patients to suffer from exertional dyspnea and fatigue, syncope, and eventually heart failure as a result of AS. These symptoms not only diminish quality of life, but mandate intervention. Currently, the primary clinical course of action is aortic valve replacement (AVR). Without such a replacement, patient survival rates after symptom onset are 50% at two years and 20% at five years, highlighting the inevitability of surgical intervention (Figure 1.1).[6,7] Notably, Figure 1.1 has been reproduced and referenced in the CAVD and AS literature continuously since its publication in 1968, as no medical therapies have affected either the natural history of this disease, or its mortality curve.[7]

AVR has entailed, until the last decade, open heart surgery and manual replacement. This procedure has been reported to result in 30-day mortality rates ranging from 2-18%.[8] The lack of alternatives to surgical replacement led to an interest in potential pharmaceutical therapies.[9] Approved therapies for atherosclerosis and hypertension were studied in patients with AS, due to both their roles as risk factors for CAVD and mechanistic overlap. Unfortunately, lipid-lowering therapy has largely failed,[10,11] while antihypertensive agents have improved cardiac function, but had little effect on valve degeneration or function.[1,12,13] Thus, the field has focused on uncovering new biological understanding, and potentially new treatment strategies.

VALVULAR AORTIC STENOSIS IN ADULTS
AVERAGE COURSE
(Post Mortem Data)
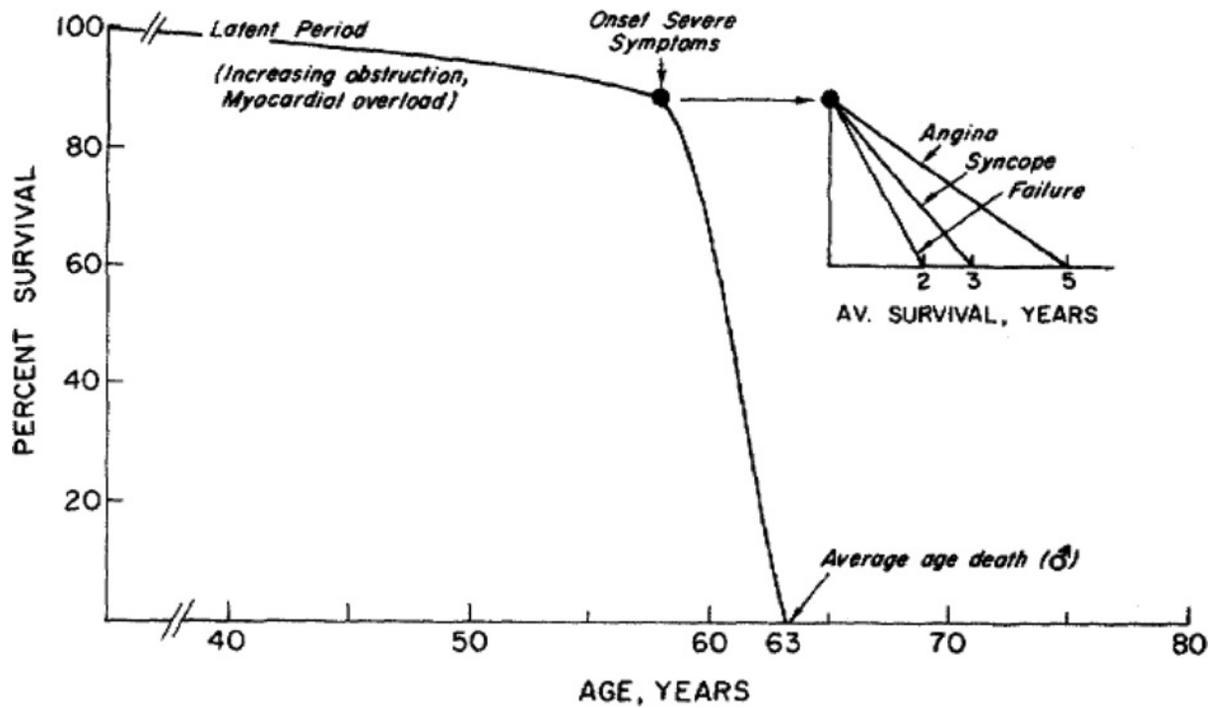
Figure 1.1. The clinical progression of aortic stenosis.
The progression of aortic stenosis involves a latent period with asymptomatic progression followed by a rapid increase in mortality after symptom onset. Reprinted, with permission, from Ross and Braunwald.[7]

In this setting, clinical care and scientific study of AV disease have undergone a revolution within the last 20 years with the invention and widespread adoption of transcatheter aortic valve replacement (TAVR). TAVR is a catheter-based approach that does not necessitate "open-heart" surgery. It involves access to the arterial side of the cardiovascular system through the radial or femoral arteries, followed by subsequent threading of various tools up the arterial system to the AV. A compressed bioprosthetic valve is then placed in the AV orifice and expanded to compress the existing diseased leaflets in the periphery of the aortic root, thus allowing the bioprosthetic valve to assume valvular function. The TAVR procedure was first performed in 2002,[14] and just 18 years later it has proven superior to surgical aortic valve replacement in nearly every situation.

The clinical field of cardiology has tested the benefit of TAVR first in high-risk surgical patients—those who are likely to have many complications from surgery and therefore receive the most benefit from a transcatheter approach—followed by progressively lower risk patients.[15,16] This recently culminated with the finding that TAVR is superior to surgical aortic valve replacement even in patients with a low-risk surgical profile.[17] This change in clinical care has shifted the landscape of scientific research into AV disease. With the ease and relative low morbidity of TAVR, long-term pharmaceutical intervention is made less efficacious for most populations. Clinicians might still opt for pharmaceutical therapy in patients with contraindications to replacement, such as a uniquely difficult approach for TAVR or high surgical risk;[18] however, many new outstanding questions in AV disease center around this intervention strategy. Among other concerns, the lifetime of these devices is not entirely understood, and their risk of recalcification remains unclear.

To that end, the central focus of this body of work is an augmented understanding of AV calcification in the TAVR era. Leveraging the experience, skills, and tools available, this body of work interrogates the role of inflammation and inflammatory pathways in CAVD. Cellular infiltrates have been observed in AV disease for decades, first noted in the calcification of

porcine bioprostheses at autopsy after AVR.[19] The appearance of such cells in bioprostheses highlights one motivation for studying inflammation in CAVD: it is a mechanism conserved across TAVR intervention. Despite this long history, the role of immune cells in CAVD is largely unknown.[20] Similarly, inflammatory pathways like those involving cyclooxygenase-2 (COX-2) and signal transducer and activator of transcription 3 (STAT3) have long been associated with fibrosis and even cardiopulmonary disease but have rarely been studied in depth in CAVD.[21,22] Thus, inflammation presents a unique nexus of study wherein (a) mechanisms are conserved across the valve replacement threshold, (b) areas of study are shared across many cardiovascular diseases, providing alternate avenues for insight and study, and (c) not yet mentioned, there is a growing scientific community interested in immunological signaling in the setting of fibrotic disease.

In addition, TAVR introduces many new clinical questions. For example, how should a clinician decide who should undergo TAVR? The transition to TAVR increases access in numerous ways: from increasing the number of potential providers to allowing for patients with higher risk-profiles to undergo AVR. This makes the question of who would benefit from AVR a more pressing one, as the capacity for delivery has increased. Some data suggests that AS phenotypes differ between sexes—with canonical understanding having a higher sensitivity for disease in male patients—perhaps driven by differences in inflammation and fibrosis.[23–26] With the expanded access brought by TAVR, it is necessary to understand how our canonical disease understanding could lead to health inequities by underserving female patients who disproportionately suffer from underrecognized AS phenotypes.

This doctoral thesis summarizes a body of work conceived to both answer old and propose new questions in AV disease. By focusing on inflammatory and immunological mechanisms, this work exists to challenge our existing notions of cardiovascular disease and ensure that any findings are translatable to patients undergoing AVR, whether surgical or transcatheter-based. It begins with a brief background of CAVD, including an extended focus on

the role of immune cells and inflammatory pathways. The middle four chapters describe studies based on the areas of interest described above. First is described a study on the impact of COX-2 inhibitors on AV disease;[27] next follows a chapter studying the unique role of STAT3 activation response to cyclic mechanical strain; then a comprehensive look at the role of macrophages in a common murine model of valve disease, concluding with translational findings on the role of STAT3 splicing in CAVD;[28] finally, a summarization of echocardiographic data from Vanderbilt University Medical Center outlines sex-dependent patterns of disease recognition in a clinical setting. A summarization of the findings from these studies, along with a discussion of their impact on the field and future directions, can be found in the final chapter.

In this era of TAVR, our molecular understanding of CAVD and where scientific inquiry is needed must be adaptable and forward-thinking. The goal of this work has been to integrate broad-ranging fields of expertise to highlight novel areas of exploration that could spark further scientific investigation in this transformational time. Through the body of work described, the author hopes to have moved the field forward and contributed to continued improving care for patients with AS.

Chapter 2: Background

Portions of this chapter adapted from:

Raddatz MA, Madhur MS, Merryman WD. Adaptive immune cells in calcific aortic valve disease. *Am J Physiol Circ Physiol*. 2019;317(1):H141-H155.[29]

Calcific Aortic Valve Disease and Aortic Stenosis

Calcific aortic valve disease (CAVD) is overwhelmingly the most common cause of aortic stenosis (AS), the third most prevalent cardiovascular disease in developed countries.[1,2] CAVD is a fibro-calcific process in which microscopic pathology like calcification and collagen deposition within the aortic valve (AV) lead to macroscopic stiffening, impeding blood flow out of the heart and causing AS. It is a disease of aging, almost never occurring before 40 years of age, and occurs most commonly in patients with other cardiovascular comorbidities like hypertension and atherosclerosis, but there is limited basic scientific understanding of how these risk factors may lead to CAVD.[3] To that end, the primary molecular causes of CAVD are generally unknown. It is estimated that 25% of the population over 65 years of age exhibits some stage of CAVD, and due to the association of CAVD with increased age, the absolute number of cases will only increase as the population of the United States ages.[1,30]

Ultimately, severe AS simultaneously decreases cardiac output and leads to increased afterload on the left ventricle during systole, causing an increase in ventricular strain and resulting in pathophysiology and symptomology common to heart failure. AS commonly presents in the clinic as dyspnea, dizziness, or decreased exercise tolerance, but can also progress to the point of syncope before patients seek medical advice. Without treatment, patient survival rates after symptom onset are 50% at two years and 20% at five years.[6]

CAVD currently has no pharmaceutical treatment: intervention is limited to surgical or transcatheter aortic valve replacements (SAVR and TAVR respectively).[1,31] The association of AS with aging suggests that many of these patients are not optimal surgical candidates, especially for an invasive procedure like SAVR which mandates thoracotomy. Some studies have estimated that ~10% of patients are "high-risk" surgical candidates,[32] and over 30% of those with severe AS eventually opted not to get the procedure.[33,34] It is likely with the prevalence of septa- and octogenarians in the AS cohort, that (1) comorbidities are common and threaten surgical outcomes in ways that surgical risk scores cannot assess and (2) patient goals may not align with undergoing invasive surgery.[35,36] However, over the last decade TAVR has changed practice, as it has rendered inoperable patients operable by providing access to AV replacement through the peripheral vasculature. The PARTNER and PARTNER 2 trials showed that TAVR is a drastic improvement over no intervention for patients who are not SAVR candidates,[15] and that TAVR may be a mild improvement over SAVR in regards to death and disabling stroke than SAVR in patients with intermediate surgical risk.[16] The PARTNER 3 trial showed further that TAVR is non-inferior to SAVR in patients with low surgical risk.[17]

Nonetheless, TAVR presents some challenges inevitable in procedural medicine. Both TAVR and SAVR patients are at risk of MI or paravalvular leak due to poor prosthetic placement, acute kidney injury, infection, and re-thickening or thrombosis of prosthetic valves.[37,38] Additionally, there are anatomical contraindications to TAVR including severe calcification, aortic root pathology such as that commonly seen in patients with bicuspid aortic valves, and unfavorable coronary ostia anatomy.[33] These patients often have other cardiovascular comorbidities or risk factors that might predict their poor tolerance of TAVR and would present an opportunity for pharmaceutical targeting either against organic CAVD in the native valve or to prevent calcification of the prosthetic valve.

Additionally, AV replacements are currently understood to have a finite lifespan inside the body.[39] Specifically, it is clear that younger patients receiving AV replacement are at high risk for deterioration of their replacement AV. These younger patients are often in the 1-2% of the population who have a congenitally bicuspid AV.[3,40,41] Patients with bicuspid AV are less likely to have other cardiovascular morbidities than the older AVR cohort, yet because of the time-limited nature of AV prosthetics are more likely to need further intervention: for example, valve-in-valve replacement.[40] This process, wherein a prosthetic valve is replaced by placing another prosthetic valve in the orifice in the initial replacement, is not without its pitfalls including poor hemodynamics, coronary artery obstruction, and retrograde paravalvular leak.[39] The specter of prosthetic failure can decrease quality of life both through real medical contraindications and psychological stress. Targeted medical therapy could prolong the lifespan of native AVs, push AVR later in life, and limit calcification of the prosthetic itself and thus valve-in-valve transcatheter procedures or other complications.

In both of the populations outlined above, medical therapy could provide for better quality of life, decreased financial burden, and increased lifespan. As it stands, no pharmaceutical trials have yielded promising results.[13] These trials for CAVD have focused on three areas. First, repeated trials have been performed with novel lipid-lowering therapies since 2005, and none have reported a difference from placebo.[10,11,42–44] Although dyslipidemia is a risk factor for AS, this pathway does not seem promising. Trials with antihypertensive agents have mitigated cardiac remodeling in AS patients, but had little effect on valve function.[12] Finally, a small number of trials have tried to directly oppose AV calcification by targeting phosphate and calcium metabolism. A retrospective study of bisphosphate use, which inhibits bone remodeling in osteoporosis, showed no effect on AS, but some have called for a prospective trial.[45,46] Additional agents targeting bone metabolism are currently being used in the ongoing SALTIRE II trial, which has not reported outcomes.[13] As seen here, our existing understanding

of CAVD has not led to successful pharmaceutical therapies. Further understanding the molecular and cellular pathogenesis of CAVD is a crucial step towards pharmaceutical therapies that would decrease disease and operation-related morbidity.

Calcific Aortic Valve Disease Pathophysiology

CAVD is thought primarily to arise from the native cells of the AV. The AV classically consists of three layers: the ventricularis, the spongiosa, and the fibrosa, going from the ventricular to the aortic side of the AV.[47,48] The ventricularis consists primarily of collagen elastin fibers that provide structure for the valve, which undergoes immense mechanical forces throughout the human lifespan.[47,49] The spongiosa consists primarily of proteoglycans, while the fibrosa is the primary source of cellular activity, including egress of hematopoietic cells, and also the location of calcification in CAVD.[1,50–52] Among valvular cells, there are two resident cell populations: aortic valve interstitial cells (AVICs) and aortic valve endothelial cells (AVECs). AVECs create the endothelium lining the interface of the valve with the circulating blood, and are embryonically derived from the secondary heart field.[53,54] AVICs are fibroblast-like cells derived from AVECs and the cardiac neural crest that make up the bulk of the valve and are thought to serve as the primary source of cellular calcification.[54,55]

Cellular calcification of AVICs is generally thought to occur by two pathways: dystrophic and osteogenic calcification. Dystrophic calcification results from myofibroblast transition, identified by increased expression of alpha-smooth muscle actin (αSMA) and cadherin-11 (CDH11).[56,57] Myofibroblast transition with αSMA expression results in increased contractility and tension on the cellular cytoskeleton, and CDH11 allows for this increased tension to be transmitted across cell-cell junctions.[57] This transition additionally results in increased metabolic activity (e.g. increased protein kinase B activity).[58] These phenomena lead to apoptosis and aggregates of necrotic calcified cells through increased mechanical stress and buildup of

metabolic byproducts.[57–59] While the dystrophic pathway is a result of what could be described as maladaptation by AVICs, osteogenic calcification results from active remodeling of the environment. AVICs differentiate into osteoblast-like cells with increased expression of RUNX2, osteocalcin, osteonectin, osteopontin, alkaline phosphatase, and other markers of the osteoblast phenotype and bone-remodeling process.[58,60,61] Diseased AVICs in the osteogenic pathway have previously been shown to form bone on their own *ex vivo*, and respond further to bone morphogenetic protein 2, a common and prolific RUNX2 activator.[62] In either of these two AVIC calcification pathways the macroscopic AV calcification process includes a mosaic of histological findings including lipid retention, mineralization, and neovascularization.[1] Primarily, CAVD histology is defined by both fibrosis and calcification. Fibrosis in the valve is characterized by excess production of dysregulated collagen fibers while calcification includes excess mineralization and in a minority of cases shows advanced bone metaplasia with osteoblast-like cells and hematopoietic osteogenic progenitor cells.[31,61,63,64] Although these are the dogmatic hallmarks of CAVD pathology, inflammatory infiltrate is near ubiquitous in diseased valves, as is discussed in a later section. Nonetheless, it has rarely been interrogated in hypothesis-driven science, and the mechanisms of immune cell contribution to CAVD are poorly described.

Common Models for the Study of Calcific Aortic Valve Disease

CAVD presents unique challenges for *in vivo* disease study for a variety of reasons. Scientific study of tissue-level biological phenomena can generally be grouped into *ex vivo*, *in vivo*, and *in vitro* studies, each of which have hurdles in the investigation of CAVD. Similar to diseases across human pathology, *ex vivo* studies of the aortic valve fill the literature, and have pushed the field forward for decades. However, for proper *ex vivo* analysis, non-diseased control tissues are needed. In the case of CAVD, these healthy controls should have little to no

cardiovascular disease, but hearts with little to no cardiovascular disease almost universally are used in heart transplant, a medical procedure whose limiting reagent is supply of replacement organs. Instead, adjacent "healthy" tissue (i.e. uninvolved in frank calcification or fibrosis) is commonly used as a control.[65]

This leads to *in vivo* models of CAVD. Various mouse models have been used for the study of CAVD.[66,67] The majority of these fall into one of three categories: models of dyslipidemia (either genetic or diet-induced) which lead to plaque-like formations in the aortic root and on the aortic valve, aortic valve injury induced my injurious mechanical or pharmaceutical stimulus, or genetic mutations meant to alter fibroblast biology.[66,67] This last category bears the most resemblance to the clinical phenomenon of CAVD and includes the *Notch1*^{+/-} mouse.[68] *Notch1*^{+/-} mice exhibit increased valvular calcification, inflammation, and molecular osteogenesis.[69] AVICs isolated from *Notch1*^{+/-} animals have increased expression of αSMA and CDH11, and increased calcific nodule formation *in vitro*, and pharmacological NOTCH1 suppression promotes calcification.[56,70] Importantly, *NOTCH1* haploinsufficiency is associated with bicuspid aortic valves and CAVD in humans, making the clinical relevance of this model a strength.[71,72] This evidence has pushed NOTCH1 into the spotlight for CAVD. However, returning to *in vivo* models, mice often must be aged six to twelve months before seeing signs of disease.[69] This has certainly dissuaded investigators from using nuanced and specific mouse models to investigate pathophysiology. Instead of using *Cre/lox* systems to probe clinically relevant echocardiography outcomes, mouse studies more often use surrogate endpoints or examine correlation of molecular staining with disease status in *ex vivo* analysis.

Finally, *in vitro* models of CAVD present their own unique issues. *In vitro* studies utilize AVICs from human CAVD patients, pigs, or mice.[73] As noted above, cells from diseased human valves or mice with common CAVD mutations (e.g. *Notch1*^{+/-}) are commonly used as a source for *in vitro* studies. Human cells provide a sufficient model, but can be difficult to obtain and

maintain. Porcine cells are easy to acquire and have higher calcification propensity, allowing for expedited testing of potential anti-calcification therapies, but experiments in porcine cells often cannot be replicated in human and murine cells, inspiring doubt about the validity of the model. The use of murine cells mandates immortalization of cell lines. The cellular yield from murine valves is expectedly small compared to larger mammals, and these cells must be expanded over multiple passages, potentially obfuscating cellular phenotypes. Common issues with *in vitro* models aside, the most egregious flaw in study of CAVD is that these models exclude any immune cell signaling and look instead at signaling of AVICs alone. While these studies have guided discovery and pushed therapeutic strategies, the omnipresence of immune cells in calcified specimens demands a consideration of their role in valvular calcification.

Hematopoietic Cells in Calcific Aortic Valve Disease

Hematopoietic Cells in the Healthy Valve

As described above, the two cell-types most commonly investigated in CAVD are AVICs and AVECS, fibroblast-like and endothelial cells of the aortic valve respectively. However, in the last decade, the physiologic presence of leukocytes has also been described, and is slowly being incorporated into calcification models. Surprisingly, up to 10-15% of murine valve cells are CD45^{+}, a marker of the hematopoietic lineage.[74] This fraction grows throughout maturation and is split primarily between CD133^{+} cells (bone marrow-derived progenitor cells) and CD11c^{+}/molecular histocompatibility complex II^{+} (MHCII^{+}) dendritic-like cells.[75] Importantly, MHCII is the primary vehicle of antigen presentation for external antigens. Antigen-presentation leads to T cell recognition of the antigen and is a primary step in the adaptive immune response. Choi, et al. first identified CD11c^{+} cells with dendritic processes in the aortic valve and further showed that their aortic wall counterparts (a) highly express MHCII and moderately express CD11c and CD86 (a co-stimulatory molecule which in conjunction with antigen presentation promotes T cell activation) at a population level and (b) could proficiently present ovalbumin to T

12

cells.[50] These characteristics explicitly confirm the presence of functional antigen-presenting cells (APCs) in the aortic valve. The most common APCs are dendritic cells, macrophages, and B cells. It has been shown that the cells in the valve express the macrophage markers CD206 and F4/80,[74] suggesting, in concert with the above data, that they may be primarily macrophages.

In physiologic states APCs serve as immune surveillance cells. Namely, they phagocytose pathogens and traffic to the lymphatic system in which they present antigens and initiate immune responses. To that end, Hajdu, et al. have shown that the hematopoietic cells in the healthy valve are constantly being replaced, as is common of immune surveillance cells in many tissues.[75] In the healthy AV, APCs would serve to initiate immune responses to valvular endocarditis or the like, but otherwise likely play a more understated role through local juxtacrine or paracrine signaling in the absence of offending pathogens.

Myeloid Cells in CAVD

Although the presence of immune cells in the healthy valve is a relatively new finding, for at least 25 years leukocytic infiltrates have been observed in non-rheumatic aortic valve disease (Table 2.1),[29] first noted in the calcification of porcine bioprostheses at autopsy after AVR.[19] Nonetheless, the role of these cells in CAVD is largely unknown.[20] Notably, in the calcified valve there is an enrichment of the macrophage population,[76–78] and an increase of CD11c^{+} as opposed to CD206^{+} macrophages.[79] CD11c positivity is a marker of inflammatory M1-like macrophages which are generally responsive to interferon gamma (IFNγ) and lipopolysaccharide (LPS) activation, efficiently secrete IL-12, tumor necrosis factor alpha (TNFα), and other acute phase reactants, and direct a pro-inflammatory immune response.[80,81] In contrast, CD206 is a marker of M2 macrophages which generally promote immunoregulation and long-term antibody production.[82] While the M1/M2 macrophage model is a simplified

dichotomization, the general concept of inflammatory and tolerogenic or immunosuppressive macrophages is useful here: an increase in M1 polarization like that found in CAVD by Li, et al. represents a heightened inflammatory state.[79] Similarly, an increase in transcripts of human leukocyte antigen (HLA) subtypes and other proteins involved in antigen presentation in calcified valves reinforces the concept of increased inflammatory activity in the pathophysiology of CAVD.[65] These results are at some level unsurprising: inflammatory cells are often recruited to sites of building pathology. However, in combination with the data on macrophages in the healthy valve, we know their phenotype in healthy and diseased states, and can investigate the trajectory between the two.

Mechanistic investigations have provided mixed results on the role of macrophages in the calcification process. The first studies have used conditioned media from macrophages. AVICs treated with conditioned media from M1 macrophages increase expression of osteogenic calcification markers—bone morphogenetic protein 2, osteopontin, and alkaline phosphatase— at the mRNA and protein levels, and antibody blockade of inflammatory cytokines TNFα and/or IL-6 decreases this calcification effect *in vitro*.[79] This would suggest a pro-calcific role for macrophages, wherein inflammatory macrophages promote AVIC calcification. However, nonspecific depletion of macrophages in hyperlipidemic mice with liposomal clodronate leads to increased valvular thickness due to expanding lipid and collagen deposits.[83] This stresses the importance of macrophage polarization and selective inhibition, as clodronate treatment depletes both M1 and M2 macrophages, which may not affect the balance between tolerogenic and inflammatory responses. Additionally, liposomal clodronate is taken up specifically by phagocytic macrophages, most potently those in circulation. It is unclear exactly which cells are depleted with liposomal clodronate treatment: both in their location (circulation, valve, etc.) and their phenotype (pro-inflammatory, patrolling monocytes, activated monocytes, etc.).

Study of macrophages in CAVD must take advantage of work done in adjacent fields. One burgeoning area of study that bears note here incorporates existing research into dystrophic calcification in CAVD. The known pro-calcification protein CDH11 described previously has also been described on macrophages in the setting of lung fibrosis.[84] In this study, the authors find that CDH11 on macrophages engage with myofibroblasts through homotypic CDH11 bonds, leading to transforming growth factor beta (TGF-β) secretion by the macrophages. This type of finding incorporates existing understanding of fibroblast biology with immunology, highlighting the way forward for the study of macrophages and other hematopoietic cells in cardiopulmonary disease.

Table 2.1. Hematopoietic cells in calcific aortic valve disease.

Cell Type		Immunological Role	Notes
Myeloid Cells			
Dendritic Cells		Initiate innate immune response, antigen-presentation	
Macrophages		Phagocytose pathogens, initiate innate immune response, antigen-presentation	
	M1-like Macrophages	Initiate inflammatory and cytotoxic immune responses	↑ in CAVD[79]
	M2-like Macrophages	Initiate tolerogenic and pro-fibrotic immune responses	↓ in CAVD[79]
Lymphocytes			
T cells			↑ in CAVD[19,76–78]
	Th Cells	Coordinate the immune response by providing "help" to other cells	
	CTLs	Kill infected cells or tumor cells	
	Regulatory T Cells	Resolve immune response, promote tolerogenic environment	In circulation; ↓ after surgical intervention[85]
	Memory-effector T Cells	Initiate immune responses to prior pathogens	In both valve and circulation[86]
	Natural Killer T Cells	Release cytokines in response to various glycolipid antigens	↑ with worsening echo metrics[87]
B cells			
	Plasma Cells	Produce antibody	
Other			
Mast Cells		Rapidly release histamines and inflammatory substances during allergic reactions	↑ in bicuspid aortic valves; increased with worsening echo[88–90]
Osteogenic Progenitor Cells		Bone formation	↑ with worsening echo; in both valve and circulation[63,91,92]

CAVD = calcific aortic valve disease, CTL = cytotoxic T lymphocyte, Th = T helper
Adapted from Raddatz, et al.[29]

Lymphocytes in CAVD

Although APCs and specifically macrophages are present in the healthy valve, T lymphocytes are characteristic of the aged and diseased valve.[19,76] This inflammatory infiltrate accompanies increased neovascularization and osseous metaplasia, hallmark histological signs of CAVD.[77] In addition, at a transcript level, five of the ten most upregulated pathways in calcified versus non-calcified aortic valves directly involve T lymphocyte-specific signaling, while nine involve the immune response.[93] Functionally, T cell prevalence in the valve is correlated with increased pressure gradient, an echocardiographic measure of AS,[87] suggesting close ties between aortic valve calcification or stiffening and T cell infiltration. Further, transcriptomic data from CAVD samples show increased granzyme, perforin, CD8, and interferon gamma (IFNγ), affirming the presence of T lymphocytes and suggesting an increased activity level.[94] IFNγ specifically has been shown to stymie macrophage capacity for calcium reabsorption and osteoclast activity through the receptor activator of nuclear factor kappa B (RANK) system.[94] This would propose an antigen-independent role for T lymphocytes in the aortic valve; however, T lymphocytes both in the valve and in circulation are more likely to be clonal in disease,[86,95] suggesting an antigen-specific immunological response. More specifically, the described T lymphocyte infiltrate involves both CD8$^+$ T cells (cytotoxic T lymphocytes [CTLs]), and CD4$^+$ T helper (Th) cells, with a tendency towards Th cell dominance.[96,97] Generally, CTLs respond at a single-cell level to kill infected cells or tumor cells while Th cells coordinate the immune response by providing "help" to other cells. Each of these cell types consists of many subtypes which have not been investigated in CAVD. In fact, there is limited data on the T cell infiltrate present in CAVD, and almost no incorporation into *in vitro* models of disease.

Inflammation in Calcific Aortic Valve Disease

AVICs in Inflammation

In addition to the identification of hematopoietic cell types in CAVD, there have been numerous studies on the role of inflammatory signaling.[98] One major area of study is AVIC expression of, and activation through, Toll-like receptors (TLRs).[99] TLRs are a mechanism of innate immunity through which cells can recognize general pathogen- or damage- associated molecular patterns (PAMPs, DAMPs) such as intracellular contents (necrosis), double-stranded RNA (dsRNA, viruses), LPS (bacteria), or dysregulated proteoglycans (non-infectious tissue-level pathology).[100] AVICs have uniquely increased expression of TLRs compared to cells from other cardiac valves,[101] and AVICs isolated from stenotic human valves have even further increased expression.[102] This TLR expression may play a role in the unique calcification propensity of the AV, as TLR signaling has been identified as a mechanism for AVIC calcification in response to numerous inflammatory or injury-associated molecules, including dsRNA and LPS.[103–106] One particularly interesting case is that of biglycan, which is dysregulated in pathology. AVIC treatment with biglycan leads to osteogenic signaling through TLRs, highlighting the capability of AVIC inflammation to further extend existing tissue pathology that may be initiated through dystrophic or osteogenic signaling.[107–109] Another well-defined avenue of AVIC calcification through TLRs is by way of LPS. LPS is derived from bacterial membranes, and is thus a marker of infection and a potent activator of inflammation and immune responses. AVICs have repeatedly been shown to respond to LPS through TLRs to trigger both dystrophic and osteogenic phenotypes through the induction of adhesion molecules and osteogenic signals like BMP2 and RUNX2.[101,103] This activity is further potentiated by treatment with interferons.[110] LPS as a mechanism of CAVD induction was replicated *in vivo* using a mouse model of 12-week LPS treatment.[111] These studies using LPS were among the first to more thoroughly investigate molecular pathways of inflammatory calcification, showing that the well-described LPS activation pathway through nuclear factor kappa-light-chain-

enhancer of activated B cells (NF-κB) was active in AVICs and partially responsible for calcification phenotypes.[101,112] NF-κB is a master regulator of inflammation and has long been described in this central role.[113] The activation of NF-κB is triggered by many inflammatory stimuli, and likewise nearly every cytokine or inflammatory marker is related directly or indirectly to NF-κB in its role as a transcription factor. Therefore, these findings regarding NF-κB in CAVD highlighted the capability of AVICs to play a part in the inflammatory cascade, and the role of inflammation as whole in CAVD.

The identification of NF-κB signaling in AVICs and as a part of the calcification process opened up a new area of research in the last decade: integration of NF-κB pathways with common models and molecules described in CAVD. Chief among these are NF-κB-activating molecules. TNF-α is a powerful activator of the NF-κB pathway and has been shown to promote both dystrophic and osteogenic signaling in AVICs.[114,115] IL-1β, a common co-signaling molecule, is associated with CAVD remodeling in the valve, and also induces AVIC calcification through NF-κB.[116,117] *In vivo*, loss of IL-1 receptor antagonist (IL-1Ra) promotes aortic valve disease.[118] Lee, et al. showed that in humans, IL-1Ra was abundant in healthy valves, and absent in stenotic valves.[119] They went on to show that IL-1Ra treatment opposed LPS-induced BMP2 expression.[119] Another commonly described circulating molecule in CAVD is low-density lipoprotein (LDL): a driver of atherosclerosis. Although there is debate about the shared or directional causality of CAVD and atherosclerosis, it is undeniable that oxidized LDL is increased in diseased AVs, exaggerates the pro-calcification effect of LPS, and is associated with faster progression of disease in the clinic.[120–123] Crucially, oxidized LDL activates NF-κB, and this activity is silenced with TLR-neutralizing antibodies.[111] Finally, RANK ligand (RANKL) has been shown to promote AVIC calcification through NF-κB,[124] and RANKL receptor antagonist osteoprotegerin has been shown to be protective against valvular calcification.[125]

In addition to activators of NF-κB, other inflammatory molecules have repeatedly been identified in CAVD models. Many of these molecules have been identified in their role as

secreted factors released from valvular cells. First among these are matrix metalloproteinases (MMPs). MMPs, specifically MMP-2 and MMP-9, have been associated with valvular remodeling in response to IL-1β,[116] and have long known to be promoted by NF-κB activity.[126] Similarly, IL-6 expression is downstream of NF-κB activity,[113] and much work has been done to outline the role of IL-6 in CAVD, which is discussed in a future section. One area of particular interest in this body of work is the association of NF-κB with signal transducer and activator of transcription 3 (STAT3). This is a well-described relationship which includes common functions, co-regulation, and cooperation in producing inflammatory responses.[127] The study of STAT3 in immunology and oncology has elevated its status as a signaling molecule of interest in biomedical research. However, the same justifications for studying STAT3 in cancer and autoimmune diseases (immune cell infiltration and fibrotic responses) can be translated to the study of CAVD.

The STAT3 Pathway

STAT3 has been implicated in fibrosis of the kidney, vasculature, and liver,[128] and in cardiology has been studied in hypertension and cardiac fibrosis.[21,129,130] In cardiac fibrosis, it was found that STAT3 activity specifically in cardiac fibroblasts promotes fibrosis in response to angiotensin II.[131,132] Notably, angiotensin II and its producer, angiotensin converting enzyme, are also associated with calcification and increased LDL in human AVs, and a retrospective study found that angiotensin receptor blockers were associated with slower progression of AS.[133–135] Like CAVD, the aforementioned fibrotic diseases are characterized by TGF-β1 expression and myofibroblast transition. To that end, TGF-β1 directly leads to phosphorylation of STAT3, and STAT3 phosphorylation is required for the fibrotic, proliferative, and autophagy effects of TGF-β1.[136–139] STAT3 activity has also been shown to activate TGF-β1, worsening fibrosis in various organs.[140] It is clear that STAT3 can often interact with TGF-β1 and cooperatively promote tissue fibrosis, while also cooperating with NF-κB to promote the inflammatory activation that is found in CAVD. These dual roles highlight STAT3 as a potential molecule of interest.

STAT3 cooperates with NF-κB by acting as a transcription factor for many inflammatory signals. STAT3 belongs to the JAK/STAT (JAK, just another kinase) family of signaling pathways, and is downstream of cytokine receptors for many common cytokines found in CAVD: IL-6, vascular endothelial growth factor (VEGF), and IL-10 among them.[141] When these cytokines bind their respective receptors on the cell surface, JAK proteins are activated intracellularly and phosphorylate STAT3. Phosphorylated STAT3 regulates expression of many inflammatory pathways and, along with NF-κB, controls initiation of inflammation.[127,142–144] More specifically, STAT3 is underlies a fibrotic and proliferative inflammatory response and promotes the Th17 T helper cell phenotype. Importantly, STAT3 also plays crucial roles in development: STAT3 global knockout is embryonically lethal,[145] and STAT3 activity in cardiomyocytes promotes a reparative program after MI.[146] These complex roles highlight the lack of understanding of STAT3 activity, even as pharmaceutical options are being developed and tested in clinical trials.[147] Altogether, STAT3 signaling is an area of interest for targeting a plethora of fibrotic diseases and may provide a new angle for targeting CAVD pathophysiology.

STAT3 in CAVD

Many inflammatory cytokines are enriched in CAVD, some of which are mentioned above; all such findings are summarized in Table 2.2. STAT3 activation is a common theme amongst these, likely due to its almost ubiquitous role in many types of inflammation. Two molecules of particular interest are TGF-β1 and IL-6. As summarized above, TGF-β1 is a key driver of dystrophic calcification in the aortic valve and cooperatively drives fibrosis with STAT3. Separately, IL-6—the most well-studied initiator of STAT3 activity—plays a key role in CAVD development. SNPs in IL-6 are protective against CAVD, murine models of CAVD are enriched for IL-6, and IL-6 administration increases myofibroblast transition *in vitro*.[68,148–151] In addition to studies of these related signaling molecules, phosphorylation of STAT3 itself is increased in *ex*

vivo CAVD specimens from human patients.[152] However, this is the extent of the limited amount of STAT3 study in CAVD.

      Similar to other CAVD pathogenic molecules, STAT3 signaling is also mechanosensitive. It has previously been shown that STAT3 phosphorylation is increased on stiff substrates, and that this activation works additively with growth factor stimulation.[153,154] Additionally, topographically sensitive glioma cell migration was ablated by blockade of STAT3 phosphorylation.[155] The mechanical environment has proven a key driver of CAVD-associated protein signatures in the case of CDH11, αSMA, and TGF-β1, and may also play a role here.[57,59,156] To that end, CDH11 knockdown decreases STAT3 phosphorylation in response to cellular confluence *in vitro*.[157,158] It is possible that STAT3 serves as a proliferative and fibrotic switch in response to CDH11 activation through mechanical tension. There has been extensive work outlining the role of CDH11 in CAVD, and this again highlights the potential role of STAT3 signaling in CAVD.[27,57,68,151]

Table 2.2. Cytokine enrichment in calcific aortic valve disease.

Cytokine	Immunological Role	STAT3 Activity	Finding
Transcription Activated by STAT3			
CCL11	Recruits eosinophils	Activated by STAT3	↑ in CAVD[65,93]
CXCL5	Recruits angiogenic neutrophils	Activates and is activated by STAT3	↑ in CAVD[65,93]
IL-17RA	Receptor for IL-17; promotes Th17 maturation	IL-17 expression is activated by STAT3	Increased in plasma of patients who progress to AVR[159]
TGFβ	Immunosuppressive; profibrotic; promotes Th17 maturation	Activates and is activated by STAT3	↑ in CAVD[160]
TNFα	Acute phase reactant	Activates and is activated by STAT3	↑ in CAVD; ↑ with increased inflammation in the valve[114,149]
Promotes STAT3 Activity			
CCL21	Recruits CCR7+ T cells	Activates STAT3	↑ in CAVD[65]
CXCL9	Recruits T cells	Activates STAT3	↑ in CAVD[65]
IL-1β	Acute phase reactant	Activates STAT3	↑ in CAVD; ↑ in valves with more severe remodeling[116]
IL-1R antagonist	Opposes IL-1 activity	Opposes IL-1 activity	↓ in AS[119]
IL-6	Acute phase reactant; promotes T cell maturation	Activates STAT3	↑ in CAVD; ↑ in valves with more severe remodeling; IL6R SNP decreases severity of AS[148–150]
IL-10	Immunosuppressive; promotes Treg maturation	Activates STAT3	Present in CAVD; SNPs in IL10 are associated with CAVD[161,162]
IL-18	Promotes T cell maturation	Activates STAT3	↑ in patients with more severe AS[163]
IL-32	Proinflammatory	Activates STAT3	↑ in CAVD[152]
IL-33	Promotes Th2 maturation	Activates STAT3	Present in AS; its receptor, sT2, is increased in plasma in patients with more severe AS, and increased in patients with AS compared to AR[164,165]
M-CSF	Promotes macrophage maturation	Activates STAT3	Present in CAVD[161]
Other			
CCL19	Recruits CCR7+ dendritic cells and T cells	-	↑ in CAVD[65]
IFNα	Acute phase reactant; promotes Th1 maturation	Regulates STAT3 in balance with STAT1	↑ in Singleton-Merten Syndrome (juvenile AV calcification)[110]
IFNγ	Acute phase reactant; promotes Th1 maturation	Regulates STAT3 in balance with STAT1	↑ in CAVD[94]

AR = aortic regurgitation, AS = aortic stenosis, AVR = aortic valve replacement, CAVD = calcific aortic valve disease, CTL = cytotoxic T lymphocyte, SNP = single nucleotide polymorphism, Th = T helper
Adapted from Raddatz, et al.[29]

STAT3 in RUNX2-Associated Calcification

In addition to general observation of STAT3-related phenomena in CAVD, STAT3 has been shown in other models to directly modulate transcription of genes related to calcification. Most important among these, STAT3 has been shown to play a necessary role in mechanosensitive expression of RUNX2 in osteoblasts.[153] RUNX2 is the major driver of osteoblast transition in aortic valve cells and is increased in *Notch1*^{+/-} valve disease, the model used in this study.[69,166,167] In other diseases, monocytes have been shown to induce STAT3 activation in mesenchymal stem cells, leading to osteoblast differentiation identified by alkaline phosphatase and RUNX2 expression.[168] This disease model appears especially relevant to CAVD, and may provide a roadmap for investigation into the role of STAT3 in CAVD. These studies highlight the capability of STAT3 signaling to promote canonical calcification pathways in CAVD.

STAT3 is also capable of negatively modulating RUNX2 expression through the alternative splice product STAT3β (Figure 2.1).[169,170] STAT3β negatively regulates canonical STAT3α activity by dimerizing with STAT3α and inhibiting transcription factor activity.[171] Interestingly, STAT3β also acts to negatively regulate RUNX2 activity in this way.[169] Neither STAT3 nor STAT3β specifically have been studied in CAVD, and their impact on AVIC calcification is unknown. However, the known relationship of STAT3 with RUNX2 activity and the ability of STAT3β to directly extinguish RUNX2 expression collectively ask pressing questions on the role of STAT3 activation in CAVD.
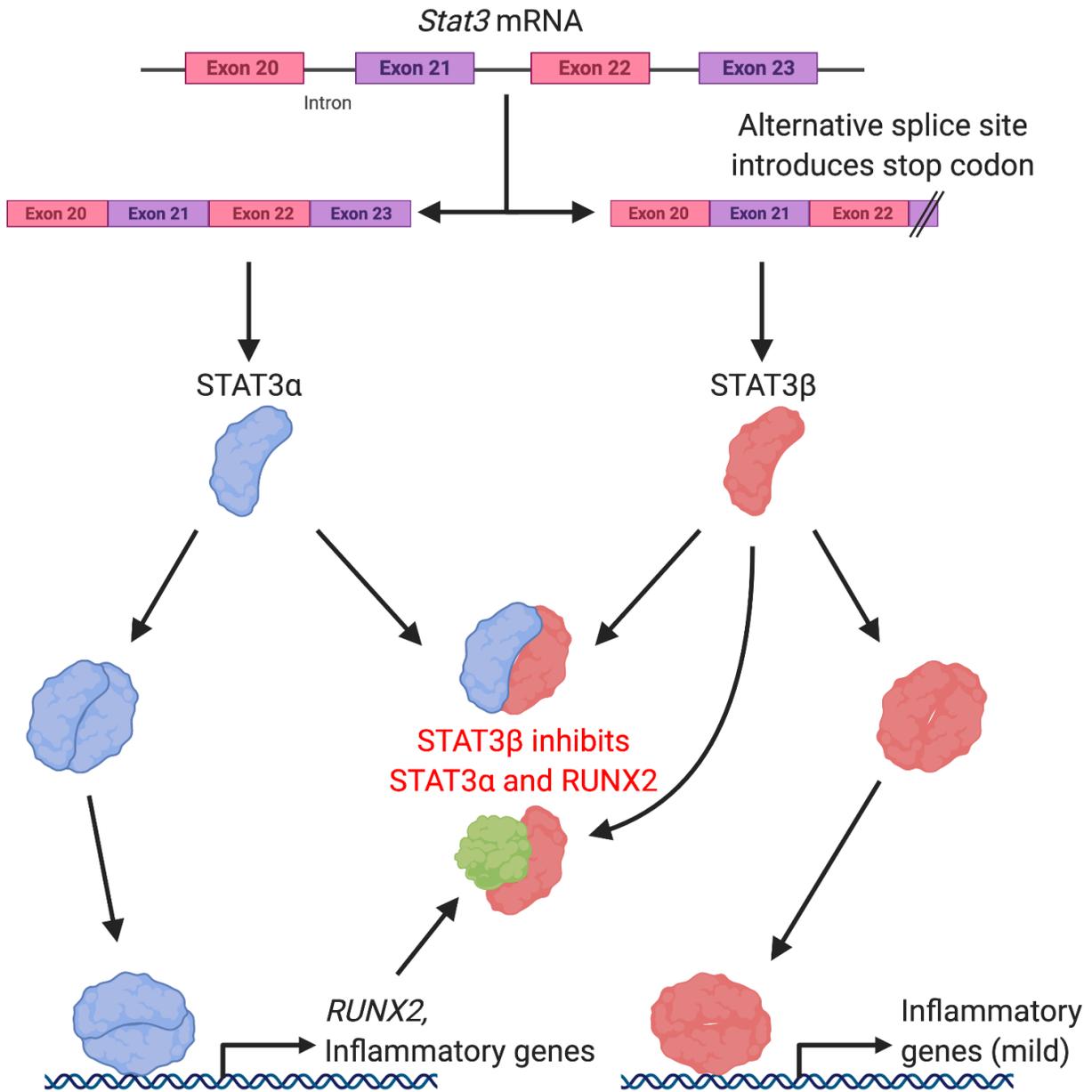
Figure 2.1. The opposing roles of STAT3 splice products.
An alternative splice site in exon 23 of *Stat3* mRNA leads to a truncated version of STAT3, STAT3β, that serves as both a transcription factor and a negative regulatory variant opposing STAT3α activity both directly and against its transcription targets.

Cyclooxygenase-2 in CAVD

Another pathway of interest discussed in this body of work is that of cyclooxygenase-2 (COX-2). COX-2 expression is promoted by both NF-κB and STAT3, placing it squarely in the inflammatory dynamic of CAVD outlined previously (Figure 2.2).[172] COX-2 functions to convert arachidonic acid to prostaglandins, physiologic signaling molecules of inflammation and pain, and is best understood in a clinical context.[173] COX-2 inhibitors were created and utilized as alternatives to pan-COX inhibitors that are commonly used in the clinic: naproxen, ibuprofen, and other NSAIDs. While pan-COX inhibitors cause gastric ulcers, which can lead to devastating clinical outcomes, COX-2 inhibitors do not carry this same risk, as they do not affect COX1 activity in the gut.[174] COX-1 is primary involved in platelet production throughout the body and cellular viability in the gut—therefore serving a somewhat protective role—but COX-2 is induced in pro-inflammatory states, making it perhaps a better target for inflammatory disease processes.[173,175] Thus, COX-2 inhibition has proven an attractive pharmaceutical goal for many disease processes. In CAVD specifically, not only might COX-2 blockade serve to inhibit inflammatory processes that promote or respond to NF-κB and STAT3 activation, but also to inhibit the role of COX-2 in bone formation, therefore connecting the osteogenic calcification pathway. It has been shown that COX-2 mediates the induction of lamellar bone formation in response to mechanical strain, and promotes the maturation of mesenchymal stem cells into osteoblasts.[176,177] Considering the heterotopic calcification characteristic of CAVD, this facet of COX-2 activity is particularly interesting. Altogether, COX-2 has many avenues through which it might affect pathophysiology.
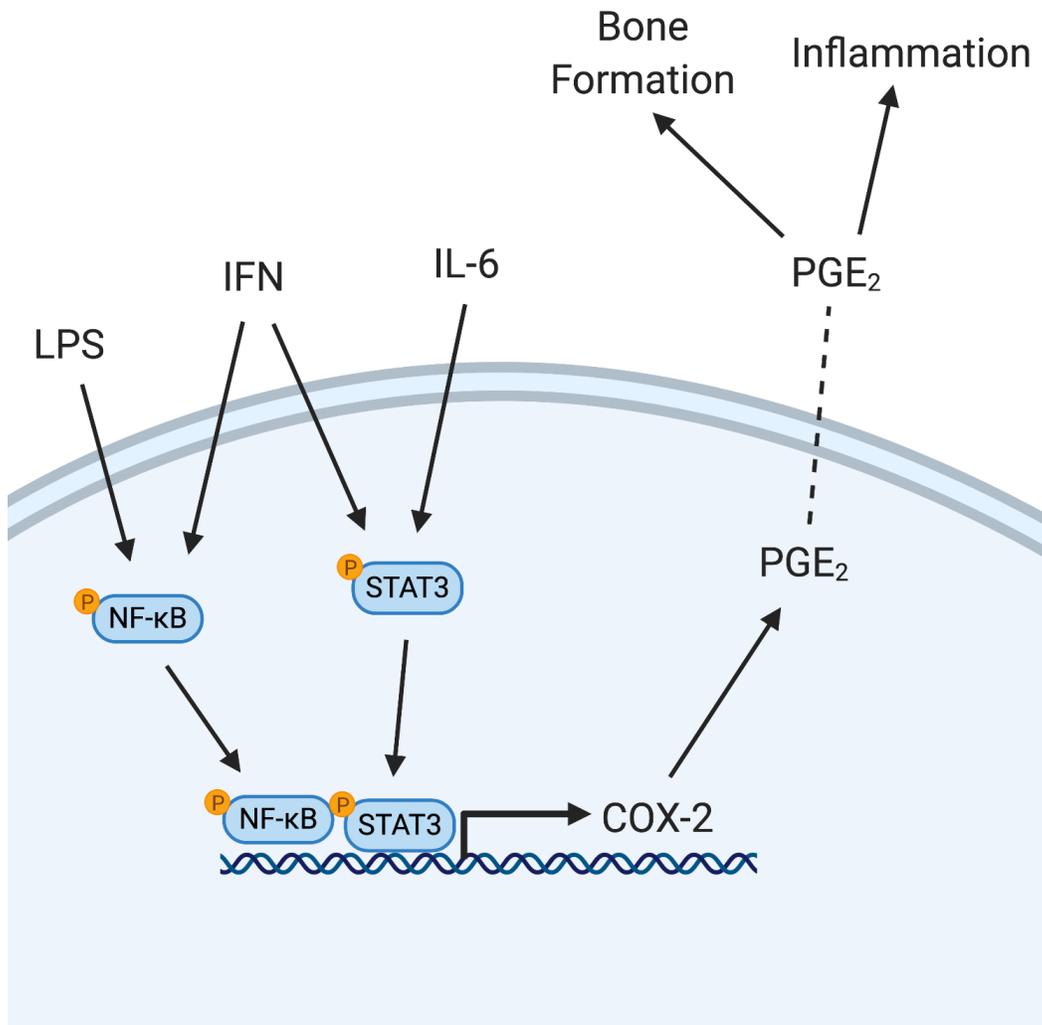
Figure 2.2. COX-2 pathway in calcific aortic valve disease.
STAT3 and NF-κB are both phosphorylated by inflammatory molecules commonly found in CAVD. Once activated, STAT3 and NF-κB both promote COX-2 expression. COX-2 converts arachidonic acid to PGE_2, which is secreted and promotes inflammation and bone formation, both of which are key findings in CAVD.

In cardiovascular disease specifically, COX-2 inhibition has had mixed results. Two sets of initial trials yielded concern. First, the APPROVe trial of the COX-2 inhibitor rofecoxib for prevention of colorectal adenoma resulted in increased incidence of MI and ischemic stroke in the rofecoxib group in 2005.[178] Simultaneously, patients were given COX-2 inhibitors after coronary artery bypass surgery for analgesia, thinking that the lack of platelet inhibition driven by COX-1 blockade might mean less risk of gastric ulceration and bleeding among other side effects. Unfortunately, these trials also showed increased incidence of MI and ischemic stroke, in addition to increased wound infection.[179,180] Follow-up basic science studies suggested that COX-2 played a significant role in protection from cardiac ischemia-reperfusion injury,[181] COX-2 inhibition decreased cardiac output and increased arrhythmogenesis,[182] and mutations in the COX-2 promoter increased incidence of ischemic stroke.[183] Nonetheless, the subsequent PRECISION trial comparing celecoxib to naproxen and ibuprofen showed no increased cardiovascular risk.[184]

Conversely, basic and translational science studies have provided evidence for a beneficial role of COX-2 blockade in cardiovascular disease. For example, it has been shown that celecoxib reduced atherosclerosis in mice.[185] In CAVD, one study found that COX-2 was increased in CAVD, celecoxib treatment decreased calcification *in vitro*, and COX-2 ablation decreased calcification *in vivo*.[186] Finally, it was found computationally that celecoxib may be capable of inhibiting CDH11 activity, providing a mechanism for inhibition of dystrophic calcification in addition to the other pathways targeted by celecoxib.[187] Considering altogether this muddled amalgamation of clinical findings regarding celecoxib; its potential capabilities as an inhibitor of osteogenesis, inflammation, and dystrophic calcification; and promising findings in CAVD, celecoxib and its analogs represent a crucial area of study for potential repurposing of current drugs for the treatment of CAVD.

Sex Differences in Aortic Stenosis

The discussion of inflammation as a significant contributor to CAVD calls into question long-standing dogma regarding prevalence of CAVD and AS in male over female patients. Heightened inflammatory states have repeatedly been identified in female patients.[188] Female patients have higher levels of inflammation throughout life as measured by acute phase reactants C-reactive protein, plasma fibrinogen, and urinary albumin,[189,190] and at least one study has identified increased anti-inflammatory capacity in male rodents.[191] Of note, these effects are complex, and do not imply monolithic comparisons across all immune and inflammatory reactions. For example, in female but not male patients, fat mass correlated with low-grade systemic inflammation, but in repeated murine studies, male mice fed a high-fat diet have an increased inflammatory response compared to female mice.[192–195] Interestingly, it has been suggested that differential expansion of macrophage phenotypes underlies this difference in mice.[196] Regardless of these complex findings in animal models, most human studies have identified increased baseline inflammation in female patients. Given a potential causation between inflammation and development of CAVD, this calls into question the association of CAVD and AS with male sex.

This association may rely on antiquated diagnostic procedures with poor sensitivity. Many papers have reported an increased risk of developing AS in male patients; however, the identification of AS in these papers is reliant primary on aortic valve peak jet velocity (V_{max}), a measure of hemodynamic obstruction.[1,197] Diagnosis of AS today begins with V_{max}, but extends to include at least aortic valve area (AVA) and left ventricle ejection fraction (EF), and can go further to functional testing augmented by dobutamine or nitroprusside, or calcification quantification by computed tomography.[198–202] These additional studies have shown that CAVD in male and female patients tends to differ in the extent of fibrosis and calcification, with calcification dominating in male patients and fibrosis in female patients.[23–25] Importantly, calcification burden, and not fibrosis, was shown to be correlated with V_{max}, the historically

prioritized measure of AS severity,[24] and only patients with "severe" AS are recommended for AVR.[202]

Prior studies have demonstrated that "discordant AS"—in short, an AS phenotype without increase in V_{max}—is common and suggested that patients with discordant AS would see a survival benefit from AVR. Different studies have found that 30-70% of those with an indexed AVA consistent with severe AS do not have a "severe" V_{max}.[26,203] This sizable volume of patients would likely benefit from AVR as Dayan, et al. and Berthelot-Richer, et al. both showed specifically that patients with discordant AS, regardless of cardiac compensation, see a benefit from AVR.[204,205] Nonetheless, this discordance can yield uncertainty regarding the severity of AS, which influences clinical management: multiple studies have found decreased referral for AVR in those with discordant AS.[203,204] Altogether, these differences in AS pathophysiology suggest that female patients have lower V_{max} and mean gradient with similar disease severity, yet clinical guidelines do not differentiate between the sexes, and as discussed above discordant AS is often deprioritized, suggesting a potential disparity in clinical care.[202]

There is limited sex-specific data on these echocardiography metrics in early disease. Because the relationship between AS severity and velocity or gradient may be different in male and female patients, female patients with low hemodynamic metrics may currently be underdiagnosed. Additionally, estimates of the prevalence of discordant AS are wide-ranging. It is possible, especially considering the role of inflammation in CAVD, that there is under-diagnosed AS in female patients that would result in a similar prevalence between sexes. As intervention becomes more accessible for patients with the expansion of transcatheter delivery of AVR, it is important to understand the magnitude of the discordant AS population, and whether care could be improved for these patients.

Chapter 3: The Cyclooxygenase-2 Inhibitor Celecoxib is Associated with Aortic Valve Stenosis

Adapted from:

Bowler MA*, Raddatz MA*, Johnson CL, Lindman BR, Merryman WD. Celecoxib Is Associated With Dystrophic Calcification and Aortic Valve Stenosis. *JACC Basic Transl Sci*. 2019;4(2):135-143.[27] (*co-first authors)

Graphical Abstract
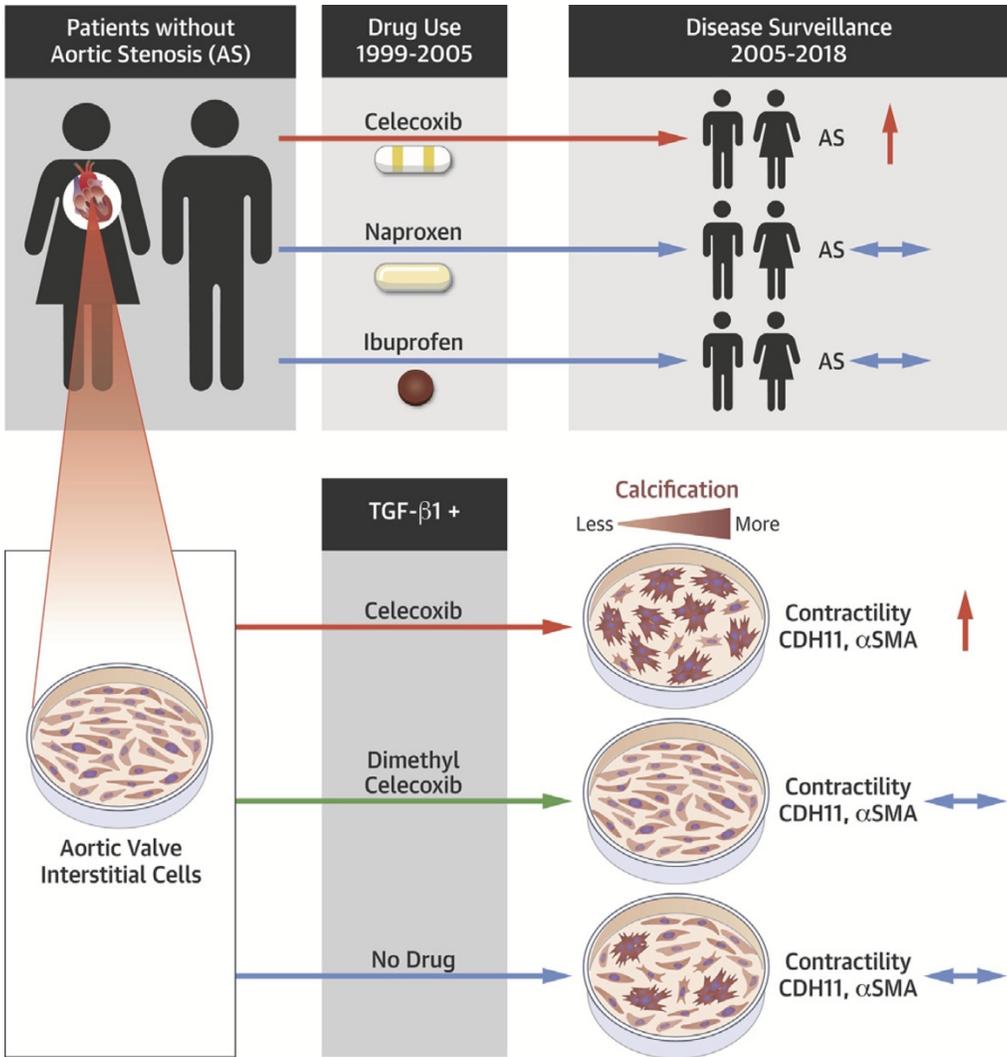
Figure 3.1. Graphical abstract for Chapter 3.
Reprinted, with permission, from Bowler, et al.[27]

Introduction

More than 25% of the US population over 65 years of age is affected by calcific aortic valve disease (CAVD).[31] This degenerative disease is the most common cause of aortic stenosis (AS), which eventually requires surgical replacement of the AV as there are no effective pharmaceutical treatments. This lack of medical therapy is a result of our inadequate understanding of the disease mechanism.[9] CAVD is believed to be mediated by AV interstitial cells (AVICs), which become activated by transforming growth factor beta 1 (TGF-β1) into myofibroblasts,[206] characterized by increased contractility, collagen deposition, and expression of smooth muscle alpha-actin (αSMA) and cadherin-11 (CDH11). When these myofibroblasts are subjected to strain, as is normal in the cardiac valve environment, this causes membrane tearing, leading to apoptosis-mediated cell death. This process has been termed the dystrophic pathway of calcification and was evident in 83% of excised human AVs (while only 13% of those showed osteogenic markers),[64] making dystrophic calcification the most prevalent mechanism of CAVD.

We recently identified and validated CDH11 as a possible therapeutic target for CAVD.[56,57,68,151] CDH11 is a mechanosensitive transmembrane cell adhesion protein known to have increased expression in calcified human AVs,[57] to be increased in the AVICs of the $Notch1^{+/-}$ murine model of CAVD,[56] and to be necessary for $in\ vitro$ formation of the calcific nodules (CNs) characteristic of CAVD.[57] Additionally, recent work has shown that blocking CDH11 with a monoclonal antibody in the $Notch1^{+/-}$ model prevents CAVD progression.[68] These findings motivated us to evaluate current FDA-approved drugs that may block CDH11 activity for CAVD, as the CDH11 antibody research program was recently halted by Roche after disappointing Phase II trials for rheumatoid arthritis. Literature review revealed that celecoxib, brand name Celebrex, and its inactive analog, dimethyl celecoxib, bind CDH11 with high affinity.[187] We therefore hypothesized that either of these drugs may prevent CAVD by blocking the homotypic CDH11 bonds between neighboring cells.

In addition to CDH11 blockade, celecoxib's activity as a COX-2 inhibitor may play a beneficial role in CAVD. COX-2 converts arachidonic acid to prostaglandins like PGE_2, which promote inflammation and bone formation.[173,175–177] It is possible that COX-2 blockade would decrease these downstream effects and mitigate AV calcification.

To evaluate this hypothesis, we treated porcine AVICs and AV endothelial cells (AVECs) with celecoxib or dimethyl celecoxib. Cells were also treated with TGF-β1 to biochemically induce myofibroblast differentiation. Cells were then subjected to well-established functional assays of CAVD such as CN formation and collagen gel contraction as well as evaluated for expression of myofibroblast markers αSMA and CDH11.[56,57,59,60,207] To assess clinical relevance, we performed a retrospective analysis of celecoxib use and AS incidence in the electronic medical record (EMR) from Vanderbilt University Medical Center (VUMC).

Methods

Clinical Data and Statistical Analysis

AS patients aged 60-89 on January 27, 2018 were identified using the Synthetic Derivative, a de-identified version of VUMC's EMR containing >2.5 million unique records. Ibuprofen and naproxen were chosen for comparison due to their similar indications and pattern of use,[208,209] and their previous use as comparators for celecoxib in the PRECISION trial.[184] The study was designed to start the drug surveillance period on 01/01/1999, the date of FDA approval of celecoxib, and end concurrently with start of the AS surveillance period on 01/01/2005, the year the APC trial identified dose-dependent cardiovascular risk,[210] and the FDA issued a black box warning on celecoxib which states that "patients with cardiovascular disease or risk factors…may be at greater risk."[211] Negative references for drug use were defined as presence of patient data prior to 01/01/2005 with complete absence of the given drug in a patient's record. Initial appearance of any of the three drugs in a patient record during the AS surveillance period (i.e. after 01/01/2005) resulted in that record being excluded from

analysis for that drug only. For example, if a record showed initiation of celecoxib use in 2001 and naproxen in 2006, that record would be included in the celecoxib analysis but excluded from the naproxen analysis, regardless of AS status. The AS surveillance period of the study extended from 01/01/2005 to 01/27/2018. All patient sets included only records with at least three logged patient care visits at VUMC during the AS surveillance period to ensure a well-annotated EMR, echocardiogram evaluation during the surveillance period to ensure appropriate assessment of the AV, and a valid body mass index (BMI) within one year of 01/01/2005. AS cases were identified by keywords and international classification of diseases (ICD) codes in the surveillance period with absence of these findings prior to or within the drug surveillance period (Table A.1). Patients with a diagnosis of AS prior to 01/01/2005 were excluded from all analyses. Patients with evidence of rheumatic valve disease in the EMR were excluded from the AS case set. Controls included all patients meeting the patient care and echo criteria, as well as at least two years of follow-up during the AS surveillance period as determined by cleaned BMI data. Myocardial infarction (MI) and ischemic stroke cases were determined using ICD codes (Table A.1).

Hypertension and diabetes case criteria were adapted from the literature and utilized a combination of ICD codes, medications, and vital measurements (Table A.2, A.3).[212–216] Records were queried for these criteria and establishment of diagnosis during the drug surveillance period and prior to the beginning of the AS surveillance period. Full EMR algorithms are included in Appendix A.

Mean available follow-up was 10.16 ± 3.14 years. Unadjusted odds ratios (ORs) and differences between cases and controls were calculated using the Fisher's exact and Mann-Whitney U tests, respectively. Given the significant association of several clinical variables with incident AS in our preliminary models, a multivariable logistic regression based on age, gender, body mass index (BMI), hypertension, diabetes, and drug use was used to calculate adjusted ORs and p-values.[217] All analyses were performed using the statistical programming language

R, version 3.4.4.[218] Use of the Synthetic Derivative is classified as non-human research by Vanderbilt University's Institutional Review Board and approval was given for this study.

In Vitro Experiments and Statistical Analysis

Porcine AV cells were isolated as previously described[57,219] and used between passages 3 and 11. Cells were evaluated with a combination of molecular and functional assays in order to understand the role of treatment with celecoxib, dimethyl celecoxib, and TGF-β1 in their propensity to calcify. The nodule assay allows for rapid screening of potential drug strategies that may prevent dystrophic calcification in vitro.[56,57,207] Briefly, cells were plated onto pronectin (AVICs) or collagen IV (AVECs) Flexcell plates, then treated with TGF-β1, and subsequently strained at 15% using the Flexcell Tension system, as previously described.[59,60] In a separate cohort, AVICs were treated with conditioned media harvested from AVEC cultures after strain. AVICs were also evaluated for contractility using a free-floating collagen gel system in which cells were plated onto gels and imaged over time to quantify the gel area. Western blots and immunofluorescence were employed to evaluate expression of myofibroblast markers CDH11 and αSMA after various treatments. All negative control images are included in Appendix B. In all cases, cells were plated simultaneously with celecoxib (Tocris 3786), dimethyl celecoxib (Sigma-Aldrich D7196), or no drug to allow for interactions with CDH11 before homotypic bonds were formed. 10 μM celecoxib and dimethyl celecoxib was chosen to match the plasma concentration found after typical doses of celecoxib in humans.[187] N was defined as independently plated samples and ≥ 3 for all experiments; more detailed methodology can be found in the supplement. All groups were compared with ANOVA in SigmaPlot version 11.0 and a p-value < 0.05 was considered significant. Normality (Shapiro-Wilk) and equal variance were tested. Normal datasets with equal variance were analyzed via One-Way ANOVA with pair-wise multiple comparisons made using the Holm-Sidak post hoc testing method. Non-normal

35

datasets were analyzed via Kruskal-Wallis One-Way ANOVA on Ranks with pair-wise multiple comparisons made using Dunn's post hoc testing method. Data are presented as mean ± SEM.

Results

In Vitro *Dystrophic Calcification Analysis*

Alizarin Red staining of calcium shows the characteristic rounded morphology of CNs formed by AVICs (Figure 3.1A). As expected, treatment with TGF-β1 increases the number of CNs under all pre-treatment conditions (Figure 3.1A-B). Unexpectedly, celecoxib pre-treatment causes a greater increase in CN number, whereas dimethyl celecoxib pre-treatment, as hypothesized, prevents TGF-β1-induced CN formation (Figure 3.1A-B). A gel contraction assay revealed that celecoxib treated AVICs appear more contractile than their untreated or dimethyl celecoxib treated counterparts, though not significantly (Figure 3.1C). TGF-β1 treatment increased contractility as well and compounded with celecoxib treatment to cause significantly more contraction than the no drug pre-treated with TGF-β1 (Figure 3.1C). Expression of myofibroblast markers αSMA and CDH11 were evaluated by western blot (Figure 3.1D-E) and immunofluorescence (Figure 3.1F). Densitometry demonstrated a significant increase in both markers only in the celecoxib pre-treated AVICs (Figure 3.1D-F). We observed no calcification of AVECs alone, as was expected, and very little calcification in AVICs treated with AVEC conditioned media (Figure 3.2).
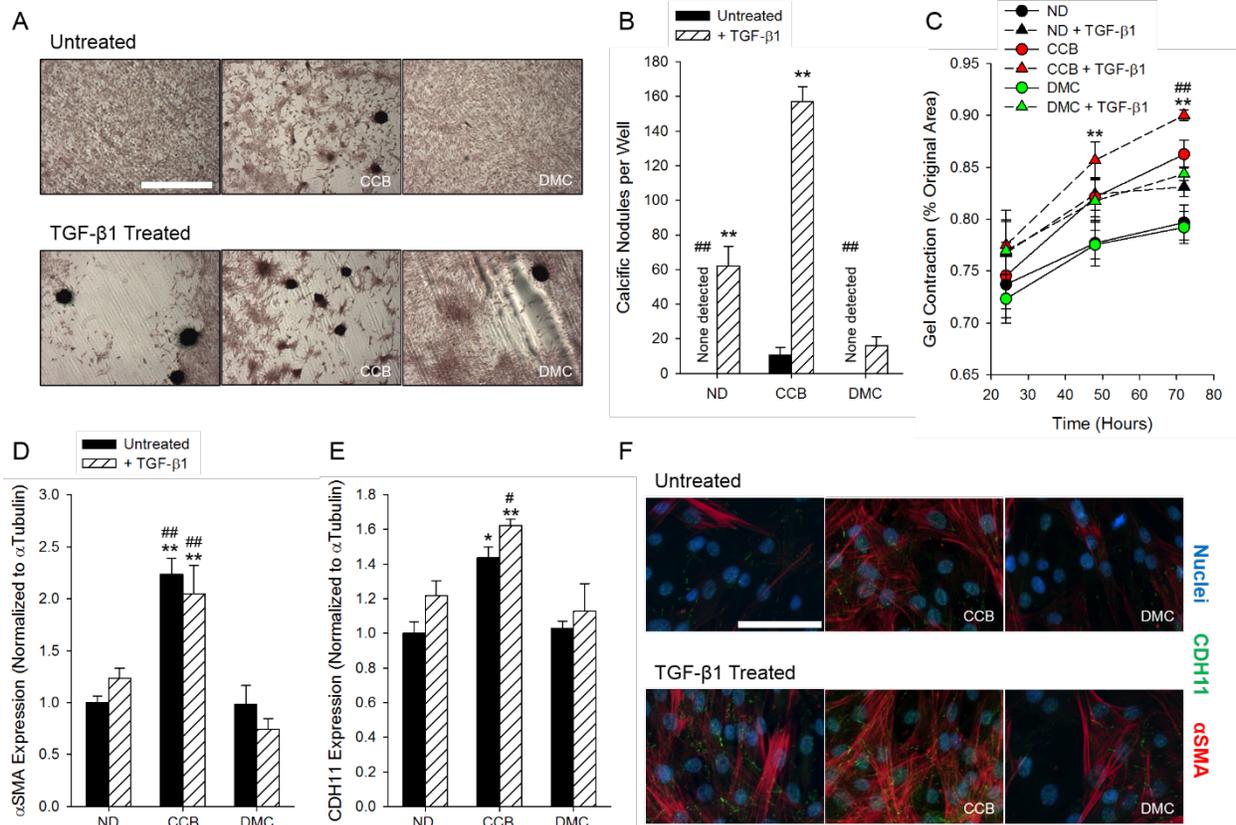
Figure 3.2. Dimethyl celecoxib prevents calcific nodule formation in aortic valve interstitial cells but celecoxib promotes calcific nodule formation through myofibroblast induction.
(A) Cyclic biaxial strain and TGF-β1 induce CN formation, identified by Alizarin Red staining. (B) Treatment with celecoxib increases the number of CNs formed in the untreated and TGF-β1 treated cases. Dimethyl celecoxib treatment reduces the number of TGF-β1 induced CNs. (C) TGF-β1 treatment increases contractility. Celecoxib pre-treatment also increases contractility to the level of ND + TGF-β1. Treatment with celecoxib increases expression of αSMA (D, F) and CDH11 (E-F). ND = no drug, CCB = celecoxib, DMC = dimethyl celecoxib, N ≥ 3, * indicates $p < 0.05$ different from ND, # indicates $p < 0.05$ different from ND + TGF-β1, ** indicates $p < 0.001$ different from same pre-treatment, ## indicates $p < 0.001$ different from ND + TGF-β1, Scale bars are 1 mm (A) and 100 μm (F). Data and figure produced by MA Bowler. Reprinted, with permission, from Bowler, et al.[27]
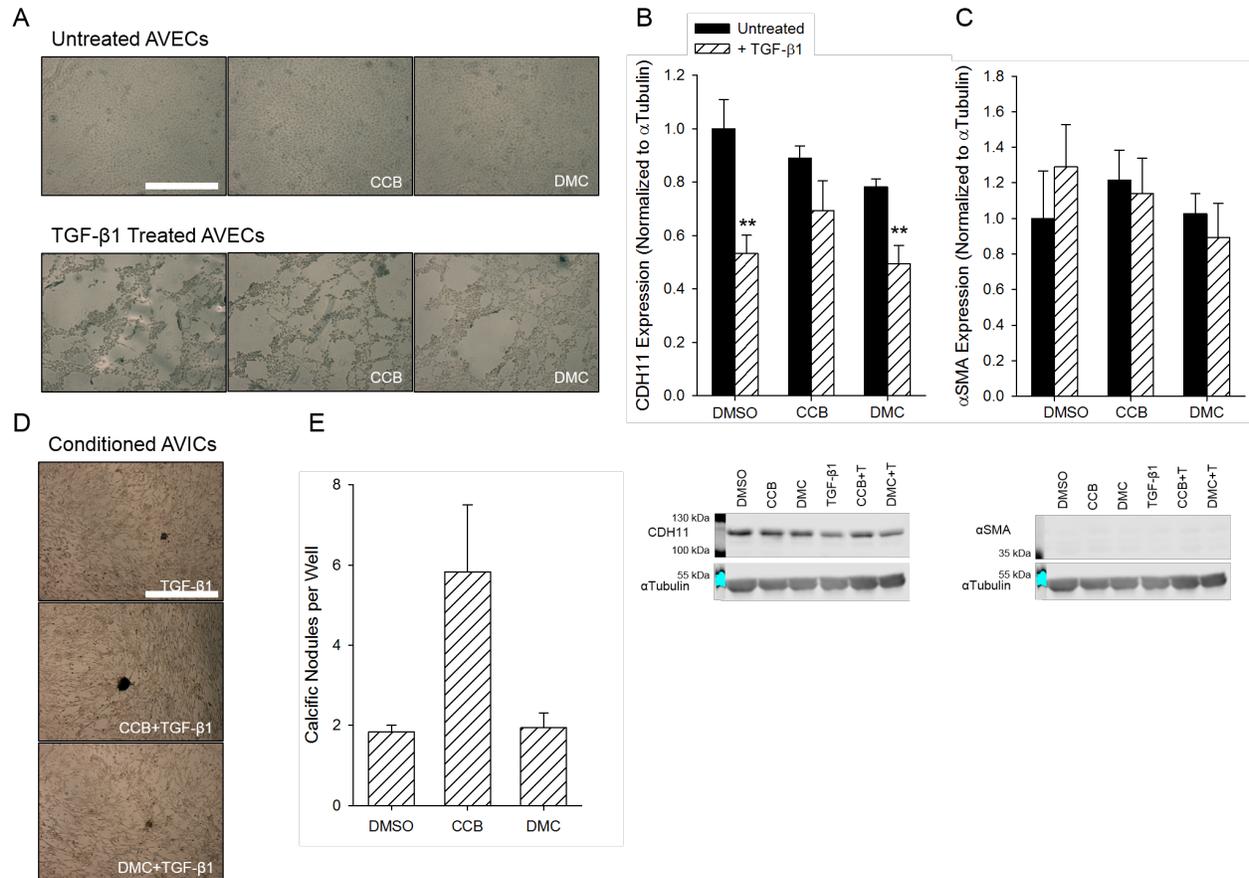
Figure 3.3. Aortic valve endothelial cells treated with celecoxib or dimethyl celecoxib and aortic valve interstitial cells cultured in their conditioned media did not calcify nor have evidence of myofibroblast activation.
(A) Representative images of AVECs stained with Alizarin Red demonstrate no calcification. (B) CDH11 is expressed in AVECs but is not affected by celecoxib or dimethyl celecoxib treatment. (C) αSMA is barely expressed, if at all, in AVECs and is unaffected by drug treatment or TGF-β1. (D) Representative images and (E) quantification of AVICs treated with conditioned media show less calcification than any directly drug treated AVICs. N ≥ 3, ** indicates p < 0.001 different from ND untreated, Scale bars are 1mm (A, D). Some data and figure produced by CL Johnson and MA Bowler. Reprinted, with permission, from Bowler, et al.[27]

Retrospective Clinical Analysis

The results obtained from these *in vitro* experiments led us to investigate possible clinical significance of celecoxib use. Approximately 8,300 de-identified patient records from VUMC met inclusion criteria and were queried for possible association of AS with celecoxib, naproxen, or ibuprofen use (Figure 3.3). In unadjusted analyses, celecoxib use was associated with increased odds of developing AS (OR 1.36, 95% CI 1.11-1.67, p=0.003) (Table 3.1). After adjustment, this association persisted (adjusted OR 1.24, 95% CI 1.00-1.53, p=0.046). Identical analyses were performed with ibuprofen and naproxen and no associations were found. To assess the consistency of this cohort with those in other celecoxib studies, we cursorily examined unadjusted ORs of celecoxib with MI and ischemic stroke and found no association, as has been reported previously (Table 3.2).[184]
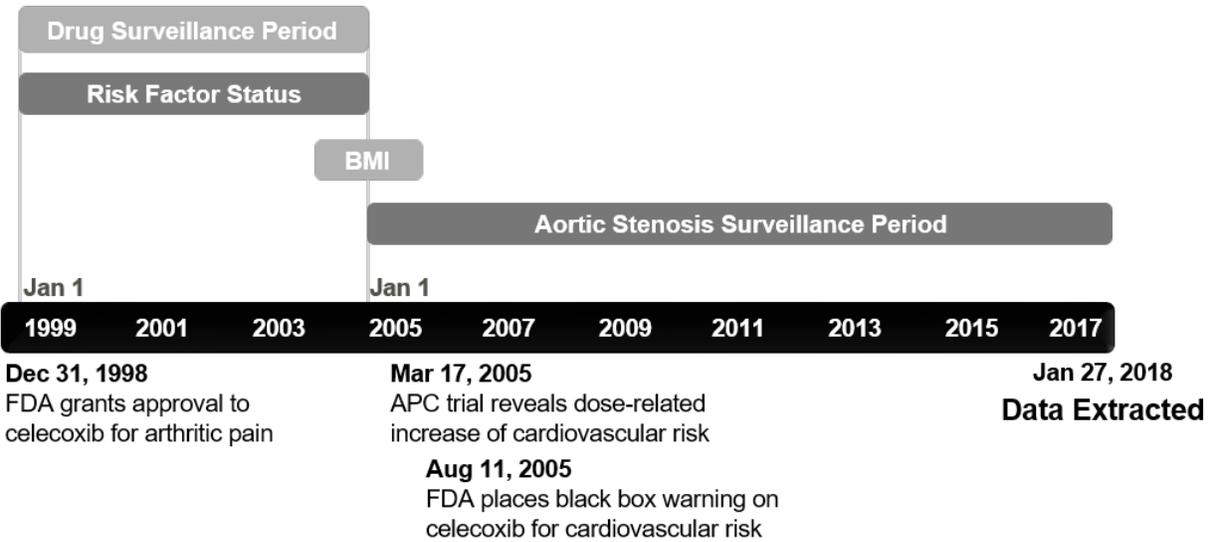
Figure 3.4. Retrospective cohort study design.
The retrospective clinical analysis described here was designed based on the approval and clinical trial history of celecoxib. Celecoxib was approved on December 31, 1998, and clinical trial results revealed a potential cardiovascular risk in early 2005, defining our drug surveillance period. BMI data were collected within one year of January 1, 2005. The aortic stenosis surveillance period extended from January 1, 2005 to January 27, 2018. Reprinted, with permission, from Bowler, et al.[27]

Table 3.1. Celecoxib use is associated with aortic stenosis.

Celecoxib

	Cases (n=574)	Controls (n=6397)	Unadjusted OR [95% CI]	Unadjusted p-value	Adjusted OR [95% CI]	Adjusted p-value
Gender %Male (n)	57.49 (330)	43.71 (2796)	1.73 [1.46, 2.06]	<0.001	1.70 [1.43, 2.03]	<0.001
Age (year) Mean ± SD	76.70 ± 4.80	72.89 ± 7.91	1.06 [1.05, 1.07]	<0.001	1.06 [1.05, 1.07]	<0.001
BMI (kg/m^2) Mean ± SD	30.67 ± 6.94	28.04 ± 6.05	1.02 [1.01, 1.03]	0.002	1.02 [1.01, 1.03]	0.003
Hypertension % (n)	54.88 (315)	40.24 (2574)	1.81 [1.52, 2.14]	<0.001	1.42 [1.19, 1.70]	<0.001
Type 2 Diabetes % (n)	24.74 (142)	15.85 (1014)	1.75 [1.43, 2.13]	<0.001	1.35 [1.09, 1.67]	0.006
Celecoxib use % (n)	23.34 (134)	18.21 (1165)	1.36 [1.11, 1.67]	0.003	1.24 [1.00, 1.53]	0.046

Ibuprofen

	Cases (n=427)	Controls (n=4724)	Unadjusted OR [95% CI]	Unadjusted p-value	Adjusted OR [95% CI]	Adjusted p-value
Gender %Male (n)	57.14 (244)	44.86 (2119)	1.64 [1.34, 2.00]	<0.001	1.59 [1.30, 1.95]	<0.001
Age (year) Mean ± SD	76.86 ± 7.82	73.15 ± 7.87	1.06 [1.05, 1.07]	<0.001	1.06 [1.05, 1.07]	<0.001
BMI (kg/m^2) Mean ± SD	30.83 ± 6.89	29.93 ± 6.94	1.02 [1.00, 1.03]	0.011	1.02 [1.01, 1.04]	0.006
Hypertension % (n)	54.33 (232)	40.60 (1918)	1.74 [1.43, 2.12]	<0.001	1.40 [1.13, 1.72]	0.002
Type 2 Diabetes % (n)	25.76 (110)	16.49 (779)	1.76 [1.40, 2.21]	<0.001	1.38 [1.08, 1.77]	0.010
Ibuprofen use % (n)	26.46 (113)	30.25 (1429)	0.83 [0.66, 1.04]	0.102	0.98 [0.78, 1.23]	0.852

Naproxen

	Cases (n=509)	Controls (n=5342)	Unadjusted OR [95% CI]	Unadjusted p-value	Adjusted OR [95% CI]	Adjusted p-value
Gender %Male (n)	57.37 (292)	45.17 (2413)	1.63 [1.36, 1.96]	<0.001	1.55 [1.29, 1.87]	<0.001
Age (year) Mean ± SD	76.50 ± 7.86	73.07 ± 7.88	1.06 [1.04, 1.07]	<0.001	1.05 [1.04, 1.07]	<0.001
BMI (kg/m^2) Mean ± SD	30.58 ± 6.81	29.83 ± 6.96	1.01 [1.00, 1.03]	0.021	1.02 [1.00, 1.03]	0.025
Hypertension % (n)	55.80 (284)	40.21 (2148)	1.88 [1.56, 2.25]	<0.001	1.55 [1.28, 1.88]	<0.001
Type 2 Diabetes % (n)	24.75 (126)	16.17 (864)	1.71 [1.38, 2.11]	<0.001	1.35 [1.07, 1.88]	0.010
Naproxen use % (n)	16.50 (84)	18.12 (968)	0.89 [0.70, 1.14]	0.364	0.92 [0.71, 1.18]	0.498

Values are % (n) or mean ± SD. ORs for age and BMI are reported per unit increase. AS = aortic stenosis, BMI = body mass index, CI = confidence interval, OR = odds ratio. Reprinted, with permission, from Bowler, et al.[27]

Table 3.2. Celecoxib use is associated with aortic stenosis, specifically, among cardiovascular diseases.

	Celecoxib	Controls	Unadjusted OR [95% CI]	Unadjusted p-value
Myocardial Infarction, % (n)	16.86 (215)	17.10 (962)	0.98 [0.84, 1.16]	0.839
Ischemic Stroke, % (n)	9.89 (134)	10.21 (600)	0.97 [0.79, 1.18]	0.727
Aortic Stenosis, % (n)	9.35 (134)	6.97 (440)	1.36 [1.11, 1.67]	0.003

Patients that matched neither case nor control criteria for a diagnosis were removed from the respective analysis. Reprinted, with permission, from Bowler, et al.[27]

Discussion

Our investigation was motivated by the need for pharmaceutical alternatives to AV replacement and the unique ability of celecoxib and dimethyl celecoxib to bind CDH11, a recently identified target for CAVD and AS. We have previously demonstrated that targeting CDH11 in vivo prevents pathologic increase in aortic jet maximum velocity,[68] a clinical metric used to define the severity of AS. Others have found that celecoxib and its inactive analog, dimethyl celecoxib, were able to bind CDH11,[187] presenting an opportunity to exploit the off-target effects of celecoxib to treat CAVD with an already FDA-approved drug. Additionally, the anti-inflammatory capabilities of COX-2 inhibition could provide additive anti-calcification effects through inhibition of the nuclear factor kappa-light-chain-enhancer of activated B cells (NF-κB) pathway, which has proven to promote disease in CAVD.[116,173] The main finding of this work was unexpected. Primarily, celecoxib, the FDA-approved drug we anticipated being a potential therapeutic for CAVD, causes calcification in vitro and is associated with AS in patients. Conversely, the inactive analog dimethyl celecoxib showed the expected benefit of CDH11 blockade. While further studies of dimethyl celecoxib are warranted, the new risk of celecoxib, a commonly prescribed drug, is the focus of our studies and discussion.

Celecoxib Promotes Myofibroblast Differentiation and Calcification In Vitro

While AVICs are widely believed to be the cells driving CAVD, we evaluated the effects of celecoxib and dimethyl celecoxib on both AVICs and AVECs, as well as effects on AVICs from drug-treated AVEC conditioned media. As AVECs showed no response to celecoxib or dimethyl celecoxib, we focused on direct effects of the drugs on AVICs. We show here that celecoxib causes an increase in both αSMA and CDH11 expression, pointing to an induction of the myofibroblast phenotype, which then leads to CN formation. Conversely, while dimethyl celecoxib treatment does not appear to change the AVIC phenotype – contractility, αSMA expression, and CDH11 expression remain unchanged – it does significantly reduce CN

43

formation. This supports our hypothesis that this beneficial effect is likely the result of dimethyl celecoxib preventing homotypic interactions of CDH11 between neighboring cells. With CDH11's cell-cell adhesions blocked, the tension between AVICs is reduced, which prevents the membrane tearing and subsequent apoptosis-mediated cell death that leads to CN formation. Given that activity in the COX-2 axis is the key difference between celecoxib and dimethyl celecoxib, we attribute celecoxib's pro-myofibroblast effect to COX-2 inhibition, which supports the notion of a protective role for COX-2 in dystrophic CN formation.

Celecoxib is Associated with Aortic Stenosis

This is not the first investigation into the impact of COX-2 inhibitors on heart disease. Most COX-2 inhibitors were pulled from the market because of adverse cardiovascular effects by 2005.[178] Celecoxib had not displayed the same adverse effects and retained FDA approval; however, the FDA mandated a cardiovascular safety trial. This study showed no increased risk of cardiovascular death, nonfatal MI, or nonfatal stroke with celecoxib use when compared to ibuprofen or naproxen.[184] However, these outcomes focus on acute, relatively short-term, and thrombotic events, and do not include valvular pathologies. Based on our in vitro data, rather than an acute thrombotic event, we suspected an increase in long-term risk of AS in these patients. Therefore, we tested our hypothesis using longitudinal clinical data. In retrospective analysis, we observed a unique association of celecoxib use with the presence of AS. The association of celecoxib and AS remained significant when adjusted for age, gender, BMI, and known AS risk factors.[1,217] The same is not observed in patients taking ibuprofen or naproxen, which have comparable major indications and clinical uses as celecoxib (acute pain, inflammatory or rheumatoid disorders, osteoarthritis, and primary dysmenorrhea), but inhibit COX1 in addition to COX-2. This suggests there is something unique about celecoxib or selective COX-2 inhibition that is associated with AS.

The Unknown Role of COX-2 in Aortic Stenosis

COX-2 expression is increased in calcified human AVs,[186] yet there is conflicting data as to whether it is a disease initiator or part of a protective response. COX-2 inhibition has been shown in the *Klotho* deficient mouse to lead to decreased AV calcification via an osteogenic mechanism assessed by cell and tissue level pathology.[210] While calcification is the most common pathology finding in AS, clinical decision making is driven by functional measures (such as aortic jet maximum velocity). However, clinical studies of celecoxib have not yet focused on valvular function or pathology, or long-term effects (> 4 years) of the drug.[178,184,210] We have shown that COX-2 inhibition can promote CN formation in porcine AVICs through the more prevalent dystrophic pathway of calcification, and a significant association between celecoxib use and AS in humans.

Collectively, these findings support further investigation of celecoxib or COX-2's role in other models of CAVD and AS, such as *Notch1*^{+/-} or *Apoe*^{-/-} mice, to clarify whether COX-2 is protective or disease-driving. COX-2 also plays a key role in modulating various immune processes, and investigating the impact of celecoxib in immunocompetent CAVD models may provide new insights into the in vivo mechanisms implicated. Clinically, a multifaceted retrospective study of functional and imaging-defined AS progression with celecoxib use may further clarify this risk. It is still unclear if celecoxib introduces novel risk or is a modifying risk factor in those already at risk. Additionally, while the efficacy of targeting CDH11 in vivo has been shown,[68] further studies of dimethyl celecoxib in relevant murine models and eventually humans could reveal a novel therapeutic for CAVD.

Limitations

Our in vitro experiments rely on porcine cells, which are a standard model for CAVD research and are potentially better examples of healthy valve cells than samples from humans, as most heart valve donors are not free of other cardiovascular pathology. Future work in human AVICs or a variety of in vivo mouse models could confirm our proposed mechanism.

Although we have imposed strict time gates and cohort selection criteria, retrospective EMR study does not allow for controlled assessment or follow-up of study participants. The retrospective nature of the clinical analysis does not allow us to quantify dosage of patients included, but contemporary literature concludes that >80% of users at the time had standard 200 mg prescriptions.[208,209] It is difficult to confidently rule in or rule out AS for patients in this large de-identified cohort of clinical records, but we tried to use definitions that would increase the accuracy of these designations. We cannot rule out that CAVD may have been present in some individuals during the drug exposure period. In addition, the retrospective nature of the study precludes conclusions about causality of CAVD. The various differences between the celecoxib and control cohorts are adjusted for when possible, but may imply additional underlying differences that are better controlled in a randomized controlled trial. For example, in our preliminary models, we assessed the impact of hyperlipidemia on AS incidence, but it was not significantly associated with AS and had no effect on the model. This may be due to incomplete retrospective data or the lack in the era queried of consistent laboratory values such as lipoprotein(a) which has since proven a reliable biomarker for the association of dyslipidemia with AS.[1] Additionally, valve morphology is a highly prevalent risk factor for CAVD, but it could not be accurately assessed in this retrospective study without consistent imaging for all subjects. An echo-driven study may provide more clarity on the impact of celecoxib in patients with a bicuspid AV. Re-analysis of the PRECISION trial data may be an effective option for assessing the potential risk outlined in this analysis.

Conclusions

Overall, these data suggest that celecoxib use is associated with the development of CAVD. Although further studies are necessary, it is likely that dimethyl celecoxib or a monoclonal antibody against CDH11 would be safer therapeutic options than celecoxib to pursue for patients with CAVD or other CDH11-mediated diseases. Considering the indications

for celecoxib, these results suggest that physicians must carefully balance the risks of COX1

inhibition in the gut with those of COX-2-specific inhibition in the AV when choosing a pain

control regimen, and use celecoxib with caution in elderly patients with risk factors for AS.

Chapter 4: Cyclic Mechanical Strain Induces an Inflammatory Phenotype in Antigen-Presenting Cells

Adapted in part from:

Raddatz MA, Clark CR, Merryman WD. Cyclic Mechanical Strain Induces an Inflammatory Phenotype in Antigen-Presenting Cells. Oral Presentation. Biomedical Engineering Society Annual Meeting. Atlanta, GA. October 20, 2018.

Introduction

As discussed previously, hematopoietic cells reside in the healthy AV and are recruited in greater number in disease states.[50,78,94,220] While some studies have considered the role of inflammation as it affects the AV, none have examined the inverse: how the unique mechanical environment in the AV can affect inflammatory signaling. Inflammation may play a targetable role in CAVD pathophysiology, and understanding how mechanical stimuli in the valve affect immune cell phenotypes could lead to novel therapies.[29,98]

Immune cells reside within many mechanically active tissues, yet the mechanobiology of these cells has been poorly characterized.[221,222] It is known that mechanical strain induces antigen-presenting cell (APC) activation and cell death.[223] Macrophages subjected to cyclic mechanical strain have been shown to downregulate phagocytosis and preferentially mature into an M2-like phenotype.[224,225] However, additional studies into immunological functions are often narrow or disease-specific. We became interested in the way that cyclic mechanical strain like that in the valve might promote an inflammatory microenvironment leading to AVIC calcification (Figure 4.1). Here, we investigated the impact of cyclic mechanical strain using a heterogeneous population of bone marrow-derived dendritic cells (BMDCs) to mimic the APCs in the valve. This study measured markers of both APC maturity and inflammatory polarization in response to mechanical strain similar to that experienced in the AV.

48
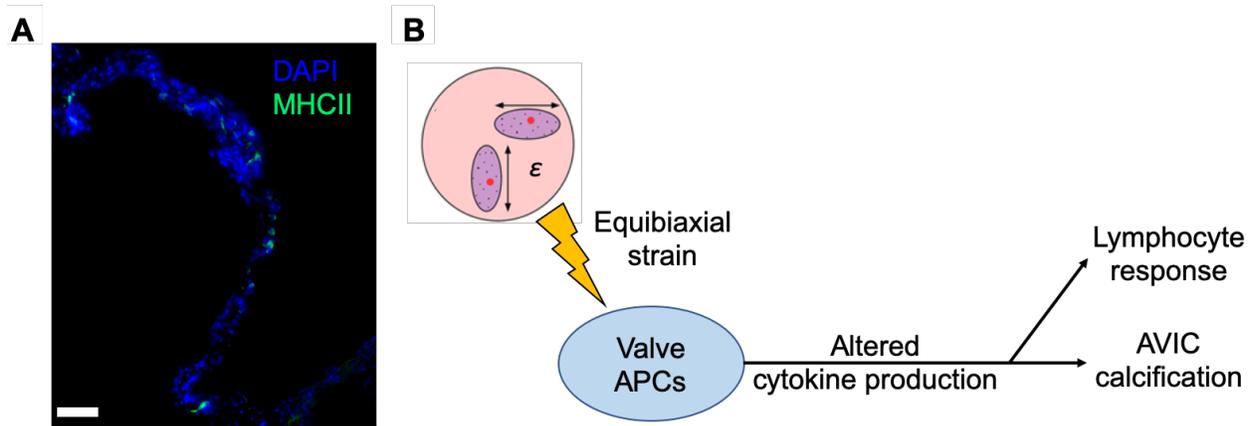
Figure 4.1. Proposed mechanism of strain-induced aortic valve calcification.
APCs in the aortic valve (A) undergo increased strain, leading to altered cytokine production and increased AVIC calcification and lymphocyte responses (B). (A) Murine aortic valve sections are stained for MHCII (green) and nuclei (DAPI, blue). Scale bar = 50 µm. APC = antigen-presenting cell.

Methods

AVICs were isolated and expanded from wild-type C57BL/6J mice as previously described.[151] Briefly, AVs were digested in 2 mg/mL collagenase in HBSS for 30 minutes at room temperature and placed in DMEM supplemented with 10% FBS, 1% penicillin/streptomycin (pen/strep), and 10 μg/mL recombinant murine interferon-γ to induce activation of the simian virus 40 T antigen. Cells were allowed to adhere to 0.1% gelatin-coated six-well tissue culture-treated plates and expanded. To allow for sustained immortal growth, cells were cultured at 33°C and 5% CO_2 when not plated for experiments. At least 12 hours prior to experiments (overnight), AVICs were incubated at 37°C and 5% CO_2 in DMEM supplemented with 10% FBS and 1% pen/strep (complete media), wherein the immortalization element degrades due to temperature changes. AVICs were seeded at 20,000 cells/cm^2 in all experiments unless otherwise noted. BMDCs were generated from wild-type C57BL/6 mice using GM-CSF and IL-4 as previously described.[226] Both cell types were seeded onto six-well BioFlex Pronectin-coated plates and exposed to 24 hours of 10% mechanical strain at 0.7 Hz. Cells were lifted using Accutase and EDTA, and analyzed via flow cytometry (FC) or quantitative real-time polymerase chain reaction (RT-qPCR). For FC, cells were blocked in Fc Block for 10 minutes at room temperature before staining with conjugated antibody for 30 minutes at 4°C.

For RT-qPCR, mRNA was isolated using Trizol (Life Technologies, Carlsbad, CA) and cDNA libraries were produced using the Superscript IV Reverse Transcriptase kit with oligo(dT) primer (ThermoFisher Scientific, Waltham, MA) as per manufacturer protocols. RT-qPCR for all targets was performed on the CFX-96 Real Time System using iQ SYBR Green Supermix (Bio-Rad, Hercules, CA). Products were confirmed by gel electrophoresis. *Gapdh* was used as a housekeeping gene. All statistics were performed on untransformed ΔCt values ("gene of interest" Ct – *Gapdh* Ct), but for clarity, gene expression was normalized and displayed as $2^{\Delta\Delta Ct}$.

For all experimental methodologies, statistical significance between strained and unstrained samples was determined with a two-tailed t test; α = 0.05.

Results

We first assayed BMDCs phenotype by visual inspection. Previous reports have highlighted the importance of actin dynamics and cellular reorganization in APC maturation.[227] After undergoing strain, BMDCs showed increased cellular spreading and projection formation as visualized by both phase-contrast microscopy and immunofluorescent staining of F-actin with phalloidin (Figure 4.2).

By flow cytometry, strained dendritic cell-like cells did not show increased markers of maturity (Figure 4.3A), but were more likely than unstrained controls to be of the inflammatory phenotype, defined here as CD11b^{hi}, Ly6C$^+$ cells (38.8% vs 31.8%; p = 0.04) (Figure 4.3B, C).[228] We continued on and performed RT-qPCR for markers for T helper (Th) 1, Th2, and Th17 inflammatory responses in order to identify any specificity of the inflammation defined by increased proportions of CD11b^{hi}/Ly6C^{hi} cells (Figure 4.4). RT-qPCR showed a significant increase only in expression of Th17 promoting transcripts *Il21* and *Il23* in strained cells. AVICs subjected to strain had a corresponding increase in the IL-23 receptor (*Il23r*).
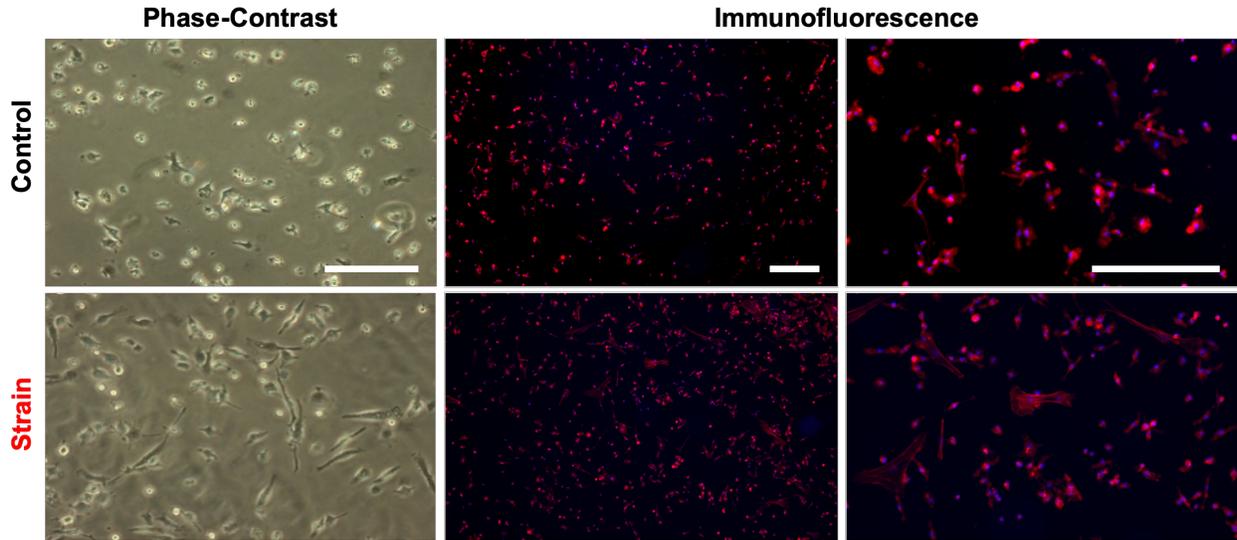
Figure 4.2. Bone marrow-derived dendritic cell imaging after equibiaxial strain.
BMDCs exposed to 10% equibiaxial strain were visualized by phase-contrast microscopy (left) and immunofluorescence (middle, magnified region right). For immunofluorescence, cells were stained with phalloidin (red) and DAPI (blue). Scale bars = 100 μm.
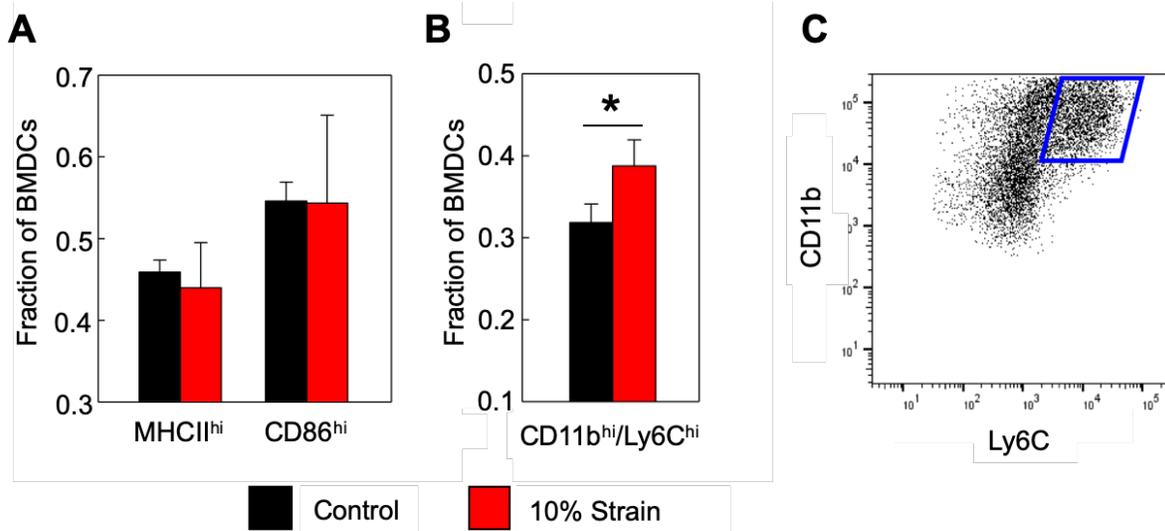
Figure 4.3. Flow cytometry analysis of bone marrow-derived dendritic cells subjected to cyclic mechanical strain.
BMDCs exposed to strain (red) did not have increased antigen presentation (A), but did have increased inflammatory maturation (B, C) compared to unstrained control (black). N = 4; * = $p < 0.05$.
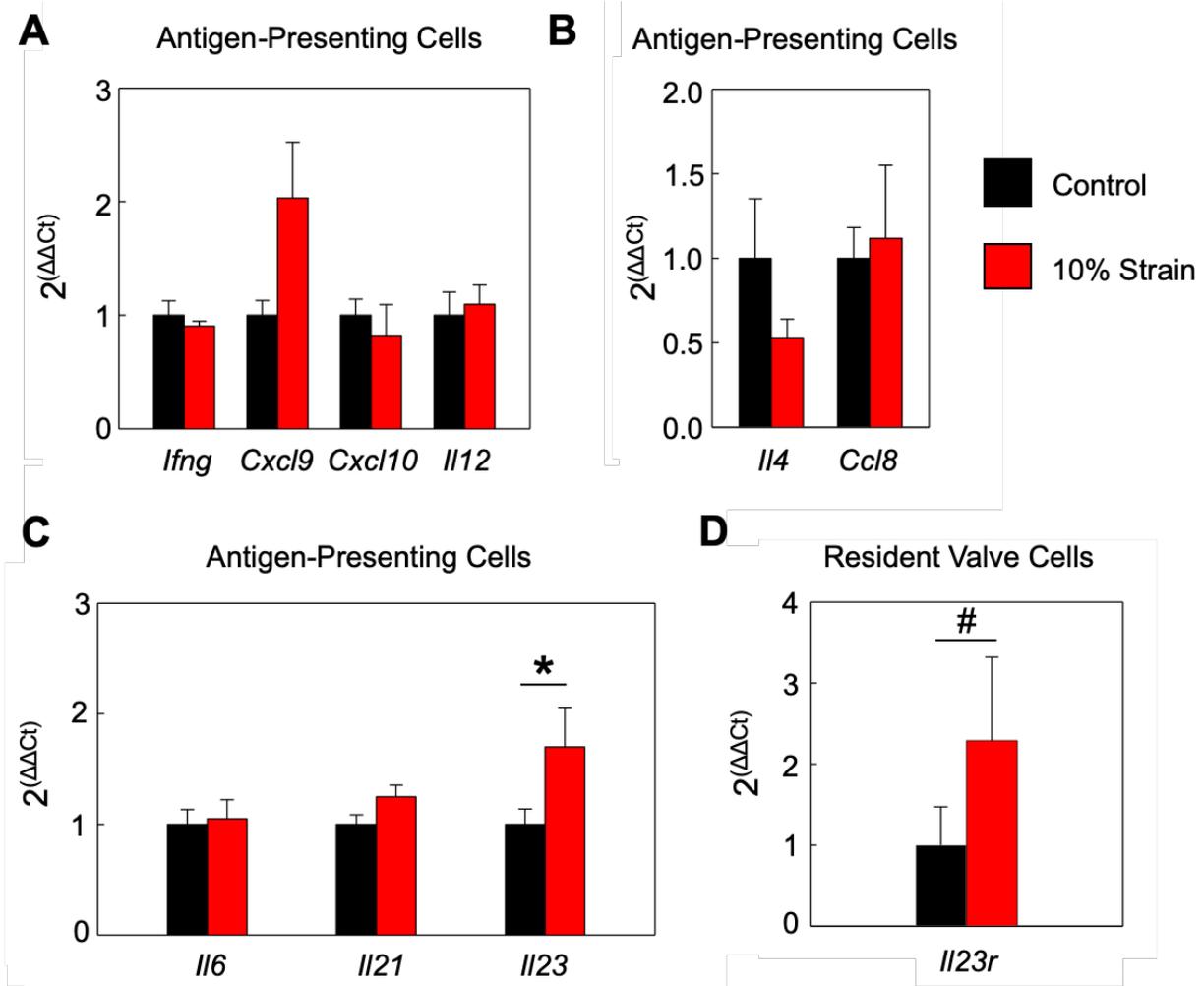
Figure 4.4. Th-specific cytokine expression in bone marrow-derived dendritic cells exposed to mechanical strain.
BMDCs exposed to cyclic mechanical strain were assayed by RT-qPCR for increased transcription of markers associated with Th1 (A), Th2 (B), and Th17 responses (C; N = 6). AVICs were assayed for the ability to respond to increased *Il23* expression (D; N = 4). * = p < 0.05; # = p < 0.10.

Discussion

We used *in vitro* systems to test the effects of cyclic mechanical strain on the inflammatory microenvironment of the AV. Cyclic mechanical strain mimicking that found in the valve does not affect BMDC expression of MHCII, a vehicle of antigen presentation, or CD86, a costimulatory molecule instrumental in driving T cell response. However, this type of strain did induce an inflammatory phenotype in the mature cells, characterized by increased cellular spreading and increased expression of CD11b and Ly6C. We used RT-qPCR to determine if these activated cells might promote a specific type of T cell response through altered cytokine production. They did not increase transcription of various cytokines promoting Th1 or Th2 inflammatory responses, but instead showed increased expression of IL-23, which promotes differentiation of CD4$^+$ T cells into Th17 cells. Separately, we confirmed the ability of AVICs to respond to IL-23 released by APCs by analyzing expression of the IL-23 receptor in strain. We found that AVICs increase transcription of IL-23R when subjected to cyclic mechanical strain. Thus, not only are APCs transcribing more IL-23 in environments of high strain, AVICs are increasing their capability to respond to this cytokine.

This data presents a dual mechanism for APC involvement in AV fibrosis and calcification. APCs are recruited to the AV wherein they are exposed to a unique mechanical environment characterized by cyclic mechanical strain.[75] This environment leads to increased cellular inflammation, characterized specifically by production of Th17-promoting cytokines. Th17 responses have previously been shown to be associated with tissue fibrosis.[229,230] Not only could activated APCs promote differentiation and recruitment of Th17 cells through the lymph system, but they could also enact cellular calcification in the AV through juxtacrine or paracrine signaling to AVICs: AVICs in the AV have the receptor for IL-23, and its expression is increased in such a mechanical environment. AVICs also have been shown to promote calcification in response to numerous other cytokines or inflammatory stimuli that may be increased in the presence of inflammatory APCs.[103,116,117,151,231]

This study highlights the potential role of a Th17 response in diseases of mechanical strain, corroborating data in the study of hypertension: Loperena, et al. found that mechanical stretch of monocytes induces an inflammatory phenotype through signal transducer and activator of transcription 3 (STAT3) activation.[232] Importantly, STAT3 is a major activator of the Th17 phenotype and induces IL-23 expression.[233,234] A crucial component of the proposed mechanism which we do not investigate here is T cell infiltration. T cells have long been identified in CAVD and associated with other disease markers.[19,76,77] No specific phenotyping of these T cells has been performed, but future studies should investigate any specific Th-subtype enriched in the immune responses in the valve. Our data suggest that perhaps these T cells would disproportionately show a Th17 phenotype. Overall, this study provides a potential mechanical etiology for fibrotic immune cell involvement in CAVD.

Chapter 5: Macrophages Promote Aortic Valve Cell Calcification and Alter STAT3 Splicing

Adapted from:

Raddatz MA, Huffstater T, Bersi MR, Reinfeld BI, Madden MZ, Booton SE, Rathmell WK, Rathmell JC, Lindman BR, Madhur MS, Merryman WD. Macrophages Promote Aortic Valve Cell Calcification and Alter STAT3 Splicing. *Arterioscler Thromb Vasc Biol*. April 2020:2020.01.24.919001.[28]

Graphical Abstract
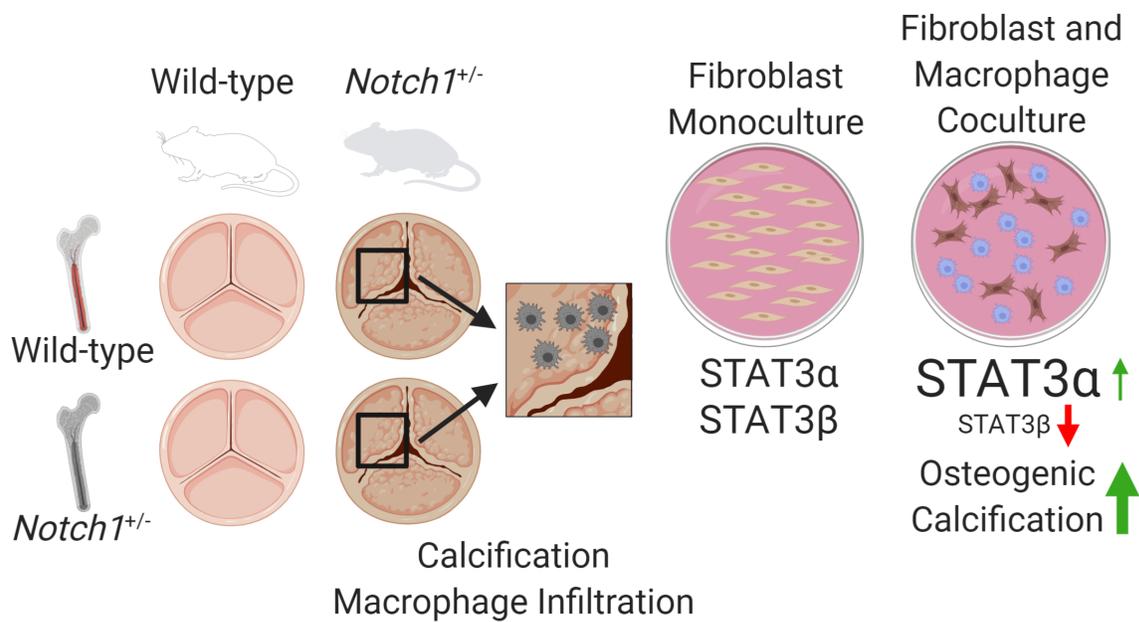
Figure 5.1. Graphical abstract for Chapter 5.
Reprinted, with permission, from Raddatz, et al.[28]

Introduction

Calcific aortic valve disease (CAVD) affects one in four people over 65 years of age and is the primary cause of aortic stenosis.[1] This prevalent and insidious disease inevitably leads to surgical or transcatheter replacement of the valve, as there are currently no pharmaceutical treatments. Understanding the cellular and molecular pathophysiology of CAVD may lead to pharmaceutical approaches for patients who are not optimal surgical candidates or prevent prosthetic valve recalcification.

CAVD studies have traditionally focused on aortic valve interstitial cells (AVICs),[73] yet no successful pharmacological strategies have emerged from this approach.[1] Recent studies have shown that inflammation and immunomodulation may play a key role in determining the calcification potential of these cells,[79,118,235] suggesting that immune signaling may be a viable target for therapeutic intervention. Immune cells are linked to CAVD,[220] and up to 10-15% of cells in the healthy murine valve express CD45, a hematopoietic lineage marker.[29,74] These cells are primarily major histocompatibility complex II positive macrophages.[50,74] Macrophages with molecular histocompatibility complex II positivity (MHCII$^+$) are more metabolically active, direct a proinflammatory immune response, and are increased in CAVD.[76,78,79] As part of this proinflammatory response, MHCII$^+$ macrophages secrete interleukin-6 (IL-6) and tumor necrosis factor α (TNFα), both of which promote calcification of AVICs.[79] However, macrophage depletion with liposomal clodronate increases disease as measured by aortic valve (AV) thickening in mice.[83] Thus, it is unclear if macrophages drive CAVD, inhibit CAVD, or respond to calcification.

Moving from cellular to molecular inflammation, STAT3 (signal transducer and activator of transcription 3) signaling is linked to both the activity of the osteogenic transcription factor RUNX2 (runt related transcription factor 2) and fibrotic inflammation in the heart.[21,129,136,168] These activities reflect the two primary pathways of AV calcification: osteogenic and dystrophic calcification, respectively.[64,236] Additionally, single nucleotide polymorphisms in the IL-6 receptor

(a major contributor to STAT3 activation) are associated with decreased severity of CAVD,[150] whereas transforming growth factor beta 1 (TGF-β1; another direct activator of STAT3) signaling is increased in CAVD and leads to calcification of AV cells *in vitro*.[156,237] Adding to the evidence, Tsai, et al. reported increased STAT3 phosphorylation in human CAVD.[152] This confluence of findings suggests that STAT3-mediated inflammation, potentially driven by macrophage-secreted factors, may promote CAVD and serve as a pharmacological target.

In order to determine the role of immune cells in CAVD, we utilized the *Notch1*^{+/-} murine CAVD model; human families with *NOTCH1* mutations have increased incidence of both CAVD and congenital bicuspid AV disease.[71] Mice with *Notch1* haploinsufficiency have increased AV calcification,[68,69] while AVICs with a *Notch1* mutation have increased calcification potential *in vitro*.[56] Interestingly, NOTCH1 has long been known to play a significant role in the differentiation and maturation of hematopoietic lineages—including specific inhibition of myeloid development—thus highlighting the potential for haploinsufficiency to affect valve calcification through infiltrating macrophages.[238–240] After assaying macrophage phenotypes in the *Notch1*^{+/-} model, we utilized bone marrow transplants and *in vitro* coculture models to assess the contribution of *Notch1*^{+/-} immune cells to AV calcification. Finally, we assessed and manipulated STAT3 activity using overexpression plasmids and phosphorylation blockade to investigate the contribution of macrophage-mediated changes in STAT3 to AVIC calcification. We found that *Notch1*^{+/-} AVICs increase recruitment and inflammatory maturation of macrophages, and that macrophages promote AVIC calcification and alter STAT3 splicing.

Methods

Animal Studies

      All animal experiments used C57BL/6J *mus musculus* animals. Bone marrow transplant experiments included both sexes, while experiments with ≤ 8 mice per group included only male mice due to the increased prevalence of CAVD in male patients. In total, 135 mice were used for this study. In the bone marrow transplant study, two mice died 8-15 weeks into the aging period. One wild-type mouse receiving *Notch1*$^{+/-}$ bone marrow died of unknown causes, and one *Notch1*$^{+/-}$ mouse receiving *Notch1*$^{+/-}$ bone marrow died after sustaining wounds from a littermate's aggression. No other deaths occurred during the aging period. All experimental protocols were approved by the Institutional Animal Care and Use Committee at Vanderbilt University.

Flow cytometry

      AVs were isolated from littermate wild-type (WT) and Notch1$^{+/-}$ mice. Cells were isolated from the AV by nine, seven-minute collagenase digestions at 37°C.[241] After each digestion, the supernatant was removed and diluted into FC buffer (PBS, 3% FBS). The cell pellet was then subjected to red blood cell lysis buffer for five minutes before quenching with FC buffer. For in vitro assays, bone marrow-derived macrophages (BMMs) and/or AVICs were lifted with Accutase. Cells were then blocked in Fc Block for 10 minutes at room temperature before staining with conjugated antibody for 30 minutes at 4°C. All antibodies are listed in Table 5.1.

Table 5.1. Antibodies for all associated methods.

Target antigen	Vendor or Source	Catalog #	Working concentration	Lot #
αSMA-Cy5.5	MilliporeSigma	C6198	IF(1:300)	058M4761V
α-Tubulin	Vanderbilt Molecular Biology Core	n/a	WB(1:1000)	n/a
CCR2-PE	BioLegend	150609	FC(1:50)	B278733
CD11b-e450	Thermo Fisher	48-0112-82	FC(1:400)	4329941
CD45-BV510	BD Biosciences	563891	FC(1:800)	9066967
CD68-AF594	BioLegend	137020	IF(1:200)	B239125
CX3CR1-PerCP/Cy5.5	BioLegend	149009	FC(1:250)	B271940
F4/80-PE/Cy7	BioLegend	123114	FC(1:400)	B265636
IL-6	Abcam	ab6672	IF(1:200)	GR3195128-21
Ly6C-FITC	BioLegend	128006	FC(1:700)	B270133
MHCII-APC	BioLegend	107614	FC(1:1600)	B255462
MHCII-FITC	Thermo Fisher	11-5321-82	IF(1:100)	4322171
Rabbit IgG-AF 647	Invitrogen	A21245	IF(1:300)	1837984
Rabbit IgG-FITC	Abcam	ab6717	IF(1:300)	731506
RUNX2	Novus Biologicals	NBP1-77461	IF(1:100)	B-1
RUNX2	Cell Signaling	12556S	WB(1:1000)	2
STAT3	Cell Signaling	9139S	WB(1:1000)	12
pSTAT3 (Y705)	Cell Signaling	9145S	WB(1:2000)	34

IF = immunofluorescence; WB = Western blot; FC = flow cytometry

Bone marrow transplants

8- to 12-week-old WT or *Notch1*^{+/-} C57BL/6J mice were given a split 12 Gy dose of radiation from a Cs^{137} source followed by retro-orbital administration of 3×10^6 bone marrow cells isolated from a sex-matched WT or *Notch1*^{+/-} donor. Mice were allowed six weeks for bone marrow reconstitution before aging on high-fat diet. After six months, mice were euthanized and bone marrow and AVs were isolated. Incidence of unanticipated death was similar between transplant groups. Two mice died 8-15 weeks into the aging period. One wild-type mouse receiving *Notch1*^{+/-} bone marrow died of unknown causes, and one *Notch1*^{+/-} mouse receiving *Notch1*^{+/-} bone marrow died after sustaining wounds from a littermate's aggression. No other deaths occurred during the aging period. Bone marrow was digested in rat tail lysis buffer overnight and genotyped for *Notch1* and the *Notch1*[del] cassette using polymerase chain reaction (PCR) to confirm successful transplants.

Histology and Immunofluorescence

Murine AVs were frozen in OCT and sectioned at 10 μm thickness. Von Kossa staining was performed by incubating with 3% Ag_2NO_3 for 40 minutes under a UV lamp, followed by incubation with 5% sodium thiosulfate for five minutes. Slides were counterstained with Nuclear Fast Red. Leaflet thickness was measured using a semi-automated MATLAB script to calculate leaflet area divided by leaflet length, resulting in average leaflet width. For immunofluorescence, slides were fixed and permeabilized with 10% formalin and 0.1% Triton-X for 15 minutes, followed by epitope blockade for one hour with 1% BSA in PBS. Primary antibody staining was performed in blocking solution overnight at 4°C. When applicable, secondary antibody staining was performed for one hour at room temperature. Slides were mounted in ProLong Gold with DAPI and imaged at 4-60X magnification. CD68^{+} and MHCII^{+} macrophages were counted manually and normalized to the area of the leaflet DAPI mask, giving macrophages/mm^2. Control images are included in Appendix B.

Aortic valve interstitial cells

AVICs were isolated from WT or Notch1$^{+/-}$ C57BL/6J mice as previously described.[151] Briefly, AVs were digested in 2 mg/mL collagenase in HBSS for 30 minutes at room temperature and placed in DMEM supplemented with 10% FBS, 1% penicillin/streptomycin (pen/strep), and 10 µg/mL recombinant murine interferon-γ to induce activation of the simian virus 40 T antigen. Cells were allowed to adhere to 0.1% gelatin-coated six-well tissue culture-treated plates and expanded. To allow for sustained immortal growth, cells were cultured at 33°C and 5% CO_2 when not plated for experiments. At least 12 hours prior to experiments (overnight), AVICs were incubated at 37°C and 5% CO_2 in DMEM supplemented with 10% FBS and 1% pen/strep (complete media), wherein the immortalization element degrades due to temperature changes. AVICs were seeded at 20,000 cells/cm^2 in all experiments unless otherwise noted.

Bone marrow-derived macrophages

Macrophages (BMMs) were generated from the bone marrow of WT or Notch1$^{+/-}$ C57BL/6J mice using M-CSF.[242] BMM generation was verified by flow cytometry for CD11b and F4/80 (Figure 5.2). Following differentiation, all experiments were carried out without M-CSF supplementation.
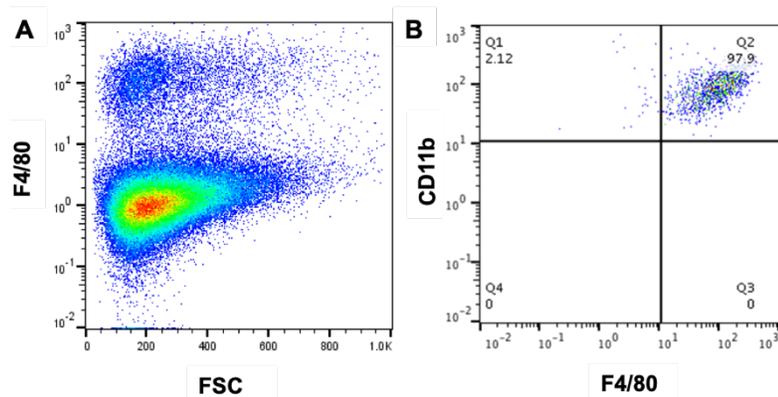
Figure 5.2. Confirmation of bone marrow-derived macrophage phenotype in coculture.
The F4/80^{hi} macrophage population is seen in AVIC-macrophage coculture (A, representative plot). Among CD45$^+$ cells, >96% were CD11b$^+$ and F4/80^{hi} in each of four biological replicates (B, representative plot). Reprinted, with permission, from Raddatz, et al.[28]

Coculture design

BMMs and AVICs were seeded at a 1:7 physiologic ratio[74] in RPMI supplemented with 10% FBS and 1% pen/strep and cultured for 48 hours before harvesting for various experiments. Transwell cocultures were seeded at the same ratio with AVICs seeded on the tissue culture-treated plate and BMMs seeded on a 0.4 μm-pore Transwell insert (Corning, Corning, NY). AVIC monoculture controls for all coculture experiments were also performed in supplemented RPMI.

Cultured media

Media was harvested from cultures after 24 hours and filtered using 0.45 μm sterile filters before use. In all cultured media experiments, RPMI supplemented with 10% FBS and 1% pen/strep was used.

Migration assay

Using a modified Transwell migration protocol,[243] 10,000 BMMs were seeded in 100 μL of uncultured media on an 8 μm-pore Transwell insert and incubated for 10 minutes at 37°C. 600 μL of cultured media was then added to the well below each insert and cells were allowed to migrate for 3 hours. Transwell inserts were then removed and fixed in 70% ethanol for 10 minutes prior to mounting in ProLong Gold with DAPI. All cells that migrated through the membrane were counted based on visualization of DAPI staining. Migration index was defined as the number of migrated cells divided by the number of migrated cells into a control condition of uncultured media.

Microarray

The Proteome Profiler Mouse Cytokine Array Kit, Panel A (R&D Systems, Minneapolis, MN) was used per the manufacturer's instructions. Briefly, protein from either cell lysates or

conditioned media was incubated with an antibody mixture and allowed to bind to the patterned membrane overnight. Antibodies were then conjugated and the membrane was imaged using an Odyssey Classic imager (Li-Cor, Lincoln, NE).

Calcific nodule assay

Cultures were treated with 5 ng/mL TGF-β1 for 24 hours followed by 24 hours of cyclic biaxial 10% mechanical strain at 1 Hz on BioFlex plates coated with Pronectin, using a FlexCell 3000 machine (FlexCell, Burlington, NC).[56] Cultures were stained for calcification using Alizarin Red S and calcific nodules were manually counted in each well by visual inspection.

Magnetic-activated cell sorting

Cells were lifted with Accutase, incubated for 15 minutes with anti-CD45 MicroBeads (Miltenyi Biotec, Bergisch Gladbach, Germany) to allow for magnetic labeling, and resuspended in MACS buffer (PBS, 0.5% BSA, 2 mM EDTA), followed by positive selection of CD45$^+$ BMMs. Further downstream analysis was conducted on the unperturbed CD45$^-$ AVICs.

Quantitative real time-polymerase chain reaction (RT-qPCR)

AVIC mRNA was isolated using Trizol (Life Technologies, Carlsbad, CA) and cDNA libraries were produced using the Superscript IV Reverse Transcriptase kit with oligo(dT) primer, as per manufacturer protocols (ThermoFisher Scientific, Waltham, MA). Quantitative real time polymerase chain reaction for all targets was performed on the CFX-96 Real Time System using iQ SYBR Green Supermix (Bio-Rad, Hercules, CA) (please see Table 5.2 for primer sequences). Products were confirmed by gel electrophoresis. Gapdh was used as a housekeeping gene. All statistics were performed on untransformed ΔCt values ("gene of interest" Ct – Gapdh Ct), but for clarity, gene expression was normalized and displayed as $2^{\Delta\Delta Ct}$.

Table 5.2. Primer sets for RT-qPCR.

Target Transcript	Forward Primer (5' to 3')	Reverse Primer (5' to 3')
Acta2	TCTGGACGTACAACTGGTATTG	GGCAGTAGTCACGAAGGAATAG
Adar1	CGGCACTATGTCTCAAGGGT	TGCGGGTATCTCCACTTGCT
Cdh11	ACACCATGAGAAGGGCAAG	ACCGGAGTCAATGTCAGAATG
Gapdh	ATGACAATGAATACGGCTACAG	TCTCTTGCTCAGTGTCCTTG
Icam1	GCAGAGGACCTTAACAGTCTAC	TGGGCTTCACACTTCACAG
Il6	CAAAGCCAGAGTCCTTCAGAG	GAGCATTGGAAATTGGGGTAG
Runx2	CCCAGCCACCTTTACCTACA	TATGGAGTGCTGCTGGTCTG
Sparc	CTGTCCCGGGTGATGGTATG	TGGAGTGTTTGCTTCTGTGC
Spp1	GTGATTTGCTTTTGCCTGTTTG	GAGATTCTGCTTCTGAGATGGG
Vegfa	AGTCTGTGCTCTGGGATTTG	GTTGGCACGATTTAAGAGGGG

Cell Proximity Analysis

Cocultures were performed on glass coverslips and stained by immunofluorescence for CD68 and either RUNX2 or alpha-smooth muscle actin (αSMA). Immunofluorescence staining was performed as described above (see *Histology and Immunofluorescence*). Immunofluorescence images were analyzed using a custom algorithm designed to determine whether the proximity of activated AVICs—as identified by RUNX2 or αSMA staining—to CD68^{+} macrophages was closer or further than expected based on Monte Carlo simulations of random macrophage placement (Figure 5.3).

In order to determine if activated AVICs were distributed unevenly throughout the coculture landscape within any given x-y field of view, an image processing algorithm was developed to test the hypothesis that activated cells were more likely to be near macrophages. After staining, images in each channel were blurred using a Gaussian filter with a standard deviation of 4 and thresholded by Otsu's thresholding method. This mask generated positive regions, which were gated by size to identify individual cells. This process was performed in each channel to identify CD68^{+} macrophages, and either RUNX2^{+} or αSMA^{+} activated AVICs.

In every image, the centroid of each activated AVIC was determined and a distance index was defined. In particular, for each identified AVIC, the location was compared to the location of each of the n identified macrophages and the distance to the nearest macrophage was recorded. All distances ≤ 10 µm were removed from the analysis to account for mistaken identification of one cell as both an AVIC and macrophage. Sensitivity analyses confirmed that this did not affect the conclusion. In order to determine the "expected distance" from the activated AVIC to the nearest macrophage, N random macrophages were placed across the x and y axes of the image and the distance from the current AVIC to the nearest random macrophage location was recorded. This randomized process was repeated 500 times in a Monte Carlo simulation, and the median distance to the nearest macrophage was recorded as the "expected distance" to the nearest macrophage. At that point, the real distance to the

nearest macrophage was divided by the expected distance and recorded as the distance index

of the activated AVIC. A density plot of the distance index of all activated AVICs is shown in

Figure 5.12. All of the above was performed using the statistical programming language, R.

Example code is included in Appendix C. The R package '*EBImage'* was used for all image

processing, and '*ggplot2*' was used for data visualization.
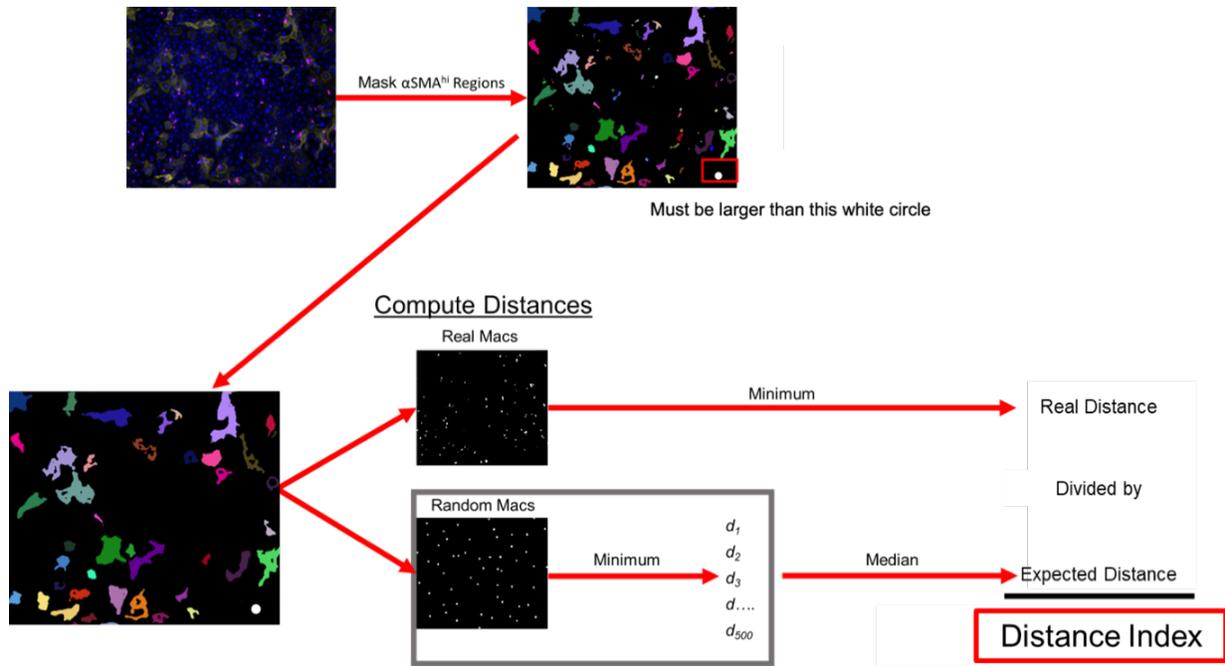
Figure 5.3. Image proximity analysis workflow.
Images were masked for activated AVICs by RUNX2 or αSMA staining and real and expected distance to the nearest macrophage calculated. Additional details are included above and in Appendix C. Reprinted, with permission, from Raddatz, et al.[28]

Western Blot

AVICs and human AVs were lysed in RIPA buffer or PBS respectively, supplemented with benzonase, sodium orthovanadate, and protease inhibitor. Lysates were denatured using SB at 100°C for 5 minutes, then 10-15 μg of protein was loaded into 15 cm 10% acrylamide gels and run at 150V for 1 hour and 45 minutes. Membrane transfer was performed at 80V for 1 hour and 45 minutes. Membranes were blocked with 5% BSA in TBST and stained in primary antibody overnight at 4°C. Membranes were then stained with fluorescent secondary antibody and imaged on an Odyssey Classic imager (Li-Cor). Quantification was performed in Image Studio Lite (Li-Cor).

Human Aortic Valve Samples

AV samples were collected at the time of replacement and separated into involved and uninvolved tissue based on the sample location relative to apparent calcification before being flash frozen in liquid nitrogen and stored at -80°C. Samples were mechanically digested with a bead homogenizer (BioSpec Products, Bartlesville, OK) in PBS supplemented with benzonase, sodium orthovanadate, and protease inhibitor. Written informed consent was obtained from patients and tissue sample collection was approved by the institutional review board at Washington University in St. Louis.

Plasmid Transfection

Prior to transfection, AVICs were serum-starved in 1 mL of DMEM with 1% FBS overnight in 12-well plates. Lipofectamine 2000 (ThermoFisher) and concentrated STAT3α, STAT3β, or vector control plasmids (Genscript, Piscataway, NJ) were diluted in Opti-MEM media (ThermoFisher) and allowed to create DNA-lipid complexes for 20 minutes. Next, 200 μL of Opti-MEM containing 4 μL of Lipofectamine and 1 μg of plasmid DNA was added to each

well. After 4 hours, media was replaced with complete media. In coculture models, macrophages were added 24 hours after transfection initiation, and in all experiments AVICs were harvested at 48 hours. Western blots confirming transfection are included in Appendix D.

Micropipette Aspiration

Micropipette aspiration was used to determine the elastic modulus of AVICs as reported previously.[156,244–246] Capillary tubes (World Precision Instruments, Sarasota, FL) were coated with Sigmacote (MilliporeSigma, St. Louis, MO), sterilized with 70% ethanol, and allowed to dry. Coated tubes were then pulled with a P-97 micropipette puller (Sutter Instrument, Novato, CA), fractured with an MF-1 microforge (Technical Products International, St. Louis, MO) to an internal diameter of approximately 6 μm, and bent to an angle allowing for the micropipette to lie parallel to the plate upon use. Pressures were applied using a custom-built pressure regulator system with an MCFS-EZ microfluidics controller (Fluigent, Le Kremlin-Bicêtre, France).

Following treatment, AVICs were lifted with Accutase, resuspended in 500 μL MACS buffer, and kept on ice until use. Aspiration was performed on at least 10 cells from each condition and biological replicate each day. Tests were performed by linearly increasing the applied suction pressure by 8 Pa/s over 60 seconds to a final aspiration pressure of 0.48 kPa. The aspirated length of each cell was measured manually from video recorded at a rate of 2 frames/s using a microscope-mounted camera (Figure 5.4).

After all data was recorded, aspirated length of each cell was measured manually and the effective stiffness (E) was determined using a half-space elastic model given below:

$$E = \varphi n \left(\frac{3r}{2\pi}\right)\left(\frac{\Delta P}{L}\right)$$

where φ(η) is the wall function and is equal to 2.1 (dimensionless parameter calculated from the ratio of the pipette inner radius to the wall thickness), r is the micropipette inner radius, and ΔP/L is the slope of the linear applied pressure vs. aspirated cell length curve.
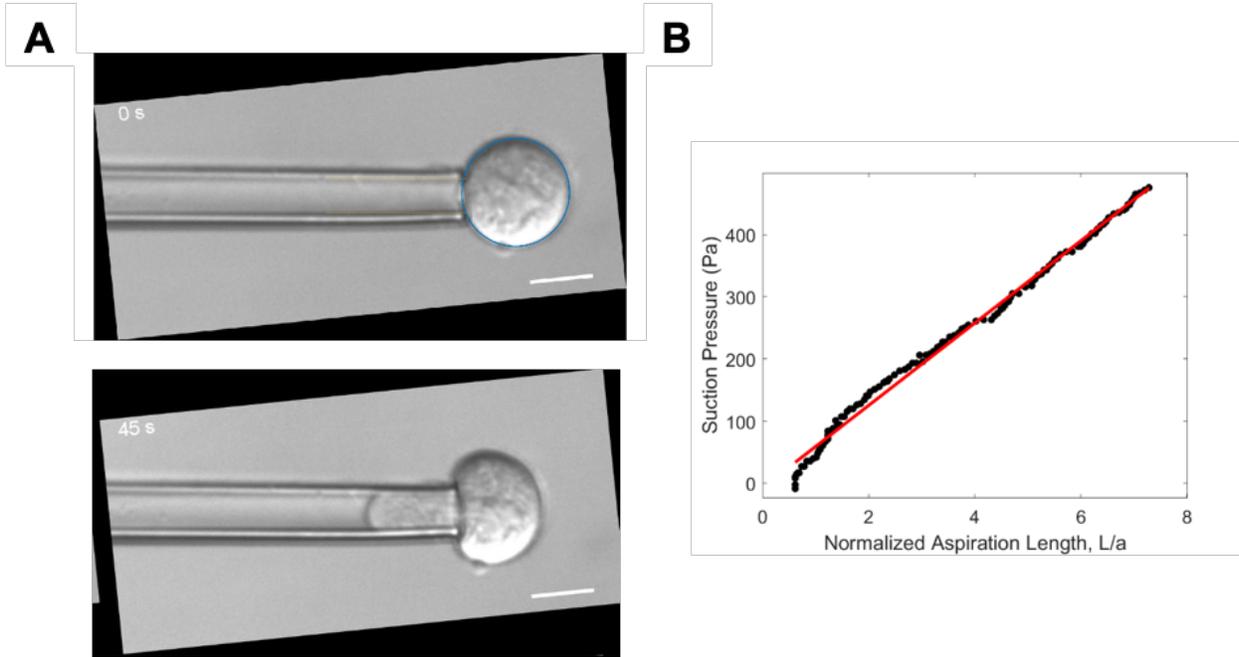
Figure 5.4. Raw micropipette analysis data.
Stabilized images of cell aspiration were recorded (A) followed by measurement of the slope of suction pressure over normalized aspiration length to determine cellular elastic modulus (B). Reprinted, with permission, from Raddatz, et al.[28]

STAT3 Blockade

Stattic (MilliporeSigma), a STAT3 tyrosine phosphorylation inhibitor (Y705) was used to block STAT3 activity. Stattic was solubilized in DMSO and added to cells in complete media. Western blots confirming STAT3 phosphorylation blockade are included in Appendix D.

Statistics

All data points are shown throughout the manuscript in addition to mean ± standard error of the mean (s.e.m.) or boxplots signifying median and first and third quartiles for non-normal data. Comparisons between normal data were performed by ANOVA followed by Student's t-test with Holm-Sidak adjustment for multiple comparisons; non-normal data were analyzed using Kruskal-Wallis or Mann-Whitney *U* test. Murine data were analyzed by aligned rank transformed ANOVA[247] to allow for two- and three-way non-parametric comparisons. All statistical analyses were performed using the statistical programming language R, version 3.5.2.[218]

Results

Notch1^{+/-} *Aortic Valves Have an Altered Myeloid Profile*

We first assessed macrophage phenotypes in the AVs of both WT and *Notch1*^{+/-} mice in young adulthood (10-12 weeks), prior to disease onset. Hematopoietic cells make up similar proportions of the AV in WT (7.1%) and *Notch1*^{+/-} (7.0%) mice (Figure 5.5A). Among hematopoietic cells, there is a majority myeloid fraction (CD11b^{+}) that is greater in the *Notch1*^{+/-} valve (Figure 5.5B) and comprised primarily of F4/80^{+} macrophages in both genotypes (Figure 5.5C). Valvular macrophages are majority CX3CR1[high]/Ly6C^{-}/CCR2^{-} in both genotypes (Figure 5.5D-F), but in the *Notch1*^{+/-} valve, macrophages show increased CX3CR1 and MHCII expression, suggesting an enhanced migratory and proinflammatory phenotype (Figure 5.5F, G).[248] When analyzing all hematopoietic cells, non-myeloid cell types include CD11b^{-}/MHCII^{+}

antigen-presenting cells, similar to previous reports (Figure 5.5H, I).[74] Simultaneously, BMMs

were generated from the same WT and *Notch1*^{+/-} mice and no differences were observed

(Figure 5.6). In summary, macrophages make up the majority of hematopoietic cells in the AV

and are different in the valves of *Notch1*^{+/-} vs WT mice.
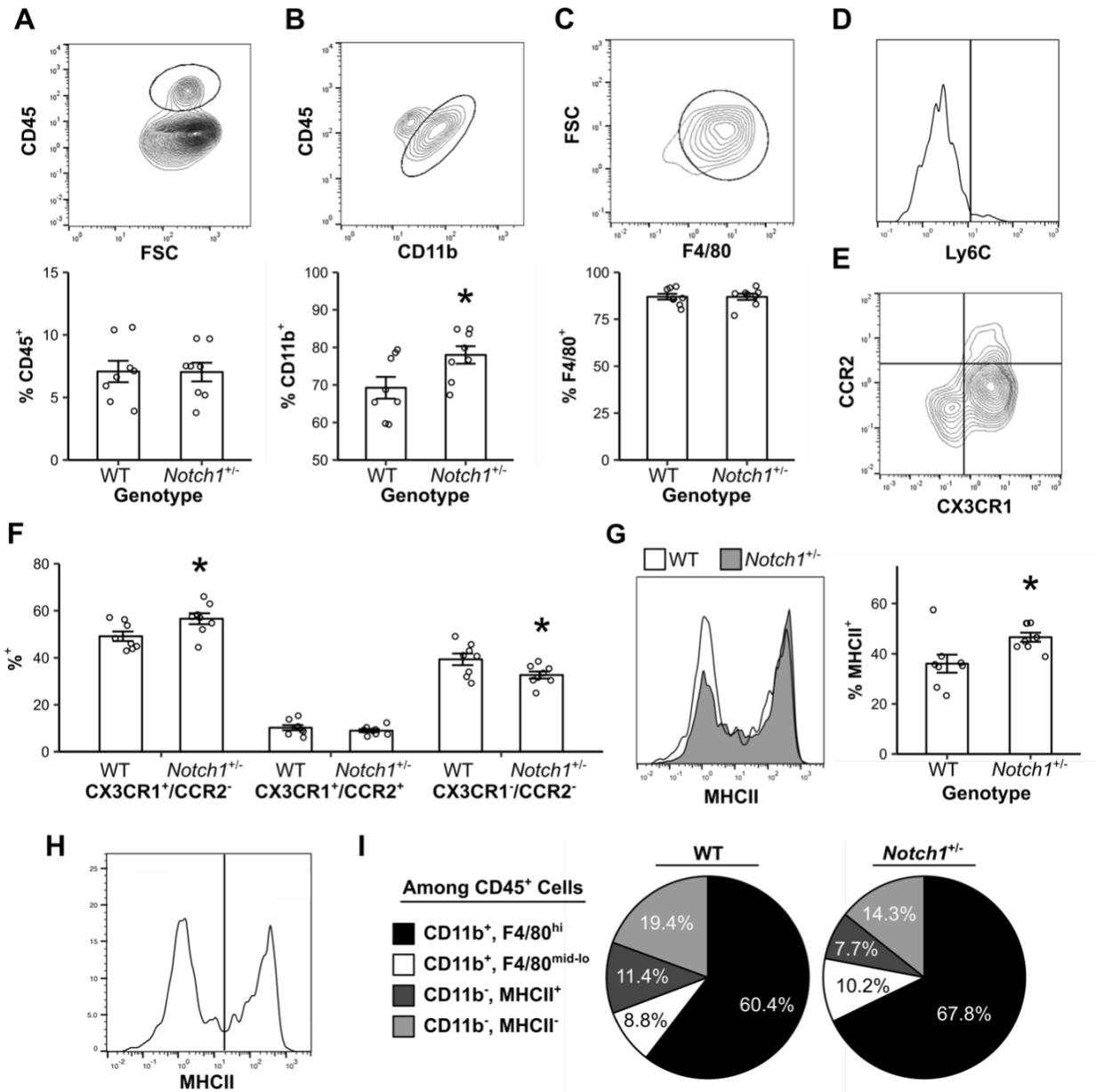
Figure 5.5. *Notch1*^{+/-} murine aortic valves have increased macrophage polarization.
Flow cytometry was performed on both WT and *Notch1*^{+/-} aortic valves for CD45 (A), followed by CD11b (B), then F4/80 (C). Macrophages were characterized by Ly6C expression (D), CX3CR1 and CCR2 expression (E, F), and MHCII expression (G, outline = WT; gray fill = *Notch1*^{+/-}). Non-myeloid hematopoietic cells were grouped by MHCII expression (H), and all cell types were plotted as average percentage of the total CD45^{+} population (I). Bar plots represent mean ± s.e.m (A-C, F, G). Representative flow plots are of WT animals (A-E, H). N = 8 biological replicates. *P < 0.05 by two-tailed *t* test. Reprinted, with permission, from Raddatz, et al.[28]
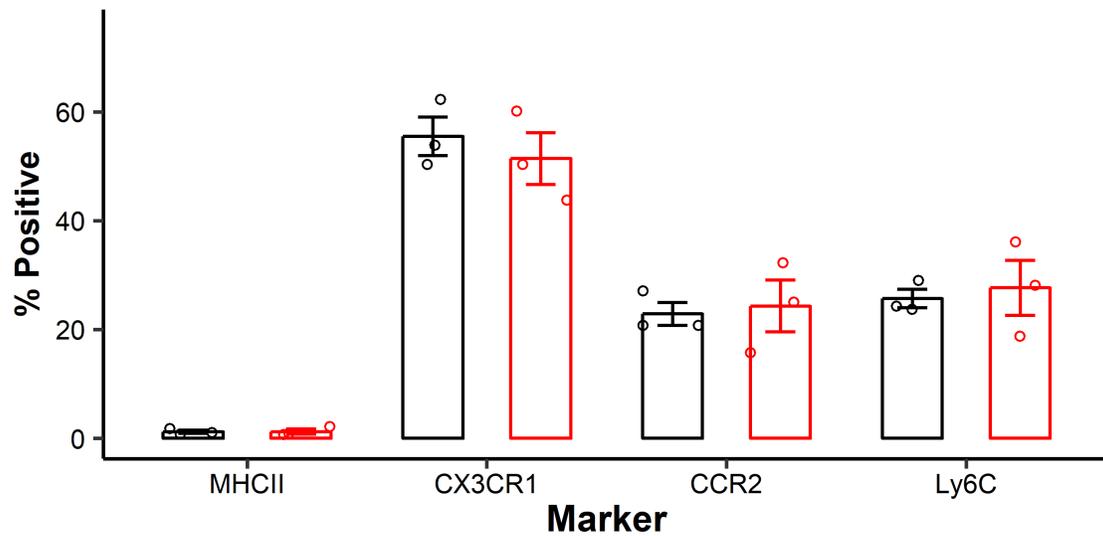
Figure 5.6. Wild-type and *Notch1*^{+/-} bone marrow-derived macrophages.
BMMs from wild-type (black) and *Notch1*^{+/-} (red) mice have no differences in various markers of maturity. Bars represent mean ± s.e.m. All data analyzed by two-tailed *t* test. Reprinted, with permission, from Raddatz, et al.[28]

Notch1 *Haploinsufficiency in Aortic Valve Cells Drives Disease and Macrophage Recruitment*

Considering the increased macrophage infiltration in *Notch1*^{+/-} mice previously reported,[69] and the altered macrophage phenotypes observed, we performed bone marrow transplants to identify if underlying differences in hematopoietic cells were driving the macrophage changes found in the *Notch1*^{+/-} CAVD model. WT and *Notch1*^{+/-} mice were transplanted with WT or *Notch1*^{+/-} bone marrow and aged for 6 months on high-fat diet to allow for disease progression. After aging, leaflet calcification was visualized by von Kossa and Alizarin Red staining (Figure 5.7A, B, Figure 5.8). Leaflet thickness was measured and body genotype, but not bone marrow genotype, was significantly associated with leaflet thickness (Figure 5.7C). The same pattern was seen with immunofluorescence staining for CD68^{+} macrophage infiltration (Figure 5.7D, E). There was no change in valve phenotype by echocardiography. Valves were additionally stained for MHCII to detect differences observed by flow cytometry (Figure 5.7F, G). Valves of *Notch1*^{+/-} mice have an increased prevalence of MHCII[+] macrophages and a lesser increase in MHCII[-] macrophages, leading to a higher MHCII[+] macrophage fraction (Figure 5.7H, I, Figure 5.9). Thus, *Notch1* haploinsufficient valve phenotypes, including differences in hematopoietic cell recruitment, are mediated by valvular cells.
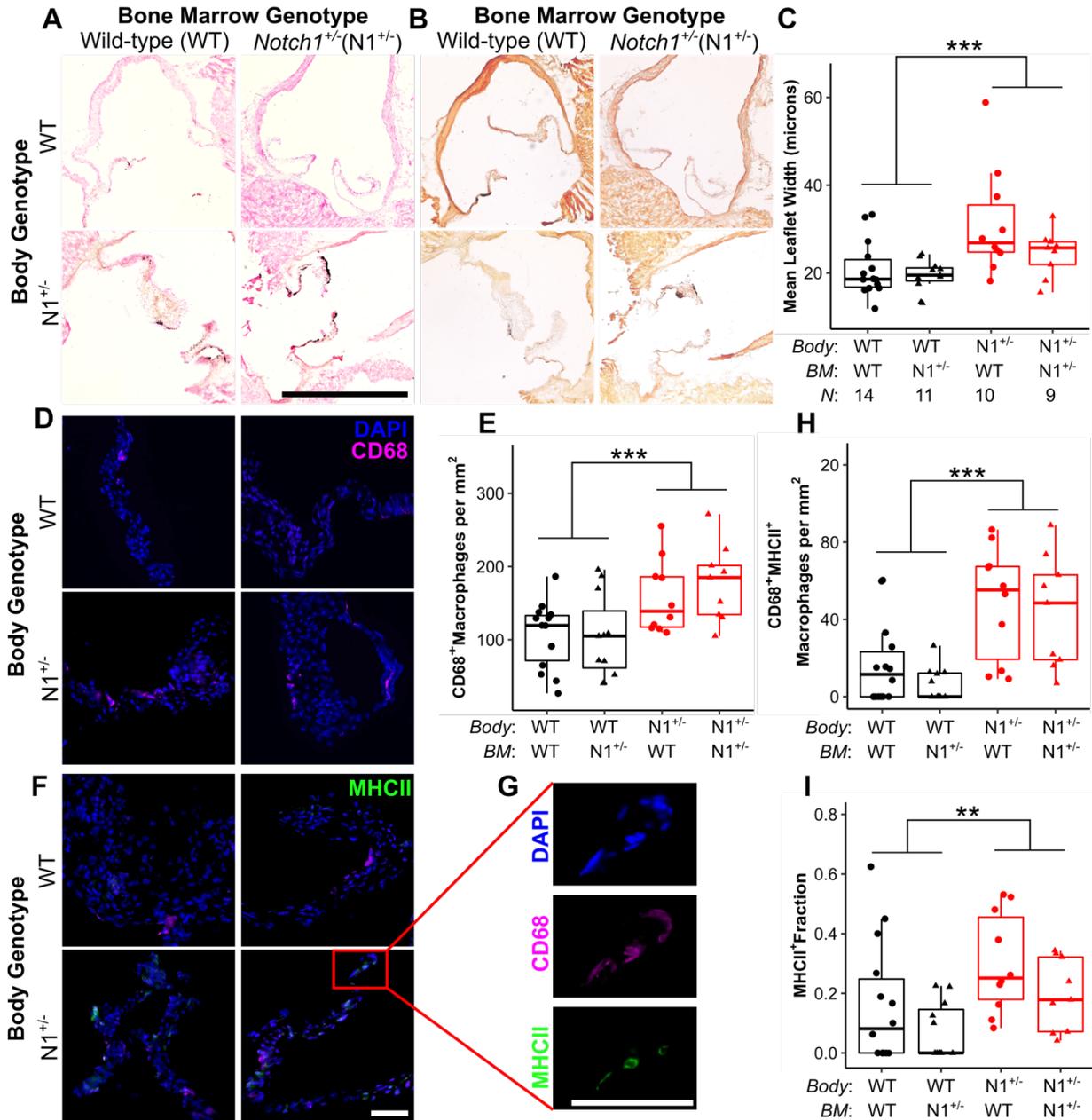
Figure 5.7. *Notch1*^{+/-} valve cells drive aortic valve disease and macrophage infiltration and maturation *in vivo*.

Following bone marrow transplant, aortic valves from *Notch1*^{+/-} (N1^{+/-}) and wild-type (WT) mice were assessed for calcification (A, B), thickness (A, C), macrophage infiltration (D, E), and macrophage maturation, as measured by MHCII positivity (F-I). (A) Aortic valves are stained for histology and calcification by von Kossa and (B) Alizarin Red; scale bar = 1 mm. (C) Leaflet thickness is plotted as mean width across the entire section. (D, F, G) Aortic valves are stained by immunofluorescence for DAPI (blue), CD68 (pink), and MHCII (green); scale bar = 100 μm. (E, H) Macrophage data is plotted as cells per mm^2 of tissue. Boxplots represent 25th, 50th, and 75th percentiles. All data were analyzed by two-way aligned rank transformed ANOVA.[247] **P < 0.01, ***P < 0.001. N = biological replicates, and is the same across panels. BM = bone marrow. Reprinted, with permission, from Raddatz, et al.[28]
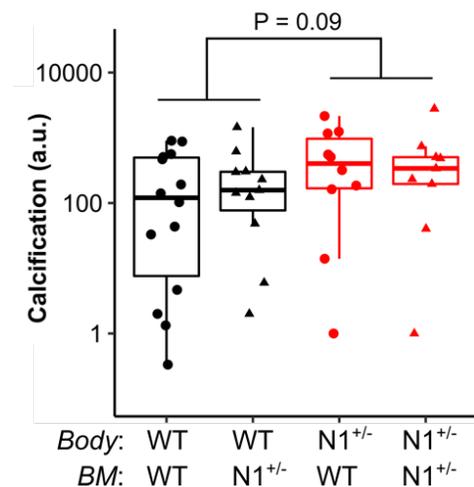
Figure 5.8. Calcification quantification in wild-type and *Notch1*^{+/-} mice.
Wild-type (WT) and *Notch1*^{+/-} (N1^{+/-}) mice with WT and N1^{+/-} bone marrow were stained for calcification with von Kossa, and positive staining was quantified. Data were analyzed by two-way aligned rank transformed ANOVA. N = 14, 11, 10, and 9 biological replicates. Reprinted, with permission, from Raddatz, et al.[28]
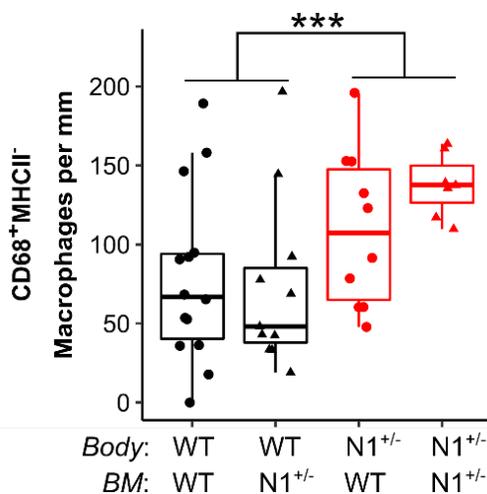
Figure 5.9. MHCII⁻ macrophages in wild-type and *Notch1*^{+/-} valves.
There is an increase in MHCII⁻ macrophages in *Notch1*^{+/-} mice regardless of bone marrow genotype. Boxplots display the 25th, 50th, and 75th percentiles. Data were analyzed by two-way aligned rank transformed ANOVA. ***P < 0.001. N = biological replicates. Reprinted, with permission, from Raddatz, et al.[28]

Notch1$^{+/-}$ *AVICs Drive Calcification and Macrophage Phenotypes* In Vitro

    With *Notch1* haploinsufficiency acting through AVICs but accompanied by a clear

difference in macrophage infiltration and phenotype, we used *in vitro* coculture models to

explore this relationship. First, we replicated the previous bone marrow transplant experiment *in*

vitro. WT and *Notch1*$^{+/-}$ AVICs and BMMs were cocultured and assayed for common

transcriptional calcification markers. *Notch1* haploinsufficiency altered coculture calcification

genes only when carried in the AVICs (Figure 5.10A-D). Assessing macrophage phenotypes,

BMMs cultured with *Notch1*$^{+/-}$ AVICs had increased CCR2 and Ly6C expression, while

macrophage genotype had no effect (Figure 5.10E, F). Additionally, both WT and *Notch1*$^{+/-}$

macrophages increased migration towards media cultured by *Notch1*$^{+/-}$ AVICs compared to WT

AVICs (Figure 5.10G, Figure 5.11). Microarray analysis of secreted factors and lysate from

Notch1$^{+/-}$ and WT AVICs revealed an increase in cytokines that induce proinflammatory

macrophage differentiation and migration (Figure 5.10H).[249,250] Raw microarray images are

included in Appendix D. The highest observed fold-change was that of IL-6, and

immunofluorescence staining of 8- to 12-week-old WT and *Notch1*$^{+/-}$ mice recapitulated this

pattern of increased IL-6 expression in *Notch1*$^{+/-}$ mice (Figure 5.10I).
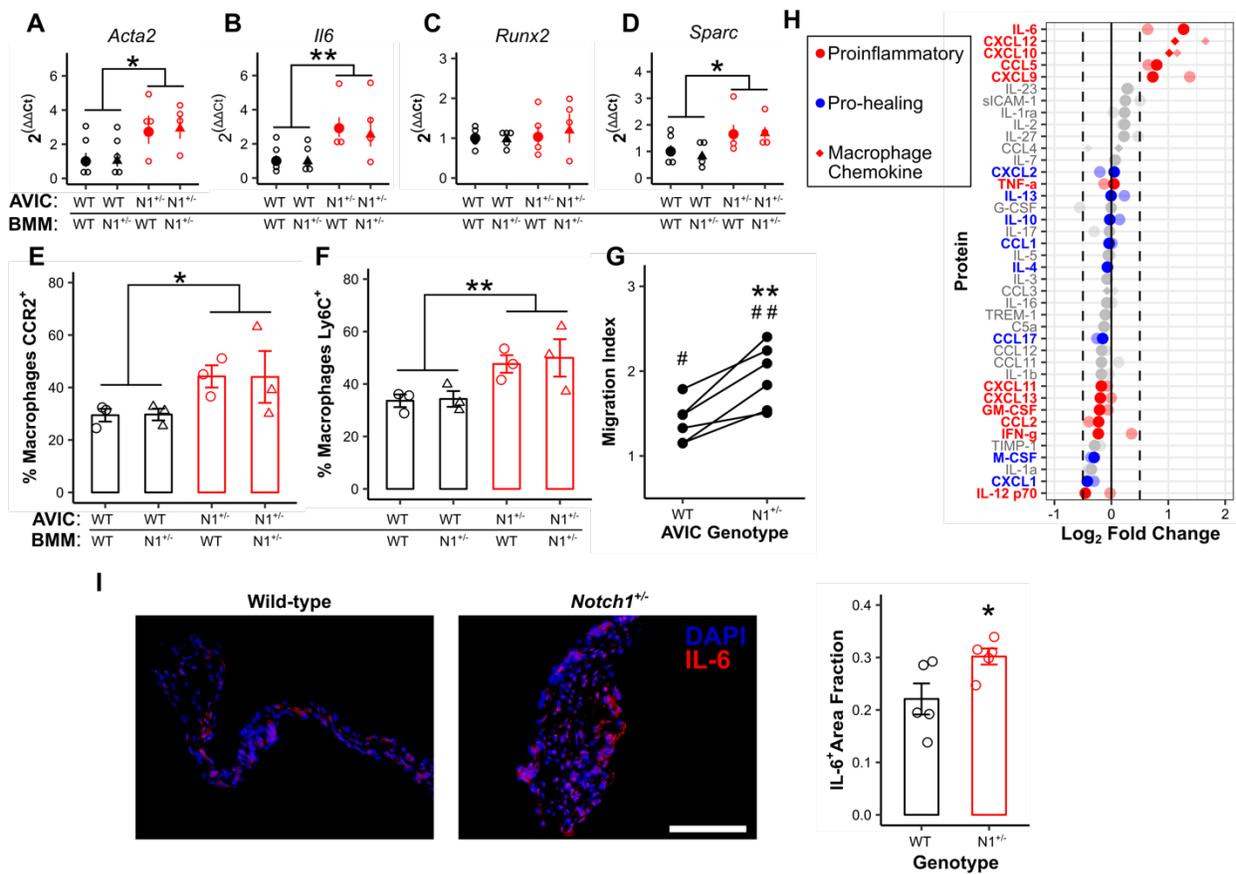
Figure 5.10. *Notch1*^{+/-} aortic valve interstitial cells promote calcification and macrophage maturation *in vitro* through altered cytokine secretion.
Wild-type (WT) and *Notch1*^{+/-} (N1^{+/-}) aortic valve interstitial cells (AVICs) were cultured with WT and N1^{+/-} bone marrow-derived macrophages (BMMs) and assayed for transcription of common markers of dystrophic (A, B) and osteogenic (C, D) calcification (N = 4). Flow cytometry for CCR2 (E) and Ly6C (F) expression was performed on BMMs (black = WT AVICs; red = N1^{+/-} AVICs; circle = WT BMMs, triangle = N1^{+/-} BMMs, N = 3). (G, N = 6) Migration assays of WT macrophages in the presence of either WT or N1^{+/-} AVIC-cultured media and uncultured media controls. (H) Cytokine microarray analysis of secreted media from WT and N1^{+/-} AVICs. Data is plotted as fold change in N1^{+/-} AVIC-cultured media compared to WT control. Full color points are cultured media; faded points are cell lysates. Points represent an average of two experiments with 3 pooled samples each. (I, N = 5) IL-6 (red) expression in WT and N1^{+/-} aortic valves; scale bar = 200 μm. All summary data represent mean ± s.e.m. Data were analyzed by two-way ANOVA on untransformed ΔCt values (A-D) or flow populations (E, F), or one-way ANOVA followed by paired, two-tailed *t* tests with Holm-Sidak corrections (G), or two-tailed *t* test (I). *P < 0.05 from wild-type AVICs, **P < 0.01 from wild-type AVICs, #P < 0.05 from control media, ##P < 0.01 from control media. N = biological replicates. Reprinted, with permission, from Raddatz, et al.[28]
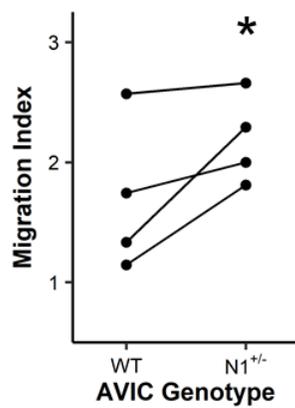
Figure 5.11. *Notch1^{+/-}* **macrophage migration towards AVIC-secreted media.**
Notch1^{+/-} AVIC-cultured media promotes macrophage migration compared to wild-type AVIC-cultured media or uncultured media control. Data were analyzed by one-way ANOVA followed by paired, two-tailed *t* tests with Holm-Sidak corrections. *$P < 0.05$ from wild-type AVICs, N = biological replicates. Reprinted, with permission, from Raddatz, et al.[28]

Macrophages Promote Osteogenic, and not Dystrophic, Calcification of AVICs

Given the observation of increased macrophage recruitment and proinflammatory maturation in the *Notch1*$^{+/-}$ model, we sought to determine how macrophages affect AVIC calcification. When cultured with macrophages, AVICs formed more calcific nodules *in vitro* (Figure 5.12A). We then cultured AVICs either in monoculture (Mono), Transwell culture with macrophages (TW), or direct coculture with macrophages (CC) (Figure 5.12B). RT-qPCR revealed increases in osteogenic calcification transcripts in both Transwell and, more profoundly, direct coculture as compared to monoculture (Figure 5.12C-E). There was no change in dystrophic calcification markers (Figure 5.12F-H). AVIC-specific expression was confirmed by immunofluorescent staining for CD68 (macrophages) and RUNX2 (Figure 5.12I). To further assess this relationship, macrophage proximity to RUNX2$^+$ and αSMA$^+$ AVICs was calculated (Figure 5.13). RUNX2$^+$ AVICs (osteoblasts, osteogenic calcification) were closer to macrophages than expected, while αSMA-positive AVICs (myofibroblasts, dystrophic) were normally distributed as expected (Figure 5.12J). Additionally, *Notch1*$^{+/-}$ animals with increased macrophage recruitment (Figure 5.7) were stained for RUNX2 and αSMA expression in the AV. RUNX2 expression alone was increased (Figure 5.12K, Figure 5.14). These data conclude that increased macrophage recruitment promotes osteogenic, but not dystrophic, AVIC calcification.
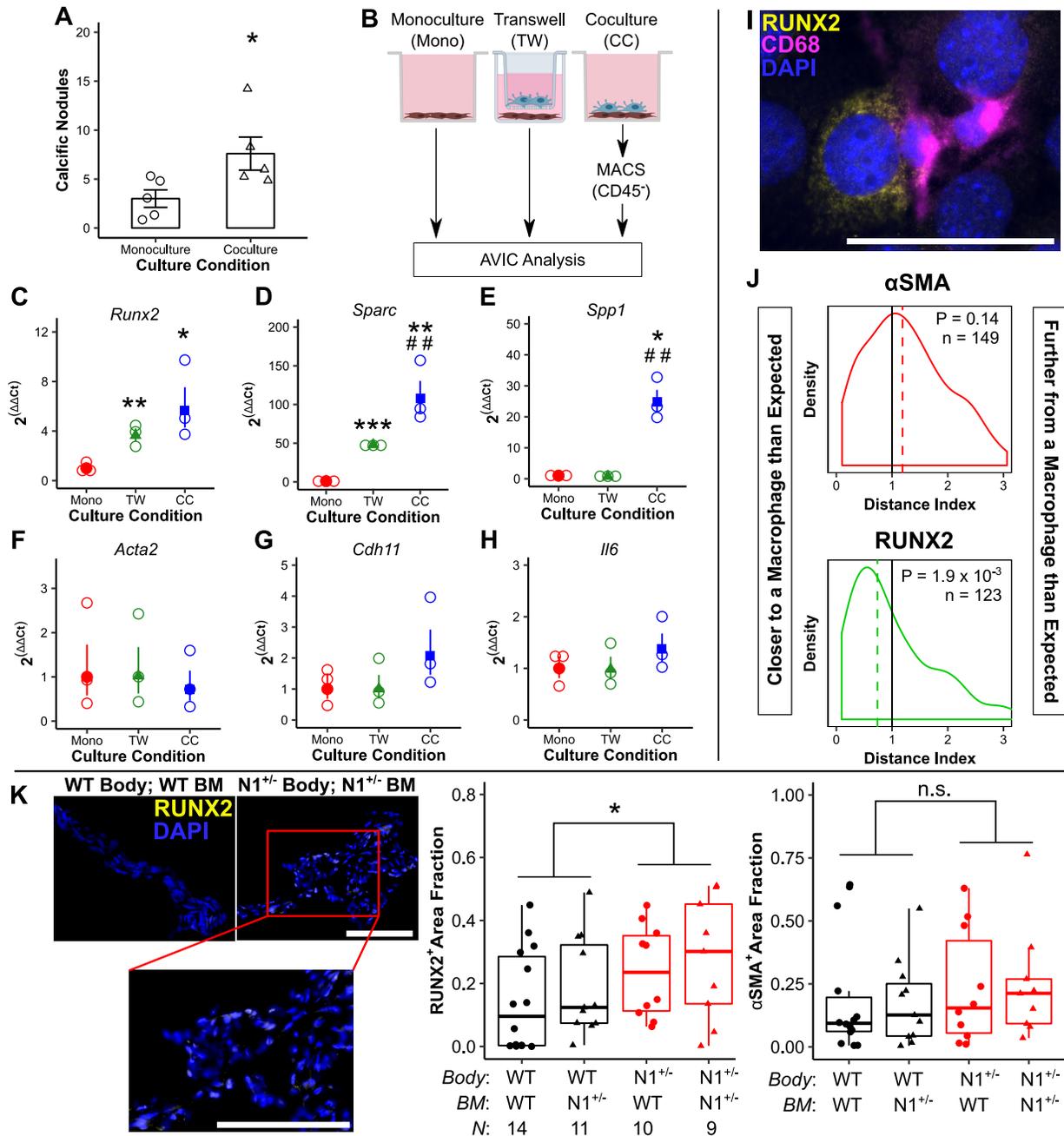
Figure 5.12. Macrophages promote osteogenic but not dystrophic calcification of aortic valve interstitial cells.

Cocultures of aortic valve interstitial cells (AVICs) with bone marrow-derived macrophages (BMMs) were assayed for calcific nodule formation (A, N = 5). AVICs cultured in monoculture (Mono), Transwell culture with BMMs (TW), or direct coculture with BMMs (CC) (B) were assayed for transcription of markers of osteogenic (C-E) and dystrophic (F-H) calcification (N = 3). Images of cocultures stained for RUNX2, CD68, and DAPI (I) were analyzed by a Monte Carlo-assisted simulation to calculate expected distance and distance index between activated AVICs and BMMs (J). Bone marrow transplanted wild-type (WT) and *Notch1*^{+/-} (N1^{+/-}) mice were stained for RUNX2 and αSMA expression (K). Scale bars = 200 µm (K) and 50 µm (I). All summary data represent mean ± s.e.m. Data were analyzed by Mann Whitney *U* test (A), one-way ANOVA followed by two-tailed *t* tests with Holm-Sidak corrections on untransformed ΔCt values (C-H), one sample Wilcoxon Signed-Rank test on log-transformed data (J), or two-way aligned rank

transformed ANOVA (K). *P < 0.05, **P < 0.01, ***P < 0.001 from monoculture AVICs (A-H) or between genotypes (K); ##P < 0.01 from Transwell AVICs. N = biological replicates (A, C-H, K) or activated AVICs across 4 biological replicates (J). Reprinted, with permission, from Raddatz, et al.[28]
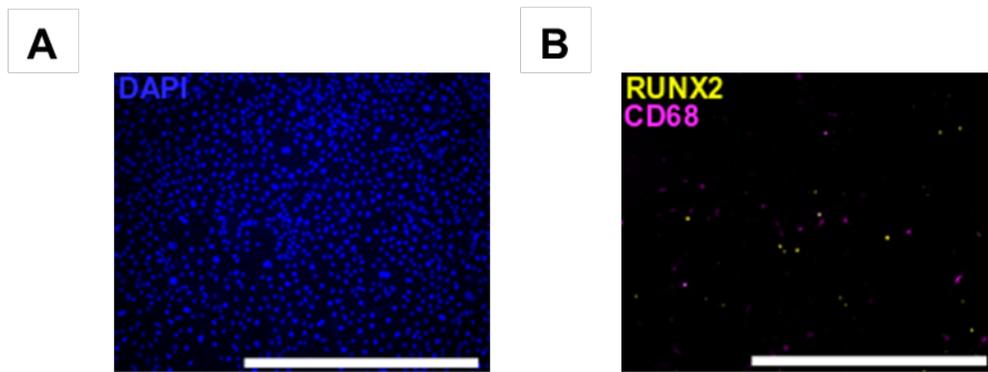
Figure 5.13. Immunofluorescence images used for image proximity analysis.
Immunofluorescent staining of aortic valve interstitial cell and macrophage co-culture for nuclei with DAPI (blue) (A) and for identification of osteogenic calcification of aortic valve interstitial cells (RUNX2, yellow) and macrophage (CD68, pink) (B). Reprinted, with permission, from Raddatz, et al.[28]
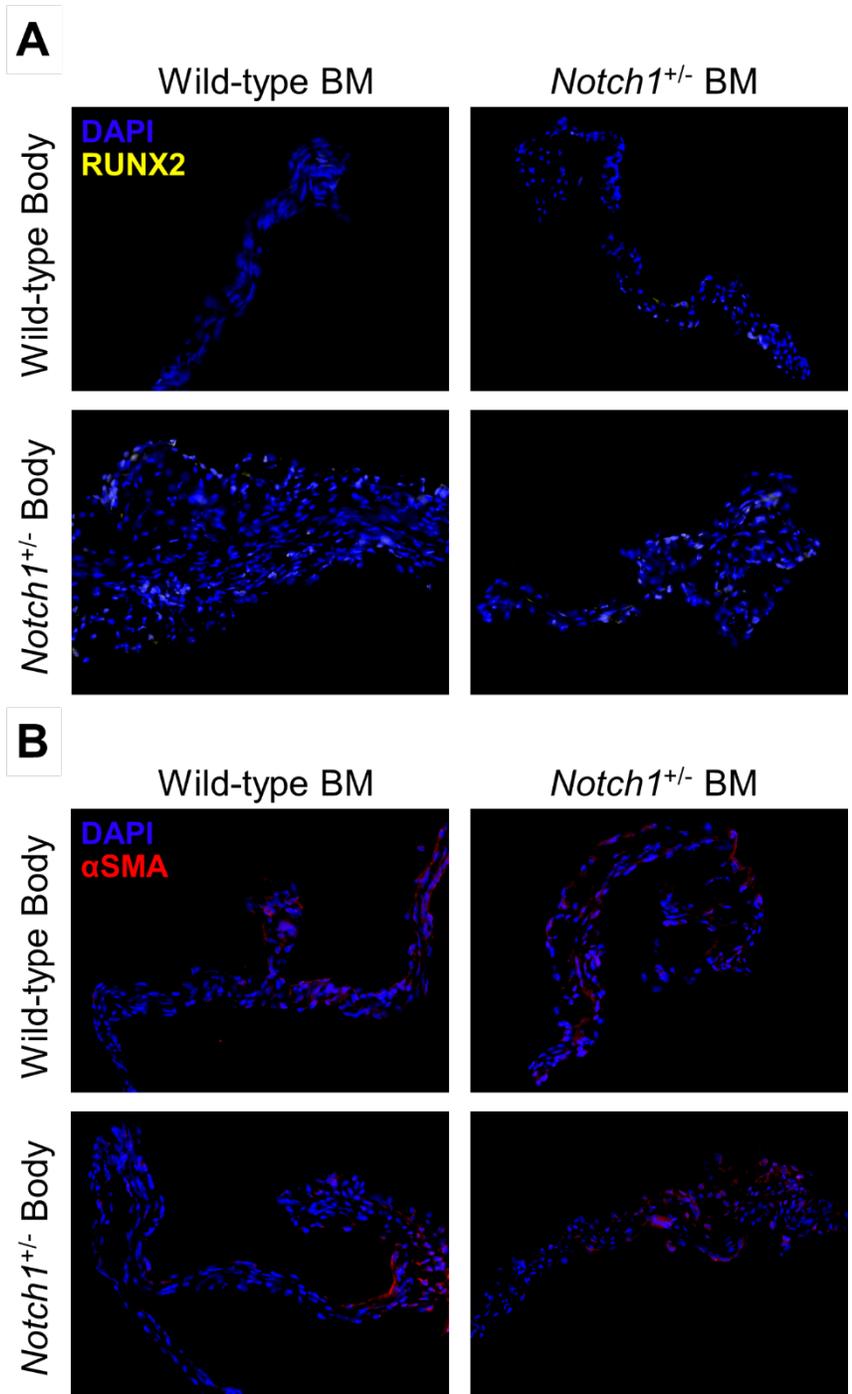
Figure 5.14. RUNX2 and αSMA expression in wild-type and *Notch1*^{+/-} murine valves.
Immunofluorescence staining of RUNX2 (A, yellow, white when overlapped with DAPI) and αSMA (B, red) in valves from wild-type (WT) and *Notch1*^{+/-} (N1^{+/-}) mice transplanted with WT or N1^{+/-} bone marrow (BM). Reprinted, with permission, from Raddatz, et al.[28]

Altered STAT3 Splicing is Present in Both In Vitro Calcification and Human Calcified Valves

In addition to canonical osteogenic signaling, we further hypothesized that STAT3-mediated inflammation played a role in RUNX2 activation based on previous studies in CAVD[152] and the role of STAT3 in other fibrotic inflammatory diseases.[21,129,136] AVICs cultured with macrophages had no increase in STAT3 phosphorylation or total STAT3 but did show a marked decrease in STAT3β expression (Figure 5.15A-E). Raw Western blot images are included in Appendix D. STAT3β is an alternative splice product of the STAT3 gene that inhibits canonical STAT3 signaling mediated through STAT3α.[171,251] RT-qPCR of STAT3 transcriptional targets *Icam1* and *Vegfa* confirmed an increase in STAT3 activity (Figure 5.15F). *Adar1* transcription increased with decreasing expression of STAT3β, opposing a previously proposed mechanism for altered STAT3 splicing (Figure 5.16).[252] Notably, STAT3 splicing was not impacted by interferons-α or -γ (Figure 5.17), which can induce *Adar1* activity.[253] To assess the role of STAT3β as an anti-calcification signaling molecule in human disease, excised AVs from patients undergoing AVR were analyzed. Leaflet tissue involved in disease (calcified) had decreased STAT3β expression and increased RUNX2 expression compared to adjacent uninvolved tissue (non-calcified) from the same patients (Figure 5.15G, H). Across all samples, RUNX2 expression negatively correlated with the STAT3β fraction (Figure 5.15I). Raw Western blot images are included in Appendix D.

Two STAT3 blockade strategies were assessed for efficacy in mitigating calcification. First, AVICs were treated with Stattic, a STAT3 phosphorylation inhibitor, and assayed for cellular stiffness and *Runx2* transcription. Stattic treatment decreased cellular stiffness but increased *Runx2* transcription in monoculture (Figure 5.18). Separately, STAT3α and -β plasmids were used to artificially manipulate STAT3 splicing (Figure 5.15J, K). Such transfections had no effect on calcification-associated transcripts in monoculture AVICs, but STAT3α overexpression increased cellular stiffness (Figure 5.15L). In the coculture model, STAT3β overexpression rescued *Runx2* transcription (Figure 5.15M).

87
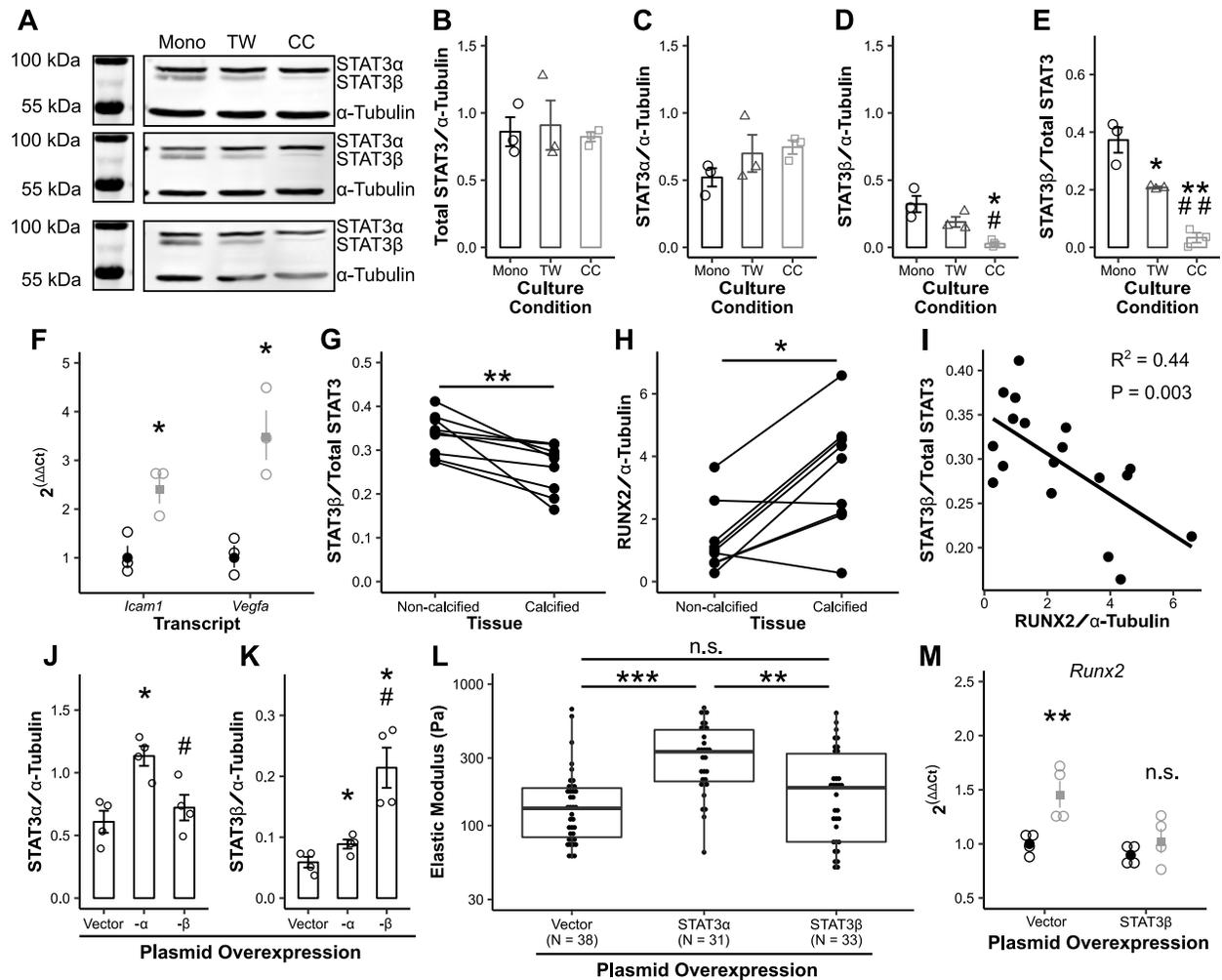
Figure 5.15. Macrophages promote osteogenic calcification of aortic valve interstitial cells and alter STAT3 splicing.
Overall STAT3 expression (A, B), STAT3α expression (C), STAT3β expression (D, E), and expression of STAT3-associated transcripts (F) across 3 biological coculture replicates (black = monoculture [Mono], gray = Transwell [TW], light gray = coculture [CC]). STAT3β and RUNX2 expression was assayed by Western blot in human aortic valves divided into calcified and non-calcified tissue (G-I, N = 9). Plasmid overexpression of STAT3α and β was performed (J, K, N = 4), and cellular stiffness measured by micropipette (L). Overexpression of STAT3β was performed prior to coculture and cocultures were assayed for *Runx2* transcription (M, N = 4). Bars and dot plots represent mean ± s.e.m. Boxplots represent 25th, 50th, and 75th percentiles. Data were analyzed by one-way ANOVA followed by two-tailed *t* tests with Holm-Sidak corrections on densitometry data (B-E, J, K) or untransformed ΔCt values (F, M); paired Mann Whitney *U* tests (G, H); linear regression (I); or Kruskal-Wallis followed by Mann Whitney *U* tests with Holm-Sidak corrections (L). *P < 0.05, **P < 0.01, ***P < 0.001 from monoculture AVICs (D-F, M), non-calcified aortic valve tissue (G, H) or vector control (J, K); #P < 0.05, ##P < 0.01 from Transwell AVICs (D-E) or STAT3α transfection (J, K). N = biological replicates (B-K, M) or tests of individual cells across 3 biological replicates in 2 independent experiments (L). Reprinted, with permission, from Raddatz, et al.[28]
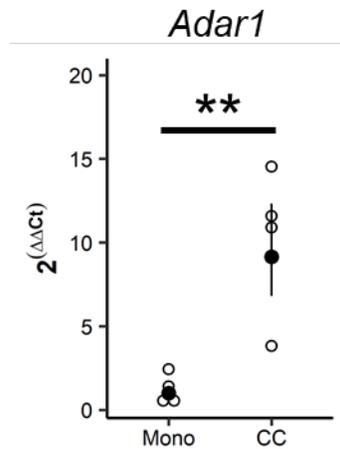
Figure 5.16. *Adar1* transcription in cocultured AVICs.
Coculture of AVICs with macrophages increases transcription of *Adar1*. Summary data represent the mean ± s.e.m. **P < 0.01 by two-tailed *t* test. Reprinted, with permission, from Raddatz, et al.[28]
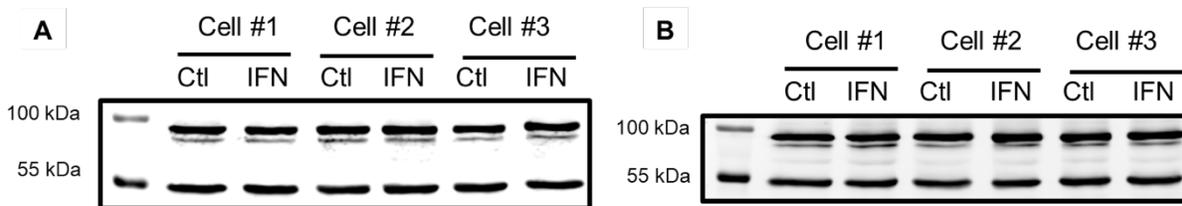
Figure 5.17. STAT3 splicing in AVICs exposed to interferons.
Culture of AVICs with either interferon (IFN) -alpha (A) or -gamma (B) does not affect STAT3 splicing. STAT3α is stained at ~88 kDa with STAT3β just below. Loading control is α-Tubulin stained at ~50 kDa. Reprinted, with permission, from Raddatz, et al.[28]
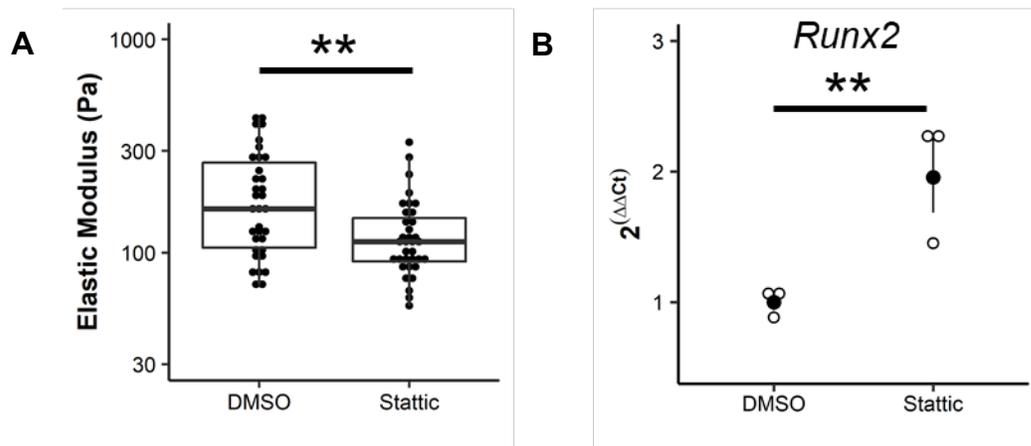
Figure 5.18. Stattic treatment of AVICs.
Treatment with 10 µM Stattic for two hours decreases cellular stiffness (A) but increases *Runx2* transcription measured after 10 additional hours in complete DMEM media (B). Boxplots display the 25th, 50th, and 75th percentiles. Summary data represent the mean ± s.e.m. (B). **P < 0.01 by Mann Whitney *U* test (A) or two-tailed *t* test on untransformed ΔCt values (B). Reprinted, with permission, from Raddatz, et al.[28]

Discussion

   While the cardiovascular immunology field has developed at a rapid pace, the role of immune cells in CAVD has remained unclear.[29] Here, we have focused on macrophages, which make up the majority of hematopoietic cells in both diseased human and healthy murine valves.[74,77] We have shown that $Notch1^{+/-}$ AVICs promote macrophage maturation and infiltration, and that macrophages promote AVIC calcification and alter STAT3 splicing. This outlines a novel inflammatory mechanism for CAVD (Figure 5.19).
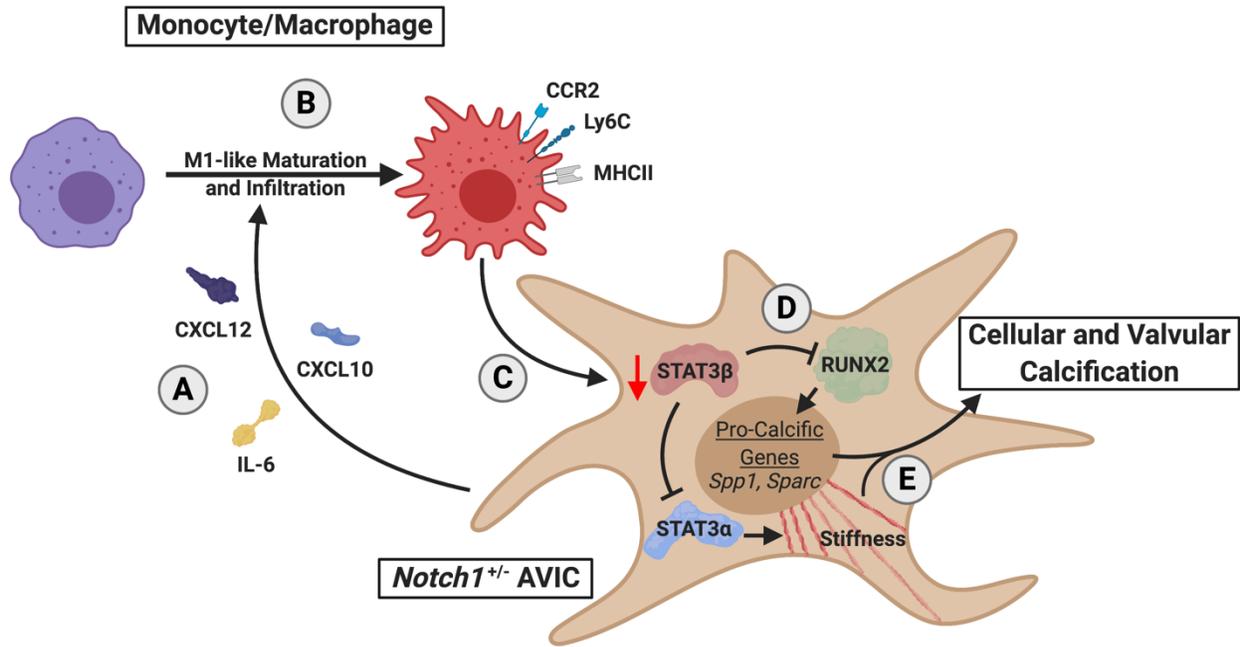
Figure 5.19. Proposed mechanism for macrophage-associated calcification in *Notch1*^{+/-} calcific aortic valve disease.

Notch1^{+/-} aortic valve interstitial cells (AVICs) secrete pro-inflammatory factors (A) leading to increased macrophage infiltration and maturation to an M1-like phenotype (B). These infiltrating macrophages alter STAT3 splice products to decrease STAT3β (C). Decrease of STAT3β removes inhibition of STAT3α and RUNX2 (D), promoting cellular stiffening and expression of osteogenic transcripts, respectively, and leading to valvular calcification (E). Reprinted, with permission, from Raddatz, et al.[28]

First, we used flow cytometry to show that the *Notch1*^{+/-} model has an increased myeloid compartment in the AV with increased CX3CR1 and MHCII positivity prior to disease progression. This aligns with previous data that murine aging and human disease correlate with proinflammatory maturation,[74,79,254] and that proinflammatory phenotypes themselves promote cellular calcification.[79,255] This suggested that perhaps differences in macrophage phenotype at baseline in *Notch1*^{+/-} mice are driving AV phenotypes. In addition, NOTCH1 is known to inhibit myeloid cell maturation, reflected in our data by an increased myeloid compartment in the *Notch1*^{+/-} valve.[239,240] Together, these data strengthened our hypothesis that altered hematopoietic cells drive disease in the *Notch1*^{+/-} model. However, bone marrow transplant experiments show that *Notch1*^{+/-} AV cells promote macrophage infiltration regardless of macrophage genotype. Contrary to our hypothesis, it seems that hematopoietic cells play their role in response to altered valve cell phenotypes. Independent of bone marrow genotype, *Notch1*^{+/-} mice had increased infiltration of MHCII[+] macrophages. Thus, *Notch1*^{+/-} valve cells are likely the instigating force behind valve pathology by both driving traditional disease markers and recruiting hematopoietic cells that then promote disease.

We built off of these findings with *in vitro* studies to explore how *Notch1*^{+/-} AVICs alter macrophage phenotypes and infiltration. Conditioned media from *Notch1*^{+/-} AVICs promotes increased migration and proinflammatory maturation of WT macrophages, relative to media from WT AVICs. Reinforcing the importance of *Notch1* haploinsufficiency in AVICs specifically, *Notch1*^{+/-} macrophages responded similarly. Notably, the proinflammatory phenotype induced *in vitro* is characterized by Ly6C and CCR2 positivity and no change in MHCII, whereas the *in vivo* data instead showed an increase in MHCII[+] macrophages but no change in Ly6C or CCR2. It is possible that this difference is due to the timelines involved. High Ly6C expression defines inflammatory monocytes and macrophages,[256,257] and CCR2 is necessary for recruitment of such Ly6C^{hi} monocytes.[258,259] Thus, the roles of Ly6C and CCR2 are in the recruitment and egress of monocytes and macrophages, but expression is variable and can decrease after

extravasation and tissue residency.[260,261] Alternatively, development of MHCII expression occurs after macrophage extravasation and allows for antigen presentation and generation of an adaptive immune response.[260,262] This would explain the observation of increased MHCII expression in macrophages within murine valves.

Cytokine microarrays on AVIC secreted media and immunofluorescence of murine AVs confirmed an increase in factors that induce migration and proinflammatory maturation. Indeed, NOTCH1 signaling has previously been shown to inhibit NF-κB activity and inflammatory cytokine production.[263,264] Together, these *in vivo* and *in vitro* phenomena provide a mechanism for macrophage involvement in NOTCH1-associated CAVD. They also highlight an additional lens for the interpretation of transcriptomic and proteomic datasets like that reported by Schlotter, et al.[65] Our results contribute to the body of literature suggesting that the effects of these secreted factors on immune cell recruitment and activation may also play a significant role in CAVD pathophysiology.

Our remaining studies focused on how macrophages alter AVIC phenotypes. We utilized a Transwell model to show that not only does the macrophage secretome promote calcification, but that physical interaction increases this effect. This is perhaps due to a macrophage-to-AVIC signal, but considering the findings that AVICs promote macrophage activation, it is also possible that physical interactions with AVICs can induce a further activated macrophage state and secretion of pro-calcification cytokines. It has also been suggested that extracellular vesicles may mediate cardiovascular calcification, and macrophage-derived vesicles may play a similar role here.[265,266] Unintuitively, macrophages promoted osteogenic calcification and not dystrophic calcification, which is characterized by cytokine production and myofibroblast transition. To test the hypothesis that myofibroblast transition was not increased *in toto*, but that myofibroblast activation was occurring closer to macrophages, we developed an image analysis algorithm. The results instead confirmed the above findings: αSMA+ myofibroblasts were normally distributed around their expected distance, while RUNX2+ osteoblast-like cells were

significantly closer to macrophages than expected. Finally, we stained AVs from bone marrow transplanted WT and *Notch1*^{+/-} mice for these same markers, and saw an increase in RUNX2 alone in the mice with increased macrophage recruitment. Thus, we show–both *in vitro* and *in vivo*–that increased exposure to macrophages is associated with osteogenic and not dystrophic calcification.

We then tested the hypothesis that STAT3 was mediating the connection between macrophage-secreted factors and RUNX2 expression. We observed a drastic shift in STAT3 splicing, resulting in a decrease in the inhibitory STAT3β splice product and an increase in the canonical STAT3α splice product. We confirmed an associated increase in canonical STAT3 signaling as measured through increased *Vegfa* and *Icam1* transcription–two signaling markers previously described in CAVD.[267,268] These phenomena translated to human AVs. STAT3β decreases in calcified regions of diseased AVs and negatively correlates with RUNX2 expression. We then used overexpression models to manipulate STAT3 splicing directly. In AVIC monoculture, manipulation of STAT3 splicing ratios altered cellular stiffness, a disease marker,[156] and in coculture this manipulation mitigated increased RUNX2 transcription.

We attempted to understand the mechanism of STAT3β rescue by blocking STAT3 activity with Stattic, a STAT3 phosphorylation inhibitor. Stattic treatment decreased cellular stiffness but increased RUNX2 expression. This leads to the conclusion that STAT3β is functioning to inhibit calcification through its own unique characteristics, perhaps requiring phosphorylation, rather than solely through an auto-inhibitory function against canonical STAT3α signaling. The ability of STAT3β to bind RUNX2 and inhibit its function as a transcription factor may be a key step in its calcification-mitigating capabilities shown here.[169]

Limitations

We have used primarily murine data throughout this manuscript. This has allowed us both to study the *Notch1*^{+/-} CAVD model, and to use coculture models with syngeneic

macrophages. Our *in vitro* models also focused on AVICs and not aortic valve endothelial cells. It is possible that *Notch1* haploinsufficiency may similarly contribute to macrophage recruitment through endothelial cell phenotypes. Second, it is possible in this murine model that there are resident hematopoietic progenitor cells in the AV that have persisted through irradiation and proliferated. However, literature in this mouse model has shown that all hematopoietic cells in the valve are perpetually recruited, rather than existing as resident cells,[75] and we have used a high radiation dose to minimize this risk. The murine model of CAVD used here is subject to relatively large variance, making some studies underpowered for phenotype detection by echocardiography. Thus, we have focused on quantitative histological and immunofluorescence methods that we believe capture with integrity the extent of disease in mice.

Conclusions

Herein, we report heightened macrophage infiltration and maturation in NOTCH1-associated CAVD driven by altered cytokine secretion of AVICs. This increased interaction between macrophages and AVICs promotes AVIC calcification and altered STAT3 splicing. Altered STAT3 splicing is found in calcified human AVs, and splicing manipulation opposes macrophage-induced calcification. These findings suggest that cellular inflammation and the STAT3 axis may play a targetable role in CAVD.

Chapter 6: Severe Aortic Stenosis in Male and Female Patients

Adapted in part from:

Raddatz MA, Gonzales HM, Farber-Eger E, Wells QS, Lindman BR, Merryman WD. Severe Aortic
Stenosis in Male and Female Patients: An Analysis of Clinical Echocardiography
Reports. In preparation.

Introduction

Aortic stenosis (AS) accounts for approximately 15,000 deaths in North America each

year, and the only effective treatment is surgical or transcatheter aortic valve replacement

(AVR).[1] Currently, AVR is recommended in patients with severe, symptomatic AS and in some

cases in those with severe, asymptomatic AS.[202] Determination of AS severity relies primarily on

the hemodynamic indices of peak jet velocity (V_{max}) or mean transvalvular gradient across the

aortic valve, and secondarily on decreased aortic valve area (AVA).[269] Commonly, patients are

considered to have severe AS when they meet both the AVA criteria (≤ 1 cm^2) and

hemodynamic criteria ($V_{max} \geq 4$ m/s or mean gradient ≥ 40 mmHg).[202] However, the guidelines

also indicate that patients with a V_{max} 3.0 – 3.9 m/s and AVA ≤ 1 cm^2 ("discordant AS") may

have severe AS if certain criteria apply.[202] A number of prior studies have demonstrated that

such a discordance between these indices is common and suggested that patients with

discordant AS would see a survival benefit from AVR.[203–205,270–272] Nonetheless, this discordance

can yield uncertainty regarding the severity of AS, which influences clinical management.[203,270]

Herein, using echocardiographic data obtained in clinical practice, we evaluated how

these indices of severe AS ($V_{max} \geq 4$ m/s and AVA ≤ 1.0 cm^2, both individually and together)

influence the proportion of patients who may be categorized as having severe AS. For each of

these groups potentially categorized as having severe AS, we evaluated how often the AS was

qualitatively described as "severe" in the clinical echocardiographic report. We were particularly interested in the relationship between sex and categorization of AS severity.

Methods

Clinical transthoracic echocardiogram reports from December 1, 2014 to October 30, 2017 were extracted from the Synthetic Derivative, a de-identified mirror of the electronic health record at Vanderbilt University Medical Center,[273] using previously described approaches that include regular expressions and natural language processing.[274,275] For each patient, all instances of echocardiographic evaluation were compiled. The report with the smallest AVA calculated by the velocity time integral (VTI) continuity equation was identified, and all data were extracted from this report. Patients with AVA ≤ 1.2 cm^2 and V_{max} ≥ 3 m/s were analyzed to include the spectrum of severe AS disease phenotypes. Patients with a severe V_{max} may have AVA > 1 cm^2 in cases of aortic regurgitation, leading to our 1.2 cm^2 criterion, and the AHA/ACC guidelines specifically state that patients with AVA ≤ 1 cm^2 but > 0.8 cm^2 should have a V_{max} ≥ 3 m/s to be considered severe, thus forming the inclusion criteria for our study.[202]

Patient records with either a procedural code for AVR prior to the echocardiography date or an ICD9/10 code for obstructive cardiomyopathy at any time were excluded. All charts with no AS characterization identified after natural language processing were reviewed manually. At the time of echocardiography, LVOT diameter and Doppler tracings were made by a sonographer and confirmed or re-measured by the echocardiographer interpreting the study. The echocardiogram was the only basis for severity characterization. Severity is stratified between "mild", "moderate", and "severe," with combinations commonly used. No patient was analyzed twice, and reports were not combined. Records missing data were excluded.

Echocardiographic metrics were compared between males and female patients using Mann-Whitney *U* tests. Binned data were compared using χ^2 tests. All statistical analysis was done using the statistical programming language R, version 3.5.2. Use of the Synthetic

Derivative is classified as nonhuman research by Vanderbilt University's institutional review board, and approval was given for this study (IRB #180320). The data used in this study is available to others for replication of our findings or further analyses and can be obtained by contacting the corresponding author.

Patient and Public Involvement

We did not directly include PPI in this study, but community representatives are involved in oversight of the database used in the study (the Synthetic Derivative) through the Vanderbilt Institute for Clinical and Translational Research.

Results

Among 807 patients (44% female) who had a recorded AVA ≤ 1.2 cm^2 and V_{max} ≥ 3 m/s, the median AVA was 0.86 cm^2 (interquartile range: 0.70 – 1.00) and median V_{max} was 3.87 m/s (interquartile range: 3.41 – 4.38) (Table 6.1). Based on the V_{max} ≥ 4 m/s criterion, 45.6% of the cohort was classified as having severe AS (Table 6.2). In contrast, based on the AVA ≤ 1.0 cm^2 criterion, 75.8% was classified as having severe AS. This represents a relative 66.3% increase in the proportion of patients that would be classified as having severe AS when using the AVA criteria instead of the V_{max} criteria, and would particularly increase the proportion of female patients considered to have severe AS (44.9% vs. 96.7% relative increase in the proportion of males vs. female patients) (Table 6.2). Using an indexed AVA (AVAi) cut-off of ≤ 0.6 cm^2/m^2, 94.1% of the cohort would be classified as having severe AS, including 99.0% of those with an AVA ≤ 1.0 cm^2.

Table 6.1. Cohort characteristics.

	All (807)	Female (355)	Male (452)	P value
Age, y	73.7 [65.7, 80.9]	75.1 [67.0, 82.5]	72.9 [64.9, 79.9]	0.03
BMI, kg/m^2	28.8 [25.3, 33.8]	29.3 [24.8, 35.8]	28.4 [25.6, 32.6]	0.04
AVA, cm^2	0.86 [0.70, 1.00]	0.80 [0.65, 0.94]	0.90 [0.75, 1.03]	<.001
AVAi, cm^2/m^2	0.43 [0.36, 0.51]	0.44 [0.36, 0.52]	0.43 [0.36, 0.50]	0.09
V_{max}, m/s	3.87 [3.41, 4.38]	3.80 [3.37, 4.30]	3.92 [3.45, 4.41]	0.02
Mean Gradient, mmHg	35.0 [26.7, 45.3]	33.0 [26.0, 43.1]	36.0 [27.5, 46.0]	0.01
Peak Gradient, mmHg	59.9 [46.7, 76.9]	57.8 [45.3, 74.0]	61.2 [47.7, 78.3]	0.03
DI	0.24 [0.20, 0.29]	0.26 [0.21, 0.30]	0.23 [0.20, 0.28]	<0.001
Ejection Fraction, %	55 [55, 63]	58 [55, 63]	55 [55, 60]	<0.001
SV, mL	78.1 [64.6, 90.4]	73.1 [58.9, 84.6]	81.8 [70.2, 94.1]	<0.001
Indexed SV, mL/m^2	39.7 [32.9, 46.3]	39.9 [33.2, 47.3]	39.4 [32.8, 45.6]	0.22
LVOT Diameter, cm	2.10 [2.00, 2.29]	2.00 [1.90, 2.00]	2.20 [2.10, 2.30]	<0.001
BSA, m^2	1.97 [1.77, 2.15]	1.78 [1.64, 1.96]	2.08 [1.93, 2.23]	<0.001

Data presented as median [25th percentile, 75th percentile]. 11 female and 16 male patients did not have reliable BMIs recorded, giving N = 344 and 436 for this metric, respectively.

Abbreviations: AVA, aortic valve area; AVAi, indexed aortic valve area; BMI, body mass index; BSA, body surface area; DI, dimensionless index; LVOT, left ventricle outflow tract; SV, stroke volume, V_{max}, peak jet velocity

Table 6.2. Aortic valve area and peak jet velocity as indices of severe aortic stenosis.

			AVA ≤ 1		
	Total	**$V_{max} \geq 4$**	**All**	**$V_{max} \geq 4$**	**$V_{max} < 4$**
Total (% of cohort)	807	368 (45.6%)	612 (75.8%)	323 (40.0%)	289 (35.8%)
Male (% of male pts)	452	216 (47.8%)	313 (69.2%)	180 (39.8%)	133 (29.4%)
Female (% of female pts)	355	152 (42.8%)	299 (84.2%)	143 (40.3%)	156 (43.9%)
% Female	44.0%	41.3%	48.9%	44.3%	54.0%
Severity					
none noted	4 (0.5%)	0 (0.0%)	2 (0.3%)	0 (0.0%)	2 (0.7%)
mild	10 (1.2%)	0 (0.0%)	5 (0.8%)	0 (0.0%)	5 (1.7%)
mild-moderate	17 (2.1%)	0 (0.0%)	8 (1.3%)	0 (0.0%)	8 (2.8%)
moderate	181 (22.4%)	10 (2.7%)	71 (11.6%)	4 (1.2%)	67 (23.2%)
moderate-severe	140 (17.3%)	28 (7.6%)	100 (16.3%)	16 (5.0%)	84 (29.1%)
severe	455 (56.4%)	326 (88.6%)	426 (69.6%)	303 (93.8%)	123 (42.6%)

Severity data presented as number (percent). Abbreviations: AVA = aortic valve area, V_{max} = peak jet velocity

101

Patients with discordant indices of severe AS (V_{max} < 4 m/s and AVA ≤ 1 cm^2) made up

35.8% of the study cohort and those with concordant indices of severe AS (Vmax ≥ 4 m/s and

AVA ≤ 1 cm^2) comprised 40.0%. Compared to those with concordant indices, those with

discordant indices were more likely to be female (54.0% vs 44.3%, p = .02) and less likely to

have their AS characterized as "severe" on the clinical echocardiography report (42.6% vs

93.8%, p < .001) (Table 6.2). This difference persisted when expanding the "severe" group to

include those characterized as "moderate-severe" (71.6% vs 98.8%, p < .001). When indexed

AVA ≤ 0.6 cm^2/m^2 replaced AVA ≤ 1 cm^2, patients with discordant indices were again less often

characterized as "severe" on the echocardiography report than those with concordant indices

(32.2% vs 90.3%, p < .001). Figure 6.1A shows data plotted by V_{max} and AVA, color coded by

the AS characterization on the echocardiography report. The percentages reported as severe

for each quadrant defined by an AVA of 1.0 cm^2 and V_{max} of 4 m/s are also shown. In Figure

6.1B, data is plotted and color coded by sex; each quadrant shows the proportion of the

population represented and the percentage female.
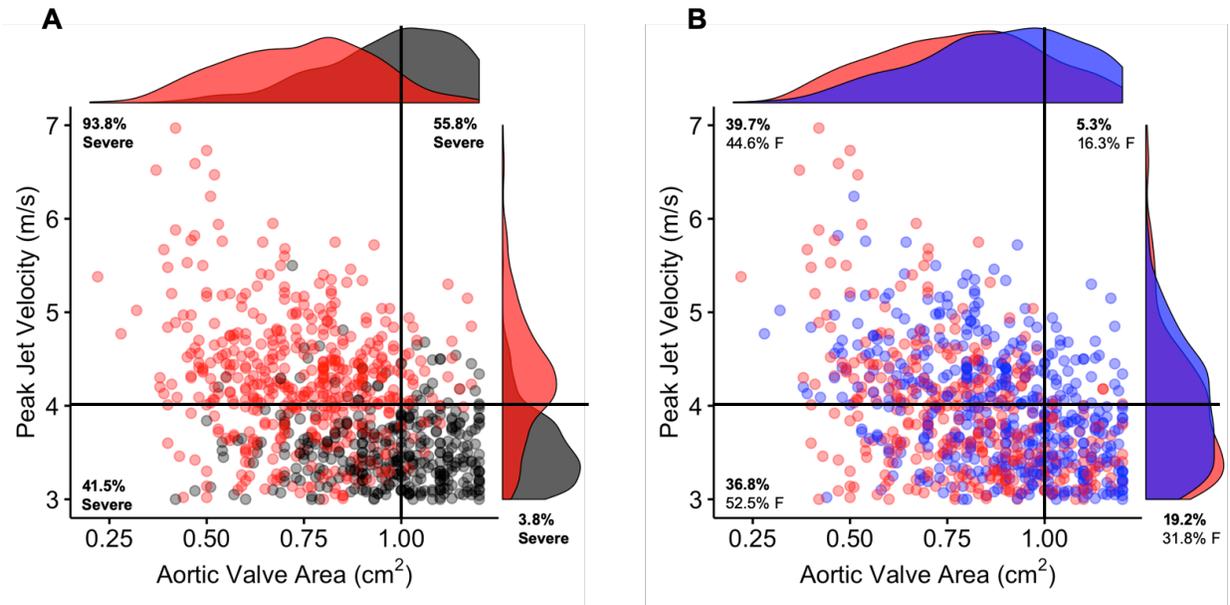
Figure 6.1. The relationships of recorded severity and sex with aortic valve area and peak jet velocity.
(A) All patients in the cohort are plotted in both one and two dimensions by aortic valve area and peak jet velocity, and color-coded by clinician characterization as severe (red) or non-severe (gray). The percentage of patients characterized as severe is annotated for each quadrant. (B) This same cohort is plotted colored by female (red) and male (blue) sex. The percentage of the cohort in each quadrant is noted, as well as the percentage of each quadrant that is comprised of female patients.

We further investigated these trends by dividing patients with discordant AS into stages as defined by AHA/ACC recommendations (Table 6.3).[202] Among those with AVA $\leq$ 1.0 cm^2, indexed AVA $\leq$ 0.6 cm^2, and Vmax < 4 m/s, patients with EF < 50% (potentially stage D2 patients depending on the results of a dobutamine echocardiogram) comprised 7.3% of the total study cohort (20.8% of those with discordant indices) and were infrequently female (27.1%); patients with EF $\geq$ 50% comprised 27.8% of the study cohort (79.2% of those with discordant indices). Among this latter group, those with paradoxical low flow, low gradient AS (stroke volume index <35 ml/m^2, stage D3 by echocardiography) represented 11.3% of the study cohort (32.2% of those with discordant indices), were disproportionately female (61.5% vs 41.8%, p < .001), and were characterized as having "severe" AS only 49.5% of the time.

Table 6.3. Left ventricle metrics and characterization of echocardiography in patients with discordant aortic stenosis.

	AVA ≤ 1, AVAi ≤ 0.6, V_{max} < 4				
	All	EF < 50	EF ≥ 50%		
			All	SVi < 35	SVi ≥ 35
Total **(% of cohort)**	283 (35.1%)	59 (7.3%)	224 (27.8%)	91 (11.3%)	133 (16.5%)
Male **(% of male pts)**	133 (29.4%)	43 (9.5%)	90 (19.9%)	35 (7.7%)	55 (12.2%)
Female **(% of female pts)**	150 (42.2%)	16 (4.5%)	134 (37.7%)	56 (15.8%)	78 (22.0%)
% Female	53.0%	27.1%	59.8%	61.5%	58.6%
Severity grading					
none	1 (0.4%)	0 (0.0%)	1 (0.4%)	1 (1.1%)	0 (0.0%)
mild	5 (1.8%)	0 (0.0%)	5 (2.2%)	3 (3.2%)	2 (1.5%)
mild-moderate	8 (2.8%)	0 (0.0%)	8 (3.6%)	4 (4.4%)	4 (3.0%)
moderate	65 (23.0%)	10 (16.9%)	55 (24.6%)	21 (23.1%)	34 (25.6%)
moderate-severe	81 (28.6%)	11 (18.6%)	70 (31.3%)	17 (18.7%)	53 (39.8%)
severe	123 (43.5%)	38 (64.4%)	85 (37.9%)	45 (49.5%)	40 (30.1%)

Severity data reported as number (percent).
Abbreviations: AVA = aortic valve area, AVAi = indexed aortic valve area, EF = ejection fraction, SVi = indexed stroke volume, V_{max} = aortic valve peak jet velocity
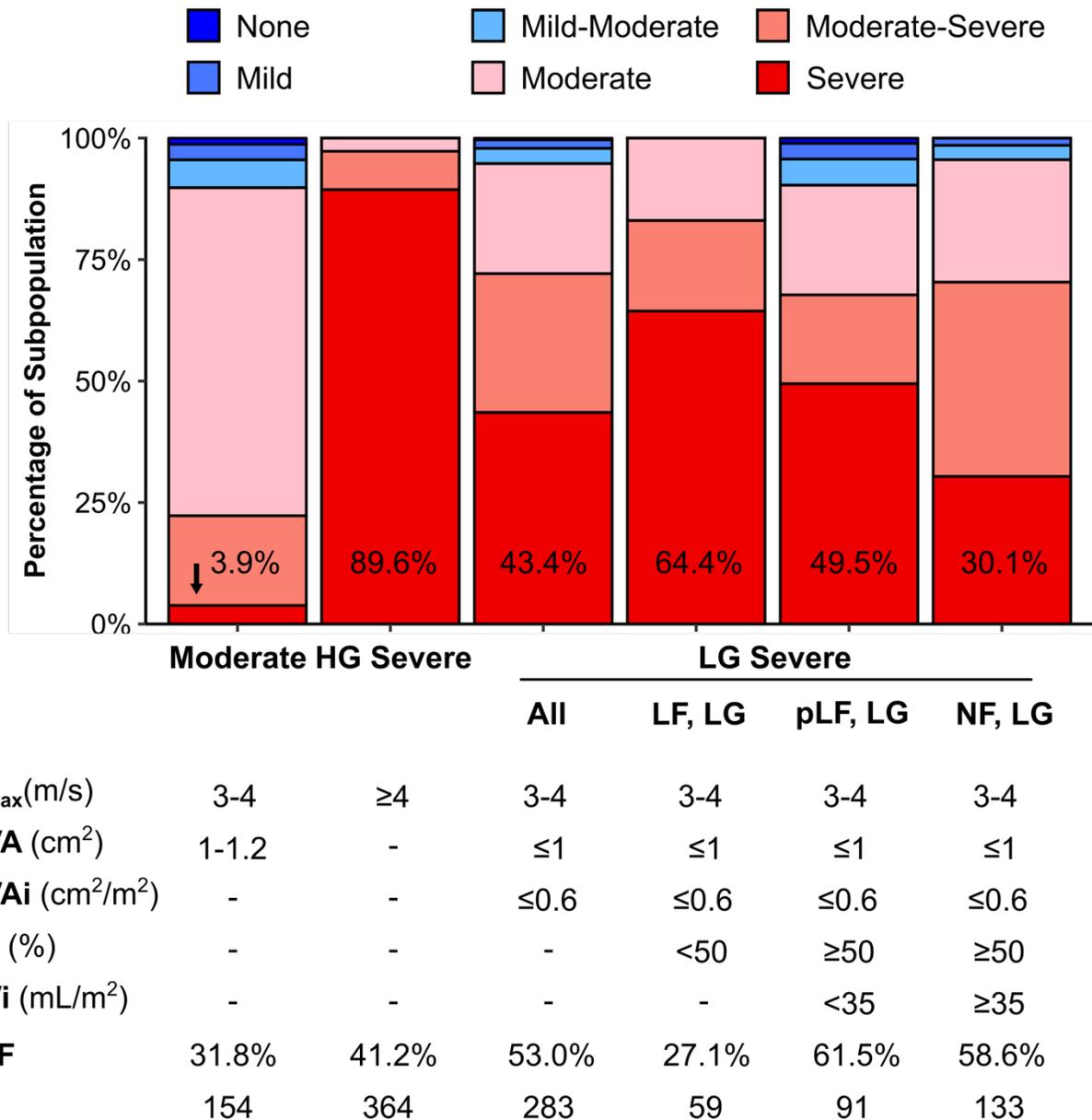
Figure 6.2. Severity characterizations for subtypes of severe aortic stenosis.
All patients in the study were categorized by echocardiographic assessment criteria, and clinician characterization was plotted. Percent categorized as severe is annotated in the chart. HG = high gradient, LF = low flow, LG = low gradient, p = paradoxical, V_{max} = peak jet velocity, AVA = aortic valve area, AVAi = indexed aortic valve area, EF = ejection fraction, SVi = indexed stroke volume, F = female

Discussion

Using data from clinical echocardiography reports of patients with AVA ≤ 1.2 cm^2 and V_{max} ≥ 3 m/s, we found that shifting from a specific definition of severe AS (V_{max} ≥ 4 m/s) to a sensitive definition (AVA ≤ 1 cm^2) resulted in a 66% relative increase in the number of patients with potentially severe AS, with a 97% relative increase for female patients. This observed increase is similar to previously reported data,[271,272] but also provides quantitative insight into how this move would affect female patients in particular. Further, while patients with concordant indices of AS severity by echocardiography are usually characterized as having severe AS (94% of the time in our study), discordant indices are common (observed almost as commonly as concordant indices among those with AVA ≤ 1 cm^2), disproportionately observed in female patients, and yield a characterization of "severe" AS a minority of the time (43%).

To our knowledge, this is the first study to demonstrate how echocardiographic data are integrated by an echocardiographer when reporting the overall AS severity in a clinical report. This has important implications, as those who receive and read an echocardiography report (particularly if they do not have expertise in valve disease or reading raw echocardiography images) may not be inclined to refer a patient with anything less than "severe AS" for AVR consideration. In this sense, the summary statement of AS severity on the clinical echocardiography report often drives subsequent clinician behavior.

With this in mind, the fact that less than half of the patients with discordant AS— including less than half of those who meet the definition of paradoxical low flow, low gradient severe AS—are reported as having "severe AS" on the clinical echocardiography report is consequential. Multiple recent studies, albeit retrospective and non-randomized, report a survival advantage from AVR for those with AVA ≤ 1 cm^2 regardless of V_{max}.[204,205,270] Berthelot-Richer, et al. reported improved survival with AVR over medical therapy for those with V_{max} 3-4 m/s, transvalvular mean gradient 25-40 mmHg, and AVA ≤ 1 cm^{2},[205] and Dayan, et al. reported improved survival with AVR for the same group, even when assessing specifically the subgroup

with preserved stroke volume index (normal flow, low gradient AS).[204] Notably, these studies did

not include, for example, valve calcium scoring to clarify the severity of AS when indices were

discordant; they included the resting echocardiographic indices alone (as in our study). Thus,

regardless of additional testing or measures of ventricular performance, patients with these

discordant indices of AS severity seem to benefit from AVR. Because the guidelines only

recommend AVR for patients with "severe AS" and patients with discordant indices of AS

severity commonly are characterized as having less than severe AS on echocardiography

reports, this undoubtedly influences clinical management decisions and leads to less and later

referrals for AVR as prior studies have shown.[203,205,270,276]

This particularly affects female patients who were disproportionately represented among

those with discordant AS in our analysis. Indeed, female patients seem to suffer from

disproportionate delay of referral for AVR.[276] The prevalence of discordant AS in female patients

could be due to several factors including differences in valve calcification and flow. Previous

studies have shown that while AS is driven primarily by calcification in male patients, there is a

more dominant fibrotic component in female patients.[24] Between these, calcification was seen to

be associated with higher gradients.[24] Female patients also tend to have a lower stroke volume

than male patients, which is associated with lower transvalvular gradients.[277]

The frequent characterization of patients with discordant AS indices as having less than

severe AS is likely due to two primary reasons. First, it is likely influenced by the explicit

prioritization in the guidelines of V_{max} and transvalvular mean gradient over AVA in the

assessment of AS severity.[202,278,279] While updates in the guidelines have increasingly allowed

for sub-groups of patients to be classified as having severe AS despite a $V_{max} < 4$ m/s, the long-

standing paradigm of prioritizing V_{max} over AVA leads to clinicians reluctant to classify a patient

as having severe AS with $V_{max} < 4$ m/s. However, the rationale for prioritizing V_{max} over AVA in

the diagnosis of severe AS is based on small studies that did not examine hard clinical events

nor compare prompt AVR versus clinical surveillance at various V_{max} or AVA thresholds.[280,281]

Second, in cases of discordant measurements, additional testing with nitroprusside,[201] dobutamine,[198] or aortic valve calcium scoring are increasingly performed to clarify whether AS is severe.[199,200] Previous work has highlighted the need for such additional testing in discordant AS.[282] Knowing this, echocardiographers may be reluctant to over-call "severe AS" when they know these additional tests may help clarify the diagnosis. However, to readers of echocardiography reports who do not commonly care for patients with AS, the diagnosis of anything other than "severe AS" on the echocardiography report may simply be interpreted as a signal to "continue watching" that patient rather than to perform an adjunctive test to clarify the true severity of stenosis.

Systems level changes may be warranted to address these challenges, which likely have adverse clinical consequences. So as to not potentially delay referral for valve replacement in patients with discordant indices of AS severity, if the echocardiographer is not going to characterize discordant AS indices (AVA < 1 cm^2 and V_{max} < 4 m/s) as severe on the clinical report, then it may be appropriate to include the following on the report: "possibly severe AS, but additional evaluation or testing are needed." This would enable the echocardiographer to not "over-call" severe AS when they believe further testing is needed, but also help ensure that these patients with discordant indices are not passively watched but instead further evaluated and, as appropriate, referred for aortic valve replacement in a timely manner. In addition, quality improvement efforts in echocardiography laboratories could reinforce that a $V_{max} \geq$ 4 m/s is not required for the diagnosis of severe AS.

Limitations

In this cross-sectional study based solely on echocardiography data, we do not have information on clinical presentation, symptoms, referral to AVR, or long-term outcomes. Further, we do not have data from dobutamine echocardiograms or valve calcium scores from computed tomography studies. Our focus was on relating the hemodynamic indices of AS

obtained on an echocardiogram to how echocardiographers assimilate that information and

report a summative characterization of AS severity. Using the resting echocardiographic indices

alone is consistent with the fact that most of the studies on the relationship between AS severity

and outcomes simply rely on these resting echocardiographic hemodynamic indices (AVA, V_{max})

and not adjunctive information from stress testing or valve calcium scores. Finally, these data

were collected from a single academic medical center, which may not be representative of other

echocardiography laboratories.

Conclusions

The proportion of patients and relative percentage of female patients potentially

categorized as having severe AS is markedly influenced by the echocardiographic indices of

severe AS used. Clinical echocardiography reports usually characterize discordant indices of

AS severity, which are common and disproportionately observed in female patients, as less than

severe, which could have adverse clinical consequences. When discordant indices of AS

severity are encountered and characterization of AS severity is uncertain, notation in the clinical

echocardiography report of the need for additional evaluation or testing may minimize the

number of patients who experience a delay in referral for aortic valve replacement.

Chapter 7: Impact and Future Directions

Treatment of calcific aortic valve disease (CAVD) has changed rapidly in the last 20 years. The introduction of the transcatheter aortic valve replacement (TAVR) has increased accessibility to aortic valve replacement and altered the landscape of the CAVD scientific community dramatically. It is in this environment that this work was devised to answer and propose questions in the field. One such question made more significant by TAVR is the role of immune cells in CAVD, as they are present in both pre- and post-replacement stenosis of the aortic valve (AV). Medical therapy that may pair with TAVR would create a formidable two-pronged therapy for aortic stenosis (AS) patients. Considering the failure of other therapies for patients with AS, inflammation and immune signaling may be the best hope. The work in Chapters 3-5 of this thesis aims to amplify this hope and sits at the nexus of cardiovascular and immunological science. It is among a growing number of studies investigating inflammation in CAVD, and it is the first to utilize *in vivo* manipulations of hematopoietic cells in a murine model of CAVD.

This shift in basic science investigation is accompanied by new areas of investigation in the clinical space. Chief among these, driven by previous work in both the basic science and clinical realms, is understanding the various phenotypes of severe AS. This understanding would allow optimized delivery of TAVR therapy to populations who would most benefit. The work in Chapter 6 begins to describe how previous guidelines may impact cardiologists' approach to different AS phenotypes in male and female patients. It is the author's hope that continued work like this may add to the evidence for improved diagnostic algorithms in CAVD and AS, leading to improved care for female patients and all with "atypical" AS.

Impact

The greatest impacts from this work come at the intersections of disparate disciplines. First among these is the intersection of cardiology and immunology. Chapter 3 outlines the association of celecoxib with AV calcification, both *in vitro* and *in vivo*. These results and the opposite impact of dimethyl celecoxib, a celecoxib analog with no effect on cyclooxygenase-2 (COX-2), suggested that COX-2 may affect calcification. COX-2 is well described as a producer of prostaglandins, a class of proinflammatory molecules. This suggested that perhaps inflammation was mediating such an effect. Further studies by another group have shown that the impact of celecoxib on calcification is mediated by the presence of glucocorticoids.[283] Glucocorticoids are commonly known as anti-inflammatory molecules, but have a wide array of functions, and could possibly be functioning here to upregulated Toll-like receptor signaling.[284] Thus, these studies have already motivated additional work on the effect of inflammation on CAVD. In addition to the mechanistic studies, our finding that celecoxib is associated with AS in humans is an impactful clinical finding that warns against the use of celecoxib in patients with mild to moderate AS, or those who are otherwise at risk of progressing to severe AS.

Continuing further at the intersection of cardiology and immunology, the work herein on macrophages and STAT3 (signal transducer and activator of transcription 3) offers new ideas regarding the involvement of myeloid cells in CAVD and proposes a potential target molecule for this mechanism of calcification. First, the work in Chapter 4 highlights the potential for increased mechanical strain to drive STAT3-associated inflammation, similar to previous work in hypertension models.[129] These findings, in combination with previous work defining the role of STAT3 in fibrotic inflammation, helped to motivate some of the following studies in Chapter 5.

The published work in Chapter 5 adds to the growing body of literature mechanistically investigating hematopoietic cells and inflammation in CAVD. Informed by the role of NOTCH1 in immunological activation, we have used bone marrow transplants to identify the role of *Notch1* haploinsufficiency in CAVD. We found that haploinsufficiency in valve cells promotes

macrophage egress to the valve, and we further outlined the ensuing role of macrophages in promoting osteogenic calcification. While at baseline this adds to the field's understanding of the *Notch1*^{+/-} model of CAVD, it additionally offers more widely applicable insights into pathophysiology.

One such area of insight is in interpreting the commonly performed studies on circulating factors, such as that performed by Aguado, et al.[235] In this study, the authors assessed the role of serum factors in promoting AV calcification. Patient serum collected pre-TAVR promotes calcification of AV interstitial cells (AVICs), while serum collected post-TAVR promotes resolution of such calcification.[235] The findings in our study highlight the role of secreted factors in their impact on hematopoietic cells. It is possible that the serum collected by Aguado, et al. also could impact recruitment of monocytes to the calcifying AV. Some studies provide preliminary results that point in this direction: An, et al. found that IL-10 genetic polymorphisms were associated with valvular calcification.[162] IL-10 is commonly understood to oppose inflammatory recruitment and activation of macrophages.[285,286] Given the "congenital" nature of genetic polymorphisms, it is quite possible that decreased macrophage recruitment and inflammatory maturation over a lifetime resulted in less macrophage egress to the valve and less macrophage-induced osteogenic calcification—so much so that this mechanism underlies the protective effect of IL-10. Especially considering the lack of studies showing an effect of IL-10 on AV cells, this macrophage theory appears promising. This is just one example of applying the macrophage recruitment paradigm to existing literature. In Chapter 6 we have shown that this mechanism promotes *Notch1*^{+/-} AV disease, a common and translatable murine model of CAVD, and thus provided a model set of experiments for future work investigating this phenomenon.

In addition, we have performed some of the first work showing a role for STAT3 splicing in cardiovascular disease. STAT3β is known to be a self-regulatory splice variant of STAT3: both modulating canonical STAT3 activity and functioning uniquely and independently from

STAT3α.[169,171,287] Previous studies have identified that STAT3β is a tumor suppressor and pointed to a promising pathophysiological mechanism in cardiovascular disease.[170,288–292] This work for the first time outlines a role for macrophages in impacting STAT3 splicing, and reports an association of altered STAT3 splicing with AV calcification. This allows for conversion and reapplication of studies in cancer immunology to cardiovascular research. The nature of STAT3β as an alternative splice product makes it difficult to study, but its activity opposing STAT3 activation can inform improved interpretation of perplexing STAT3 data,[291,293] especially considering the complex and almost ubiquitous roles it can play in a wide array of cellular functions.[130]

Transitioning to clinical studies, the findings reported in Chapter 6 are the first to report the way echocardiographic reports of AS are read in practice. These data represent a crucial set of information that can guide future reform in the care of AS. We have shown that echocardiogram readers are hesitant to adjudicate AS with discordant metrics as "severe," even when the patients in question qualify explicitly for such a status by way of decreasing left ventricle function. Additionally, we highlight that this disproportionately impacts female patients, who are overrepresented in these "under-diagnosed" groups.

It is important to consider these sex-related findings in the context of sex differences in modern cardiovascular care. The most obvious example is myocardial infarction (MI). First, there was an identification that mortality after MI is higher in female patients.[294] This was then associated with a lack of delivery of optimal care to female patients; in 2019 a study estimated that in England and Wales, female patients with MI suffered over 8,000 deaths that would have been prevented if they had been given the same level of care as their male counterparts.[295,296] In the case of AS, the most important and impactful care that a patient can be prescribed is a referral for AVR; therefore, patient status at time of AVR reflects how far the disease was allowed to progress before clinicians thought it appropriate to refer for care. Fuchs, et al. report that female patients referred for AVR have a smaller AV area (AVA, both raw and indexed) and

a higher mean transvalvular gradient.[276] Female patients also more often reported symptoms associated with AS.[276]

Altogether, this suggests that AS in female patients often has progressed further prior to referral for appropriate care: similar to the findings in MI. In the case of MI, we have begun to understand that female patients are likely under-treated because they more often present with unique symptoms that aren't well-described in the literature than male patients.[297] Similarly, in AS we have shown that female patients are more likely to have discordance in the two major metrics of AS: AVA and peak jet velocity (V_{max}), and that patients in this group are less likely to be characterized as "severe" by echocardiogram readers. This hesitation undoubtedly leads to deferred referral for AVR like that described above. In the case of MI, there is an extensive push in the field to increase awareness of the "atypical" presentations seen more often in female patients. Crucially, this awareness will improve care for patients of all sexes and genders who present with "atypical" symptoms. In AS, we now know that patients with discordant metrics see benefit from AVR. [204,205,270] The data in this thesis clearly outlines a need for increased awareness of the severity of discordant AS, as improved care will better the lives of both female and male patients.

Future Directions

Although there is a vast array of studies that can be informed by the findings described here, there are a handful of approaches that are of priority following this data. The first area of focus is on the utility of STAT3 blockade as a therapeutic strategy in cardiovascular disease. Although STAT3 activation seems to have a pathological role in hypertension,[129] many studies have described the beneficial effect of STAT3 in the setting of MI and heart failure.[146,298,299] Reinforcing these bidirectional findings in CAVD, we found that STAT3 phosphorylation blockade with Stattic worsens some measures of AV cell calcification while improving others. Thus, it is unlikely that broad-spectrum STAT3 blockade will be a viable candidate for valvular or

cardiovascular therapies, as it is near impossible to separate these dual mechanisms. Alternatively, STAT3β provides a potential avenue for such a therapy. Although it is capable of negative regulation of STAT3α, it also shares some functions of STAT3α and carries out unique functions unrelated to STAT3α.[251,300–303] For example, STAT3β rescues the prenatal lethality associated with total STAT3 knockout.[251] However, STAT3β also shows cell-type specific activation,[301] unique roles in some inflammatory states,[302] and in some cases greater response to IL-6 than STAT3α.[303] All of these data point to STAT3β as a unique molecule that may allow for targeting of the pathological aspects of the STAT3 signaling pathway, while preserving some necessary STAT3 functions. Experiments manipulating STAT3 splicing in various mouse models of cardiovascular disease would shed light on the potential utility of this strategy. This strategy has proven promising in the study of atherosclerosis, where STAT3β-specific knockout significantly worsens disease in mice.[304] Unfortunately, long-term administration of agents that alter STAT3 splicing such as morpholinos—stable oligonucleotides that, in this application, interact with the STAT3 splice site—is likely cost-prohibitive in the aging model of CAVD, which takes 6 to 12 months to develop disease. Use of the STAT3β knockout animal described previously would be optimal if it can be obtained.[302,304] Otherwise, using morpholinos, exploration of STAT3 splicing in animal models of myocardial infarction or heart failure may be more useful as the disease models are much shorter, and necessary for eventual translation in any case as CAVD is commonly coincident with coronary artery disease or ventricular dysfunction in human patients. In order to pursue further investigation of STAT3 splicing in AS or any other disease, it will be important to understand its effects on cardiac function at large. In short, the first necessary steps would be assessing STAT3 splicing in murine models of cardiovascular currently used in the Merryman laboratory.

Nuclear factor kappa-light-chain-enhancer of activated B cells (NF-κB) signaling provides an additional area of follow-up for the studies in this thesis. Among other things, simply assaying for NF-κB phosphorylation and activity in the coculture model would be of interest. We

would expect phosphorylation and activity to increase in coculture with macrophages. Similarly, assaying for NF-κB changes in response to transient transfection with STAT3β would provide new information for how STAT3β might directly or indirectly, through inhibition of STAT3α, oppose inflammation driven by NF-κB, which is implicated in AV calcification. Known interactions between STAT3α and NF-κB provide a foundation for these future studies. For example, STAT3α is capable of binding to NF-κB and displacing IκB, a negative regulator of NF-κB, therefore promoting NF-κB translocation to the nucleus and subsequent activity.[305] This represents a mechanism of NF-κB promotion by IL-6 that could have particular relevance in CAVD. Multiple studies have found that STAT3α binds to NF-κB *in vivo*, serving to both promote and inhibit NF-κB activity,[305–307] and still others have shown that STAT3α can make posttranslational modifications to NF-κB, decreasing nuclear export and increasing its activity as a transcription factor.[308] It is possible that STAT3β is incapable of binding NF-κB in these promotional capacities, or otherwise opposes typical NF-κB activation by STAT3α. This would be an area of great interest as it could make the STAT3β finding even more widely relevant. Because NF-κB is broadly expressed and functional, targeting it would be near impossible in a chronic inflammatory disease like CAVD; however, if fine-tuning some amount of control with STAT3 splicing is an option, it could have vast therapeutic potential. Future studies in our laboratory should first assay p65 phosphorylation (a component of NF-κB activation) in AVICs exposed to macrophages and in AVICs transfected with STAT3 splice-product overexpression plasmids.

Separately, our results concerning macrophage recruitment to the AV highlight novel avenues for exploration through various mechanisms. For example, as summarized above, Aguado, et al. showed that post-TAVR serum opposes calcification of AVICs.[235] It would be interesting to assess the impact of this serum on macrophages: simple migration assays or flow cytometry of macrophages cultured in this serum may reveal insights into how TAVR affects the inflammatory state of the circulatory system. Additionally, you might repeat experiments like this

one on cocultures of macrophages and AVICs. Perhaps post-TAVR serum would differentially activate macrophages and mitigate macrophage-induced calcification. This model of exploration could be replicated with many of the current experimental models for studying CAVD. For example, cultured media from novel knockout cell lines could be used to culture macrophages, which might then be assayed for activation. Studies like these may eventually be of use in the design of TAVR bioprostheses. Stents and other transcatheter-based therapies are commonly loaded with bioactive molecules to improve healing or long-term engraftment.[309,310] It is possible that loading of a TAVR bioprosthesis with IL-10, given the data reported by An, et al. wherein IL-10 mutations beget AV calcification,[162] might decrease incidence of restenosis. This concept could also be replicated with other anti-inflammatory molecules, either organic or engineered. *In vitro* studies like those described above could help guide the types of bioactive molecules that would be loaded onto such bioprostheses.

In direct follow-up to the macrophage studies in this work, a few particular experiments would be useful. First would be *in vivo* depletion of macrophages for assessment of their effect on CAVD. Previous studies have shown that liposomal clodronate treatment increases AV thickening;[83] however, these experiments were performed in hamsters and clodronate only affects cells that phagocytose while in circulation, selecting for a specific subset of circulating monocytes. In addition to repeating these experiments in mice, either a macrophage-depleting antibody or Cre-inducible diphtheria toxin receptor, perhaps directed against CSF1R-expressing cells,[311] could provide a more targeted system for testing the effects of macrophages in CAVD. Separately, treating mice with an anti-IL6 receptor antibody like tocilizumab (or the murine analog MR16-1) would allow for mechanistic investigation into the role of increased IL-6 expression in the valves of *Notch1*^{+/-} mice.[312] We show that cytokine secretion from the valve cells of *Notch1*^{+/-} mice increases macrophage extravasation and maturation *in vitro*, and that macrophages in turn promote calcification of valve cells. Based on these data, one would expect IL-6 receptor blockade to mitigate macrophage egress from circulation into the valve and

ensuing calcification. This could be replicated with other therapies targeting macrophage egress from circulation. Because the translational potential of macrophage depletion is limited, IL-6 receptor blockade should take priority in future work.

It is also worth considering whether a more acute model of CAVD, such as the wire injury model performed by Honda, et al.,[313] may allow for more direct mechanistic investigations. Many immunomodulating reagents, like the antibodies mentioned here, are not feasible to administer for the length of time required in the aging model, but a model that takes less than four weeks would enable more finely tuned experimental design. Such experimental design will be necessary to move the study of CAVD forward in this time of immunobiology.

Additional studies of adaptive immunity in CAVD are also indicated both by this work and others. Although not included here, we have found that in the $Notch1^{+/-}$ model of disease T cells do not have differential activation or maturation. However, multiple prior studies have shown the clonality of T cells in CAVD and the potential effect they could have on calcification.[86,94,95] Similarly, B cells in the valve correlate with increased severity.[314] It is quite possible that the recruitment of these cells, like macrophages as shown in Chapter 6, comes in response to disease-initiating cells in the valve. And like macrophages, these cells could also promote calcification upon egress into the valve. Further *in vitro* studies mimicking immunocompetent valves are necessary to identify molecular and cellular mechanisms. Similarly, studies like the *in vitro* studies in Chapters 4 and 5 should be followed up with T cell stimulation studies with the resulting activated APCs or macrophages. For example, these APCs (or cocultures as a whole) could be cocultured with T cells and T cell proliferation and cytokine production then measured by flow cytometry. Model experiments to guide experimental design can be found in Kirabo, et al.[315] and Haniffa, et al.[316] Haniffa, et al. specifically showed the immunomodulatory capabilities of fibroblasts, highlighting the potential for this direction of future investigations.[316] This type of work could give substantial direction to further immunological studies in CAVD.

The identification of clonal T cells highlights the role of adaptive immunity in CAVD.[86,94,95] Novel methods of T cell antigen discovery using the T cell receptors on these clonal T cells have the potential to identify antigens in CAVD.[317–319] This would be an enormous development in the field. Recent work in hypertension has identified the role of isolevuglandin-protein adducts as a pathogenic antigen.[315,320] The creation of these antigenic structures occurs in parallel with production of oxidized low-density lipoprotein,[321] which has been shown to be enriched in calcified AVs and promote osteogenesis in AVICs,[120,322] and is associated with faster AS progression to AVR or death in patients.[121] Considering the association of hypertension with faster progression of AV calcification and hemodynamic obstruction, this mechanism may be promising.[134,323] As the field moves to incorporate cardiovascular immunology into the existing body of knowledge, simply staining diseased AVs for isoketals as in Kirabo, et al. would be an incredible first step to pair with the innate immunity findings in this thesis.[315]

In summary, there is a succinct set of outstanding questions following this work: (1) How does modifying STAT3 splicing affect NF-κB activity? (2) Does targeting STAT3 splicing have translational potential in cardiovascular disease? (3) Does targeting macrophage recruitment mitigate CAVD in the $Notch1^{+/-}$ model? and (4) Do the pro-calcification effects of macrophage recruitment in $vivo$ involve lymphocytes and the adaptive immune system? These questions could each be multiple manuscripts worth of ideas, but each also involves a fairly simple first set of experiments. First, regarding STAT3 splicing and NF-κB, AVICs should be isolated after culture with macrophages and increased p65 nuclear translocation and phosphorylation confirmed. Manipulation of STAT3 splicing with plasmid overexpression should also be performed and p65 activity similarly assessed. Second, regarding translational potential, cardiac tissue from (a) the ligation model of myocardial infarction, (b) the transaortic constriction model of heart failure, and (c) the angiotensin II model of hypertension heart failure should be assayed for altered STAT3 splicing.[324] Similar to the CAVD tissues assayed in Chapter 5, we would expect these tissues to have decreased STAT3β. Pilot cohorts of anti-STAT3α morpholino

treatment could be used in any of these models following promising observational results (Figure 7.1). The third question at hand is the recruitment of macrophages. Here, the first strategy worth assessing is IL-6 receptor blockade due to its translational potential. This should be performed in *Notch1*^{+/-} mice from 6 to 9 months of age at least. This may prove challenging due to the lengthy period of therapeutic administration, but MR16-1 has previously been used with biweekly injection, making it a relatively low-burden treatment (Figure 7.2).[312] Finally, regarding the adaptive immune system question, there are two preliminary experiments. First, the aforementioned staining for isoketals is a low-investment step that could identify common pathogenesis with hypertension. Second, assessing the ability of macrophages in coculture with AVICs to promote T cell proliferation and cytokine production could create a generalizable model for T cell involvement. This would involve coculture of the three cell types and ensuing assessment of T cell phenotypes by flow cytometry. It has been shown previously that fibroblast-like cells can modulate T cell activation in coculture with dendritic cells, and this experimental model could be used for AVIC investigations.[316] This second experimental set-up would serve both to further define the effects of AVICs, both wild-type and *Notch1*^{+/-}, on macrophage maturation as measured by their signaling to T cells, and to assess direct effects on T cells in this model of CAVD. Altogether, these four sets of experiments would serve as foundations for further courses of study in this area.

	AVIC and Macrophage Coculture	Human CAVD	AVIC STAT3 Manipulation	Myocardial Infarction Models	Heart Failure Models
STAT3 Splice Changes	✓	✓	N/A	?	?
NF-κB Changes	?	✓	?	✓	✓
Morpholino Treatment	N/A	N/A	N/A	?	?

Figure 7.1. Future directions for investigation of STAT3 splicing in cardiovascular disease.
The first two areas of investigation discussed are related to STAT3 splicing in cardiovascular disease as shown here. The first area of investigation involves assessment of NF-κB activity, seen incorporated into the relevant models in the left three columns of the table. The second area involves assessment of STAT3 splicing in other models of cardiovascular disease as seen in the right two columns. Checkmarks indicate phenomena previously identified. Green checkmarks indicate results in this dissertation. Question marks indicate areas of further investigation. AVIC = aortic valve interstitial cell.

Assess for: Stenosis, Calcification, Macrophage Infiltration

Notch1$^{+/-}$

Bi-weekly anti-IL-6-receptor antibody injections

Euthanize and assess as shown above

1 month	2 months	3 months	4 months	5 months	6 months	7 months	8 months	9 months
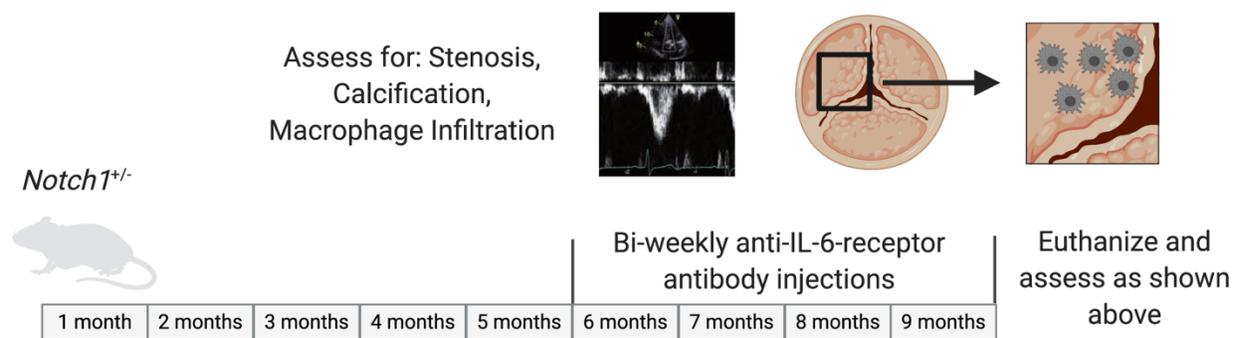
Figure 7.2. Study design for investigation of macrophage recruitment in CAVD via IL-6.
The third area of investigation discussed is treatment of mouse models of CAVD with IL-6-receptor blocking antibodies. This could be performed using the study design shown here.

Bibliography

1. Lindman BR, Clavel M-A, Mathieu P, et al. Calcific aortic stenosis. *Nat Rev Dis Prim*. 2016;2(1):16006.

2. Benjamin EJ, Virani SS, Callaway CW, et al. Heart Disease and Stroke Statistics—2018 Update: A Report From the American Heart Association. *Circulation*. 2018;137(12):CIR.0000000000000558.

3. Roberts WC, Ko JM. Frequency by Decades of Unicuspid, Bicuspid, and Tricuspid Aortic Valves in Adults Having Isolated Aortic Valve Replacement for Aortic Stenosis, With or Without Associated Aortic Regurgitation. *Circulation*. 2005;111(7):920-925.

4. Goldstone AB, Chiu P, Baiocchi M, et al. Mechanical or Biologic Prostheses for Aortic-Valve and Mitral-Valve Replacement. *N Engl J Med*. 2017;377(19):1847-1857.

5. Isaacs AJ, Shuhaiber J, Salemi A, Isom OW, Sedrakyan A. National trends in utilization and in-hospital outcomes of mechanical versus bioprosthetic aortic valve replacements. *J Thorac Cardiovasc Surg*. 2015;149(5):1262-1269.e3.

6. Otto CM. Timing of aortic valve surgery. *Heart*. 2000;84(2):211-8.

7. Ross J, Braunwald E. Aortic Stenosis. *Circulation*. 1968;38(1s5).

8. Tjang YS, van Hees Y, Körfer R, Grobbee DE, van der Heijden GJMG. Predictors of mortality after aortic valve replacement. *Eur J Cardio-thoracic Surg*. 2007;32(3):469-474.

9. Hutcheson JD, Aikawa E, Merryman WD. Potential drug targets for calcific aortic valve disease. *Nat Rev Cardiol*. 2014;11(4):218-231.

10. Cowell SJ, Newby DE, Prescott RJ, et al. A Randomized Trial of Intensive Lipid-Lowering Therapy in Calcific Aortic Stenosis. *N Engl J Med*. 2005;352(23):2389-2397.

11. Rossebø AB, Pedersen TR, Boman K, et al. Intensive Lipid Lowering with Simvastatin and Ezetimibe in Aortic Stenosis. *N Engl J Med*. 2008;359(13):1343-1356.

12. Bull S, Loudon M, Francis JM, et al. A prospective, double-blind, randomized controlled trial of the angiotensin-converting enzyme inhibitor Ramipril In Aortic Stenosis (RIAS trial). *Eur Heart J Cardiovasc Imaging*. 2015;16(8):834-41.

13. Marquis-Gravel G, Redfors B, Leon MB, Généreux P. Medical Treatment of Aortic Stenosis. *Circulation*. 2016;134(22):1766-1784.

14. Cribier A, Eltchaninoff H, Bash A, et al. Percutaneous transcatheter implantation of an aortic valve prosthesis for calcific aortic stenosis: First human case description. *Circulation*. 2002;106(24):3006-3008.

15. Leon MB, Smith CR, Mack M, et al. Transcatheter Aortic-Valve Implantation for Aortic Stenosis in Patients Who Cannot Undergo Surgery. *N Engl J Med*. 2010;363(17):1597-1607.

16. Leon MB, Smith CR, Mack MJ, et al. Transcatheter or Surgical Aortic-Valve Replacement in Intermediate-Risk Patients. *N Engl J Med*. 2016;374(17):1609-1620.

17. Mack MJ, Leon MB, Thourani VH, et al. Transcatheter aortic-valve replacement with a balloon-expandable valve in low-risk patients. *N Engl J Med*. 2019;380(18):1695-1705.

18. Kappetein AP, Head SJ, Généreux P, et al. Updated standardized endpoint definitions for transcatheter aortic valve implantation: The valve academic research consortium-2 consensus document. *J Am Coll Cardiol*. 2012;60(15):1438-1454.

19. Olsson M, Dalsgaard CJ, Haegerstrand A, Rosenqvist M, Rydén L, Nilsson J. Accumulation of T lymphocytes and expression of interleukin-2 receptors in nonrheumatic stenotic aortic valves. *J Am Coll Cardiol*. 1994;23(5):1162-1170.

20. Levy RJ, Schoen FJ, Howard SL. Mechanism of calcification of porcine bioprosthetic aortic valve cusps: Role of T-lymphocytes. *Am J Cardiol*. 1983;52(5):629-631.

21. Kurdi M, Zgheib C, Booz GW. Recent Developments on the Crosstalk Between STAT3 and Inflammation in Heart Function and Disease. *Front Immunol*. 2018;9(December):1-10.

22. Lovgren AK, Jania LA, Hartney JM, et al. COX-2-derived prostacyclin protects against bleomycin-induced pulmonary fibrosis. *Am J Physiol - Lung Cell Mol Physiol*. 2006;291(2):144-156.

23. Thaden JJ, Nkomo VT, Suri RM, et al. Sex-related differences in calcific aortic stenosis: correlating clinical and echocardiographic characteristics and computed tomography aortic valve calcium score to excised aortic valve weight. *Eur Heart J*. 2016;37(8):693-699.

24. Aggarwal SR, Clavel M-A, Messika-Zeitoun D, et al. Sex Differences in Aortic Valve Calcification Measured by Multidetector Computed Tomography in Aortic Stenosis. *Circ Cardiovasc Imaging*. 2013;6(1):40-47.

25. Simard L, Côté N, Dagenais F, et al. Sex-Related Discordance Between Aortic Valve Calcification and Hemodynamic Severity of Aortic Stenosis. *Circ Res*. 2017;120(4):681-691.

26. Clavel M-A, Messika-Zeitoun D, Pibarot P, et al. The Complex Nature of Discordant Severe Calcified Aortic Valve Disease Grading. *J Am Coll Cardiol*. 2013;62(24):2329-2338.

27. Bowler MA, Raddatz MA, Johnson CL, Lindman BR, Merryman WD. Celecoxib Is Associated With Dystrophic Calcification and Aortic Valve Stenosis. *JACC Basic to Transl Sci*. 2019;4(2):135-143.

28. Raddatz MA, Huffstater T, Bersi MR, et al. Macrophages Promote Aortic Valve Cell Calcification and Alter STAT3 Splicing. *Arterioscler Thromb Vasc Biol*. 2020;40(6):e153–e165.

29. Raddatz MA, Madhur MS, Merryman WD. Adaptive immune cells in calcific aortic valve disease. *Am J Physiol Circ Physiol*. 2019;317(1):H141-H155.

30. Coffey S, Cox B, Williams MJA. The Prevalence, Incidence, Progression, and Risks of Aortic Valve Sclerosis: A Systematic Review and Meta-Analysis. *J Am Coll Cardiol*. 2014;63(25):2852-2861.

31. Rajamannan NM, Evans FJ, Aikawa E, et al. Calcific aortic valve disease: Not simply a degenerative process: A review and agenda for research from the national heart and lung and blood institute aortic stenosis working group. *Circulation*. 2011;124(16):1783-1791.

32. Dewey TM, Brown D, Ryan WH, Herbert MA, Prince SL, Mack MJ. Reliability of risk algorithms in predicting early and late operative outcomes in high-risk patients undergoing aortic valve replacement. *J Thorac Cardiovasc Surg*. 2008;135(1):180-187.

33. Jones BM, Krishnaswamy A, Tuzcu EM, et al. Matching patients with the ever-expanding range of TAVI devices. *Nat Rev Cardiol*. 2017;14(10):615-626.

34. Iung B, Cachier A, Baron G, et al. Decision-making in elderly patients with severe aortic stenosis: Why are so many denied surgery? *Eur Heart J*. 2005;26(24):2714-2720.

35. Lindman BR, Perpetua E. Incorporating the Patient Voice Into Shared Decision-Making for the Treatment of Aortic Stenosis. *JAMA Cardiol*. 2020;97(2):158-164.

36. van Beek-Peeters JJAM, van Noort EHM, Faes MC, et al. Shared decision making in older patients with symptomatic severe aortic stenosis: a systematic review. *Heart*. January 2020:heartjnl-2019-316055.

37. Svensson LG, Blackstone EH, Rajeswaran J, et al. Comprehensive Analysis of Mortality Among Patients Undergoing TAVR. *J Am Coll Cardiol*. 2014;64(2):158-168.

38. Otto CM. Informed Shared Decisions for Patients with Aortic Stenosis. *N Engl J Med*. 2019;380(18):1769-1770.

39. Arsalan M, Walther T. Durability of prostheses for transcatheter aortic valve implantation. *Nat Rev Cardiol*. 2016;13(6):360-367.

40. Masri A, Svensson LG, Griffin BP, Desai MY. Contemporary natural history of bicuspid aortic valve disease: a systematic review. *Heart*. 2017;103(17):1323-1330.

41. Tzemos N, Therrien J, Yip J, et al. Outcomes in adults with bicuspid aortic valves. *JAMA*. 2008;300(11):1317-25.

42. Chan KL, Teo K, Dumesnil JG, Ni A, Tam J. Effect of Lipid Lowering With Rosuvastatin on Progression of Aortic Stenosis. *Circulation*. 2010;121(2):306-314.

43. van der Linde D, Yap SC, van Dijk APJ, et al. Effects of Rosuvastatin on Progression of Stenosis in Adult Patients With Congenital Aortic Stenosis (PROCAS Trial). *Am J Cardiol*. 2011;108(2):265-271.

44. Dichtl W, Alber HF, Feuchtner GM, et al. Prognosis and Risk Factors in Patients With Asymptomatic Aortic Stenosis and Their Modulation by Atorvastatin (20 mg). *Am J Cardiol*. 2008;102(6):743-748.

45. Aksoy O, Cam A, Goel SS, et al. Do Bisphosphonates Slow the Progression of Aortic Stenosis? *J Am Coll Cardiol*. 2012;59(16):1452-1459.

46.   Dweck MR, Newby DE. Osteoporosis Is a Major Confounder in Observational Studies Investigating Bisphosphonate Therapyin Aortic Stenosis. *J Am Coll Cardiol*. 2012;60(11):1027.

47.   Sacks MS, David Merryman W, Schmidt DE. On the biomechanics of heart valve function. *J Biomech*. 2009;42(12):1804-1824.

48.   Thubrikar M. *The Aortic Valve*. Routledge; 2018.

49.   Sotiropoulos F, Le TB, Gilmanov A. Fluid Mechanics of Heart Valves and Their Replacements. *Annu Rev Fluid Mech*. 2016;48(1):259-283.

50.   Choi J, Do Y, Cheong C, et al. Identification of antigen-presenting dendritic cells in mouse aorta and cardiac valves. *J Exp Med*. 2009;206(3):497-505.

51.   Rippel RA, Ghanbari H, Seifalian AM. Tissue-Engineered Heart Valve: Future of Cardiac Surgery. *World J Surg*. 2012;36(7):1581-1591.

52.   Towler DA. Molecular and Cellular Aspects of Calcific Aortic Valve Disease. *Circ Res*. 2013;113(2):198-208.

53.   Verzi MP, McCulley DJ, De Val S, Dodou E, Black BL. The right ventricle, outflow tract, and ventricular septum comprise a restricted expression domain within the secondary/anterior heart field. *Dev Biol*. 2005;287(1):134-145.

54.   Wu B, Wang Y, Xiao F, Butcher JT, Yutzey KE, Zhou B. Developmental Mechanisms of Aortic Valve Malformation and Disease. *Annu Rev Physiol*. 2017;79(1):21-41.

55.   Lincoln J, Alfieri CM, Yutzey KE. Development of heart valve leaflets and supporting apparatus in chicken and mouse embryos. *Dev Dyn*. 2004;230(2):239-250.

56.   Chen J, Ryzhova LM, Sewell-Loftin MK, et al. Notch1 Mutation Leads to Valvular Calcification Through Enhanced Myofibroblast Mechanotransduction. *Arterioscler Thromb Vasc Biol*. 2015;35(7):1597-1605.

57.   Hutcheson JD, Chen J, Sewell-Loftin MK, et al. Cadherin-11 regulates cell-cell tension necessary for calcific nodule formation by valvular myofibroblasts. *Arterioscler Thromb Vasc Biol*. 2013;33(1):114-120.

58.   Yip CYY, Chen JH, Zhao R, Simmons CA. Calcification by valve interstitial cells is regulated by the stiffness of the extracellular matrix. *Arterioscler Thromb Vasc Biol*. 2009;29(6):936-942.

59.   Fisher CI, Chen J, Merryman WD. Calcific nodule morphogenesis by heart valve interstitial cells is strain dependent. *Biomech Model Mechanobiol*. 2013;12(1):5-17.

60.   Chen J, Peacock JR, Branch J, David Merryman W. Biophysical Analysis of Dystrophic and Osteogenic Models of Valvular Calcification. *J Biomech Eng*. 2015;137(2):020903.

61.   Rajamannan NM, Subramaniam M, Rickard D, et al. Human aortic valve calcification is associated with an osteoblast phenotype. *Circulation*. 2003;107(17):2181-2184.

62.   Mohler ER, Chawla MK, Chang AW, et al. Identification and characterization of calcifying valve cells from human and canine aortic valves. *J Heart Valve Dis*. 1999;8(3):254-60.

63. Gössl M, Khosla S, Zhang X, et al. Role of Circulating Osteogenic Progenitor Cells in Calcific Aortic Stenosis. *J Am Coll Cardiol*. 2012;60(19):1945-1953.

64. Mohler ER, Gannon F, Reynolds C, Zimmerman R, Keane MG, Kaplan FS. Bone formation and inflammation in cardiac valves. *Circulation*. 2001;103(11):1522-1528.

65. Schlotter F, Halu A, Goto S, et al. Spatiotemporal Multi-omics Mapping Generates a Molecular Atlas of the Aortic Valve and Reveals Networks Driving Disease. *Circulation*. 2018;138(4):377-393.

66. Sider KL, Blaser MC, Simmons CA. Animal Models of Calcific Aortic Valve Disease. *Int J Inflam*. 2011;2011(Ldl):1-18.

67. Roosens B, Bala G, Droogmans S, Van Camp G, Breyne J, Cosyns B. Animal models of organic heart valve disease. *Int J Cardiol*. 2013;165(3):398-409.

68. Clark CR, Bowler MA, Snider JC, David Merryman W. Targeting Cadherin-11 Prevents Notch1-Mediated Calcific Aortic Valve Disease. *Circulation*. 2017;135(24):2448-2450.

69. Nus M, MacGrogan D, Martínez-Poveda B, et al. Diet-induced aortic valve disease in mice haploinsufficient for the notch pathway effector RBPJK/CSL. *Arterioscler Thromb Vasc Biol*. 2011;31(7):1580-1588.

70. Nigam V, Srivastava D. Notch1 represses osteogenic pathways in aortic valve cells. *J Mol Cell Cardiol*. 2009;47(6):828-834.

71. Garg V, Muth AN, Ransom JF, et al. Mutations in NOTCH1 cause aortic valve disease. *Nature*. 2005;437(7056):270-274.

72. Majumdar U, Garg V. Notch1 Signaling and Aortic Valve Disease : From Human Genetics to Mouse Models. *J Pediatr Cardiol Card Surg*. 2017;1(1):12-17.

73. Bowler MA, Merryman WD. In vitro models of aortic valve calcification: solidifying a system. *Cardiovasc Pathol*. 2015;24(1):1-10.

74. Hulin A, Anstine LJ, Kim AJ, et al. Macrophage Transitions in Heart Valve Development and Myxomatous Valve Disease. *Arterioscler Thromb Vasc Biol*. 2018:ATVBAHA.117.310667.

75. Hajdu Z, Romeo SJ, Fleming PA, Markwald RR, Visconti RP, Drake CJ. Recruitment of bone marrow-derived valve interstitial cells is a normal homeostatic process. *J Mol Cell Cardiol*. 2011;51(6):955-965.

76. Mazzone A, Epistolato MC, De Caterina R, et al. Neoangiogenesis, T-lymphocyte infiltration, and heat shock protein-60 are biological hallmarks of an immunomediated inflammatory process in end-stage calcified aortic valve stenosis. *J Am Coll Cardiol*. 2004;43(9):1670-1676.

77. Coté N, Mahmut A, Bosse Y, et al. Inflammation is associated with the remodeling of calcific aortic valve disease. *Inflammation*. 2013;36(3):573-581.

78. Skowasch D, Schrempf S, Wernert N, et al. Cells of primarily extravalvular origin in degenerative aortic valves and bioprostheses. *Eur Heart J*. 2005;26(23):2576-2580.

79. Li G, Qiao W, Zhang W, Li F, Shi J, Dong N. The shift of macrophages toward M1 phenotype promotes aortic valvular calcification. *J Thorac Cardiovasc Surg*. 2017;153(6):1318-1327.e1.

80. Mantovani A, Sica A, Sozzani S, Allavena P, Vecchi A, Locati M. The chemokine system in diverse forms of macrophage activation and polarization. *Trends Immunol*. 2004;25(12):677-686.

81. Mantovani A, Sica A, Locati M. Macrophage polarization comes of age. *Immunity*. 2005;23(4):344-346.

82. Martinez FO, Gordon S. The M1 and M2 paradigm of macrophage activation: time for reassessment. *F1000Prime Rep*. 2014;6(March):1-13.

83. Calin MV, Manduteanu I, Dragomir E, et al. Effect of depletion of monocytes/macrophages on early aortic valve lesion in experimental hyperlipidemia. *Cell Tissue Res*. 2009;336(2):237-248.

84. Lodyga M, Cambridge E, Karvonen HM, et al. Cadherin-11–mediated adhesion of macrophages to myofibroblasts establishes a profibrotic niche of active TGF-β. *Sci Signal*. 2019;12(564):eaao3469.

85. Shimoni S, Bar I, Meledin V, Gandelman G, George J. Circulating regulatory T cells in patients with aortic valve stenosis: Association with disease progression and aortic valve intervention. *Int J Cardiol*. 2016;218:181-187.

86. Winchester R, Wiesendanger M, O'Brien W, et al. Circulating Activated and Effector Memory T Cells Are Associated with Calcification and Clonal Expansions in Bicuspid and Tricuspid Valves of Calcific Aortic Stenosis. *J Immunol*. 2011;187(2):1006-1014.

87. Mazur P, Mielimonka A, Natorska J, et al. Lymphocyte and monocyte subpopulations in severe aortic stenosis at the time of surgical intervention. *Cardiovasc Pathol*. 2018;35:1-7.

88. Šteiner I, Stejskal V, Žáček P. Mast cells in calcific aortic stenosis. *Pathol Res Pract*. 2018;214(1):163-168.

89. Wypasek E, Natorska J, Grudzień G, Filip G, Sadowski J, Undas A. Mast cells in human stenotic aortic valves are associated with the severity of stenosis. *Inflammation*. 2013;36(2):449-456.

90. Milutinovic A, Petrovič D, Zorc M, et al. Mast Cells Might Have a Protective Role against the Development of Calcification and Hyalinisation in Severe Aortic Valve Stenosis. *Folia Biol*. 2016;62:160-166.

91. Takahashi K, Satoh M, Takahashi Y, et al. Dysregulation of ossification-related miRNAs in circulating osteogenic progenitor cells obtained from patients with aortic stenosis. *Clin Sci*. 2016;130(13):1115-1124.

92. Egan KP, Kim JH, Mohler ER, Pignolo RJ. Role for circulating osteogenic precursor cells in aortic valvular disease. *Arterioscler Thromb Vasc Biol*. 2011;31(12):2965-2971.

93. Guauque-Olarte S, Droit A, Tremblay-Marchand J, et al. RNA expression profile of calcified bicuspid, tricuspid, and normal human aortic valves by RNA sequencing. *Physiol Genomics*. 2016;48(10):749-761.

94. Nagy E, Lei Y, Martínez-Martínez E, et al. Interferon-γ Released by Activated CD8 + T Lymphocytes Impairs the Calcium Resorption Potential of Osteoclasts in Calcified Human Aortic Valves. *Am J Pathol*. 2017;187(6):1413-1425.

95. Wu HD, Maurer MS, Friedman RA, et al. The Lymphocytic Infiltration in Calcific Aortic Stenosis Predominantly Consists of Clonally Expanded T Cells. *J Immunol*. 2007;178(8):5329-5339.

96. Šteiner I, Krbal L, Rozkoš T, Harrer J, Laco J. Calcific aortic valve stenosis: Immunohistochemical analysis of inflammatory infiltrate. *Pathol Res Pract*. 2012;208(4):231-234.

97. Mosch J, Gleissner CA, Body S, Aikawa E. Histopathological assessment of calcification and inflammation of calcific aortic valves from patients with and without diabetes mellitus. *Histol Histopathol*. 2017;32(3):293-306.

98. Mathieu P, Bouchareb R, Boulanger M-C. Innate and Adaptive Immunity in Calcific Aortic Valve Disease. *J Immunol Res*. 2015;2015:851945.

99. García-Rodríguez C, Parra-Izquierdo I, Castaños-Mollor I, López J, San Román JA, Crespo MS. Toll-like receptors, inflammation, and calcific aortic valve disease. *Front Physiol*. 2018;9(MAR):1-8.

100. Akira S, Takeda K. Toll-like receptor signalling. *Nat Rev Immunol*. 2004;4(7):499-511.

101. Meng X, Ao L, Song Y, et al. Expression of functional Toll-like receptors 2 and 4 in human aortic valve interstitial cells: potential roles in aortic valve inflammation and stenosis. *Am J Physiol Physiol*. 2008;294(1):C29-C35.

102. Yang X, Fullerton DA, Su X, Ao L, Cleveland JC, Meng X. Pro-Osteogenic Phenotype of Human Aortic Valve Interstitial Cells Is Associated With Higher Levels of Toll-Like Receptors 2 and 4 and Enhanced Expression of Bone Morphogenetic Protein 2. *J Am Coll Cardiol*. 2009;53(6):491-500.

103. Babu AN, Meng X, Zou N, et al. Lipopolysaccharide Stimulation of Human Aortic Valve Interstitial Cells Activates Inflammation and Osteogenesis. *Ann Thorac Surg*. 2008;86(1):71-76.

104. Fernández-Pisonero I, López J, Onecha E, et al. Synergy between sphingosine 1-phosphate and lipopolysaccharide signaling promotes an inflammatory, angiogenic and osteogenic response in human aortic valve interstitial cells. *PLoS One*. 2014;9(10):1-11.

105. Zhan Q, Song R, Li F, et al. Double-stranded RNA upregulates the expression of inflammatory mediators in human aortic valve cells through the TLR3-TRIF-noncanonical NF-κB pathway. *Am J Physiol Cell Physiol*. 2017;312(4):C407-C417.

106. Zhan Q, Song R, Zeng Q, et al. Activation of TLR3 Induces Osteogenic Responses in Human Aortic Valve Interstitial Cells through the NF-κB and ERK1/2 Pathways. *Int J Biol Sci*. 2015;11(4):482-493.

107. Song R, Ao L, Zhao K, et al. Soluble biglycan induces the production of ICAM-1 and MCP-1 in human aortic valve interstitial cells through TLR2/4 and the ERK1/2 pathway. *Inflamm Res*. 2014;63(9):703-710.

108. Song R, Fullerton DA, Ao L, Zheng D, Zhao K, Meng X. BMP-2 and TGF-β1 mediate biglycan-induced pro-osteogenic reprogramming in aortic valve interstitial cells. *J Mol Med*. 2015;93(4):403-412.

109. Song R, Zeng Q, Ao L, et al. Biglycan Induces the Expression of Osteogenic Factors in Human Aortic Valve Interstitial Cells via Toll-Like Receptor-2. *Arterioscler Thromb Vasc Biol*. 2012;32(11):2711-2720.

110. Parra-Izquierdo I, Castaños-Mollor I, López J, et al. Calcification Induced by Type I Interferon in Human Aortic Valve Interstitial Cells Is Larger in Males and Blunted by a Janus Kinase Inhibitor. *Arterioscler Thromb Vasc Biol*. 2018:ATVBAHA.118.311504.

111. Zeng Q, Song R, Fullerton DA, et al. Interleukin-37 suppresses the osteogenic responses of human aortic valve interstitial cells in vitro and alleviates valve lesions in mice. *Proc Natl Acad Sci*. 2017;114(7):1631-1636.

112. Gee T, Farrar E, Wang Y, et al. NFκB (Nuclear Factor κ-Light-Chain Enhancer of Activated B Cells) Activity Regulates Cell-Type-Specific and Context-Specific Susceptibility to Calcification in the Aortic Valve. *Arterioscler Thromb Vasc Biol*. 2020;40(3):638-655.

113. Baeuerle PA, Henkel T. Function and Activation of NF-kappaB in the Immune System. *Annu Rev Immunol*. 1994;12(1):141-179.

114. Kaden JJ, Kiliç R, Sarikoç A, et al. Tumor necrosis factor alpha promotes an osteoblast-like phenotype in human aortic valve myofibroblasts: a potential regulatory mechanism of valvular calcification. *Int J Mol Med*. 2005;16(5):869-72.

115. Yu Z, Seya K, Daitoku K, Motomura S, Fukuda I, Furukawa K-I. Tumor Necrosis Factor- Accelerates the Calcification of Human Aortic Valve Interstitial Cells Obtained from Patients with Calcific Aortic Valve Stenosis via the BMP2-Dlx5 Pathway. *J Pharmacol Exp Ther*. 2011;337(1):16-23.

116. Kaden JJ, Dempfle CE, Grobholz R, et al. Interleukin-1 beta promotes matrix metalloproteinase expression and cell proliferation in calcific aortic valve stenosis. *Atherosclerosis*. 2003;170(2):205-211.

117. Nadlonek N, Lee JH, Reece TB, et al. Interleukin-1 beta induces an inflammatory phenotype in human aortic valve interstitial cells through nuclear factor kappa beta. *Ann Thorac Surg*. 2013;96(1):155-162.

118. Isoda K, Matsuki T, Kondo H, Iwakura Y, Ohsuzu F. Deficiency of Interleukin-1 Receptor Antagonist Induces Aortic Valve Disease in BALB/c Mice. *Arterioscler Thromb Vasc Biol*. 2010;30(4):708-715.

119. Lee JH, Meng X, Weyant MJ, Reece TB, Cleveland JC, Fullerton DA. Stenotic aortic valves have dysfunctional mechanisms of anti-inflammation: Implications for aortic stenosis. *J Thorac Cardiovasc Surg*. 2011;141(2):481-486.

120. Zeng Q, Song R, Ao L, et al. Augmented osteogenic responses in human aortic valve cells exposed to oxLDL and TLR4 agonist: A mechanistic role of Notch1 and NF-κB interaction. *PLoS One*. 2014.

121. Capoulade R, Chan KL, Yeang C, et al. Oxidized phospholipids, lipoprotein(a), and progression of calcific aortic valve stenosis. *J Am Coll Cardiol*. 2015;66(11):1236-1246.

122. Yeang C, Wilkinson MJ, Tsimikas S. Lipoprotein(a) and oxidized phospholipids in calcific aortic valve stenosis. *Curr Opin Cardiol*. 2016;31(4):440-450.

123. Cote C, Pibarot P, Despres J-P, et al. Association between circulating oxidised low-density lipoprotein and fibrocalcific remodelling of the aortic valve in aortic stenosis. *Heart*. 2008;94(9):1175-1180.

124. Kaden JJ, Dempfle C-E, Kılıç R, et al. Influence of receptor activator of nuclear factor kappa B on human aortic valve myofibroblasts. *Exp Mol Pathol*. 2005;78(1):36-40.

125. Weiss RM, Lund DD, Chu Y, et al. Osteoprotegerin Inhibits Aortic Valve Calcification and Preserves Valve Function in Hypercholesterolemic Mice. Lionetti V, ed. *PLoS One*. 2013;8(6):e65201.

126. Yokoo T, Kitamura M. Dual regulation of IL-1 beta-mediated matrix metalloproteinase-9 expression in mesangial cells by NF-kappa B and AP-1. *Am J Physiol Physiol*. 1996;270(1):F123-F130.

127. Grivennikov SI, Karin M. Dangerous liaisons: STAT3 and NF-κB collaboration and crosstalk in cancer. *Cytokine Growth Factor Rev*. 2010;21(1):11-19.

128. Knight D, Mutsaers SE, Prêle CM. STAT3 in tissue fibrosis: Is there a role in the lung? *Pulm Pharmacol Ther*. 2011;24(2):193-198.

129. Loperena R, Van Beusecum JP, Itani HA, et al. Hypertension and increased endothelial mechanical stretch promote monocyte differentiation and activation: roles of STAT3, interleukin 6 and hydrogen peroxide. *Cardiovasc Res*. 2018;(July):1-17.

130. Haghikia A, Ricke-Hoch M, Stapel B, Gorst I, Hilfiker-Kleiner D. STAT3, a key regulator of cell-to-cell communication in the heart. *Cardiovasc Res*. 2014;102(2):281-289.

131. Yue H, Li W, Desnoyer R, Karnik SS. Role of nuclear unphosphorylated STAT3 in angiotensin II type 1 receptor-induced cardiac hypertrophy. *Cardiovasc Res*. 2010;85(1):90-99.

132. Sano M, Fukuda K, Kodama H, et al. Autocrine/Paracrine Secretion of IL-6 Family Cytokines Causes Angiotensin II-Induced Delayed STAT3 Activation. *Biochem Biophys Res Commun*. 2000;269(3):798-802.

133. Côté N, Pibarot P, Pépin A, et al. Oxidized low-density lipoprotein, angiotensin II and increased waist cirumference are associated with valve inflammation in prehypertensive patients with aortic stenosis. *Int J Cardiol*. 2010;145(3):444-449.

134. Capoulade R, Clavel MA, Mathieu P, et al. Impact of hypertension and renin-angiotensin system inhibitors in aortic stenosis. *Eur J Clin Invest*. 2013;43(12):1262-1272.

135. O'Brien KD, Shavelle DM, Caulfield MT, et al. Association of Angiotensin-Converting Enzyme With Low-Density Lipoprotein in Aortic Valvular Lesions and in Human Plasma. *Circulation*. 2002;106(17):2224-2230.

136. Chakraborty D, Šumová B, Mallano T, et al. Activation of STAT3 integrates common profibrotic pathways to promote fibroblast activation and tissue fibrosis. *Nat Commun*. 2017;8(1).

137. Zhang L, Xu X, Yang R, et al. Paclitaxel attenuates renal interstitial fibroblast activation and interstitial fibrosis by inhibiting STAT3 signaling. *Drug Des Devel Ther*. 2015;9:2139-2148.

138. Tang LY, Heller M, Meng Z, et al. Transforming growth factor-β (TGF-β) directly activates the JAK1-STAT3 axis to induce hepatic fibrosis in coordination with the SMAD pathway. *J Biol Chem*. 2017;292(10):4302-4312.

139. Yuan Y, Zhang Y, Han X, et al. Relaxin alleviates TGFβ1-induced cardiac fibrosis via inhibition of Stat3-dependent autophagy. *Biochem Biophys Res Commun*. 2017;493(4):1601-1607.

140. Xu MY, Hu JJ, Shen J, et al. Stat3 signaling activation crosslinking of TGF-β1 in hepatic stellate cell exacerbates liver injury and fibrosis. *Biochim Biophys Acta - Mol Basis Dis*. 2014;1842(11):2237-2245.

141. Yu H, Pardoll D, Jove R. STATs in cancer inflammation and immunity: A leading role for STAT3. *Nat Rev Cancer*. 2009;9(11):798-809.

142. Wang SW, Sun YM. The IL-6/JAK/STAT3 pathway: Potential therapeutic strategies in treating colorectal cancer (Review). *Int J Oncol*. 2014;44(4):1032-1040.

143. Johnson DE, O'Keefe RA, Grandis JR. Targeting the IL-6/JAK/STAT3 signalling axis in cancer. *Nat Rev Clin Oncol*. 2018;15(4):234-248.

144. Heinrich PC, Behrmann I, Muller-Newen G, Schaper F, Graeve L. Interleukin-6-type cytokine signalling through the gp130/Jak/STAT pathway. *Biochem J*. 1998;334(2):297-314.

145. Takeda K, Noguchi K, Shi W, et al. Targeted disruption of the mouse Stat3 gene leads to early embryonic lethality. *Proc Natl Acad Sci*. 1997;94(8):3801-3804.

146. Jacoby JJ, Kalinowski A, Liu M-G, et al. Cardiomyocyte-restricted knockout of STAT3 results in higher sensitivity to inflammation, cardiac fibrosis, and heart failure with advanced age. *Proc Natl Acad Sci*. 2003;100(22):12929-12934.

147. Huynh J, Chand A, Gough D, Ernst M. Therapeutically exploiting STAT3 activity in cancer — using tissue repair as a road map. *Nat Rev Cancer*. 2019;19(2):82-96.

148. El Husseini D, Boulanger M-CC, Mahmut A, et al. P2Y2 receptor represses IL-6 expression by valve interstitial cells through Akt: Implication for calcific aortic valve disease. *J Mol Cell Cardiol*. 2014;72:146-156.

149. Toli K, Paraskevas KI, Poulakou M V, et al. Association between plasma levels and immunolocalization of cytokines in heart valve lesions: a possible target for treatment? *Expert Opin Ther Targets*. 2008;12(10):1209-1215.

150. Wypasek E, Potaczek DP, Lamplmayr M, Sadowski J, Undas A. Interleukin-6 receptor Asp358Ala gene polymorphism is associated with plasma C-reactive protein levels and severity of aortic valve stenosis. *Clin Chem Lab Med*. 2014;52(7).

151. Bowler MA, Bersi MR, Ryzhova LM, Jerrell RJ, Parekh A, Merryman WD. Cadherin-11 as a regulator of valve myofibroblast mechanobiology. *Am J Physiol Circ Physiol*. 2018;315(6):H1614-H1626.

152. Tsai C-L, Chiu Y-M, Lee Y-J, et al. Interleukin-32 plays an essential role in human calcified aortic valve cells. *Eur Cytokine Netw*. 2018;29(1):36-47.

153. Dalagiorgou G, Piperi C, Adamopoulos C, et al. Mechanosensor polycystin-1 potentiates differentiation of human osteoblastic cells by upregulating Runx2 expression via induction of JAK2/STAT3 signaling axis. *Cell Mol Life Sci*. 2017;74(5):921-936.

154. Schrader J, Gordon-Walker TT, Aucott RL, et al. Matrix stiffness modulates proliferation, chemotherapeutic response, and dormancy in hepatocellular carcinoma cells. *Hepatology*. 2011;53(4):1192-1205.

155. Agudelo-Garcia PA, De Jesus JK, Williams SP, et al. Glioma Cell Migration on Three-dimensional Nanofiber Scaffolds Is Regulated by Substrate Topography and Abolished by Inhibition of STAT3 Signaling. *Neoplasia*. 2011;13(9):831-IN22.

156. Merryman WD, Youn I, Lukoff HD, et al. Correlation between heart valve interstitial cell stiffness and transvalvular pressure: Implications for collagen biosynthesis. *Am J Physiol - Hear Circ Physiol*. 2006;290(1):224-231.

157. Geletu M, Mohan R, Arulanandam R, et al. Reciprocal regulation of the Cadherin-11/Stat3 axis by caveolin-1 in mouse fibroblasts and lung carcinoma cells. *Biochim Biophys Acta - Mol Cell Res*. 2018;1865(5):794-802.

158. Geletu M, Arulanandam R, Chevalier S, et al. Biochimica et Biophysica Acta Classical cadherins control survival through the gp130 / Stat3 axis. *BBA - Mol Cell Res*. 2013;1833(8):1947-1959.

159. Ljungberg J, Janiec M, Bergdahl IA, et al. Proteomic Biomarkers for Incident Aortic Stenosis Requiring Valvular Replacement. *Circulation*. 2018:CIRCULATIONAHA.117.030414.

160. Jian B, Narula N, Li Q, Mohler ER, Levy RJ. Progression of aortic valve stenosis: TGF-β1 is present in calcified aortic valve cusps and promotes aortic valve interstitial cell calcification via apoptosis. *Ann Thorac Surg*. 2003;75(2):457-465.

161. Wang R, Chen W, Ma Z, Li L, Chen X. M1/M2 macrophages and associated mechanisms in congenital bicuspid aortic valve stenosis. *Exp Ther Med*. 2014;7(4):935-940.

162. An Y, Wang YT, Ma YT, et al. IL-10 genetic polymorphisms were associated with valvular calcification in Han, Uygur and Kazak populations in Xinjiang, China. *PLoS One*. 2015;10(6):1-12.

163. Naito Y, Tsujino T, Wakabayashi K, et al. Increased interleukin-18 expression in nonrheumatic aortic valve stenosis. *Int J Cardiol*. 2010;144(2):260-263.

164. Lancellotti P, Dulgheru R, Magne J, et al. Elevated plasma soluble sT2 is associated with heart failure symptoms and outcome in aortic stenosis. *PLoS One*. 2015;10(9):1-10.

165. Sawada H, Naito Y, Hirotani S, et al. Expression of interleukin-33 and ST2 in nonrheumatic aortic valve stenosis. *Int J Cardiol*. 2013;168(1):529-531.

166. Mathieu P, Boulanger M-C. Basic Mechanisms of Calcific Aortic Valve Disease. *Can J Cardiol*. 2014;30(9):982-993.

167. Zhang M, Liu X, Zhang X, et al. MicroRNA-30b is a multifunctional regulator of aortic valve interstitial cells. *J Thorac Cardiovasc Surg*. 2014;147(3):1073-1080.e2.

168. Nicolaidou V, Wong MM, Redpath AN, et al. Monocytes induce STAT3 activation in human mesenchymal stem cells to promote osteoblast formation. *PLoS One*. 2012;7(7).

169. Ziros PG, Georgakopoulos T, Habeos I, Basdra EK, Papavassiliou AG. Growth hormone attenuates the transcriptional activity of Runx2 by facilitating its physical association with Stat3β. *J Bone Miner Res*. 2004;19(11):1892-1904.

170. Bharadwaj U, Kasembeli M, Eckols T, et al. Monoclonal Antibodies Specific for STAT3β Reveal Its Contribution to Constitutive STAT3 Phosphorylation in Breast Cancer. *Cancers (Basel)*. 2014;6(4):2012-2034.

171. Caldenhoven E, van Dijk TB, Solari R, et al. STAT3β, a Splice Variant of Transcription Factor STAT3, Is a Dominant Negative Regulator of Transcription. *J Biol Chem*. 1996;271(22):13221-13227.

172. Rumzhum NN, Ammit AJ. Cyclooxygenase 2: its regulation, role and impact in airway inflammation. *Clin Exp Allergy*. 2016;46(3):397-410.

173. Turini ME, DuBois RN. Cyclooxygenase-2: A Therapeutic Target. *Annu Rev Med*. 2002;53(1):35-57.

174. Simon LS, Weaver AL, Graham DY, et al. Anti-inflammatory and Upper Gastrointestinal Effects of Celecoxib in Rheumatoid Arthritis. *JAMA*. 1999;282(20):1921.

175. Vane JR, Bakhle YS, Botting RM. Cyclooxygenases 1 and 2. *Annu Rev Pharmacol Toxicol*. 1998;38(1):97-120.

176. Forwood MR. Inducible cyclo-oxygenase (COX-2) mediates the induction of bone formation by mechanical loading in vivo. *J Bone Miner Res*. 2009;11(11):1688-1693.

177. Zhang X, Schwarz EM, Young DA, Puzas JE, Rosier RN, O'Keefe RJ. Cyclooxygenase-2 regulates mesenchymal cell differentiation into the osteoblast lineage and is critically involved in bone repair. *J Clin Invest*. 2002;109(11):1405-1415.

178. Bresalier RS, Sandler RS, Quan H, et al. Cardiovascular Events Associated with Rofecoxib in a Colorectal Adenoma Chemoprevention Trial. *N Engl J Med*. 2005;352(11):1092-1102.

179. Ott E, Nussmeier NA, Duke PC, et al. Efficacy and safety of the cyclooxygenase 2 inhibitors parecoxib and valdecoxib in patients undergoing coronary artery bypass surgery. *J Thorac Cardiovasc Surg*. 2003;125(6):1481-1492.

180. Nussmeier NA, Whelton AA, Brown MT, et al. Complications of the COX-2 Inhibitors Parecoxib and Valdecoxib after Cardiac Surgery. *N Engl J Med*. 2005;352(11):1081-1091.

181. Shibata R, Sato K, Pimentel DR, et al. Adiponectin protects against myocardial ischemia-reperfusion injury through AMPK- and COX-2–dependent mechanisms. *Nat Med*. 2005;11(10):1096-1103.

182. Wang D, Patel V V., Ricciotti E, et al. Cardiomyocyte cyclooxygenase-2 influences cardiac rhythm and function. *Proc Natl Acad Sci*. 2009;106(18):7548-7552.

183. Kohsaka S, Volcik KA, Folsom AR, et al. Increased risk of incident stroke associated with the cyclooxygenase 2 (COX-2) G−765C polymorphism in African-Americans: The Atherosclerosis Risk in Communities Study. *Atherosclerosis*. 2008;196(2):926-930.

184. Nissen SE, Yeomans ND, Solomon DH, et al. Cardiovascular Safety of Celecoxib, Naproxen, or Ibuprofen for Arthritis. *N Engl J Med*. 2016;375(26):2519-2529.

185. Jacob S, Laury-Kleintop L, Lanza-Jacoby S. The Select Cyclooxygenase-2 Inhibitor Celecoxib Reduced the Extent of Atherosclerosis in Apo E-/- Mice. *J Surg Res*. 2008;146(1):135-142.

186. Wirrig EE, Gomez MV, Hinton RB, Yutzey KE. COX2 Inhibition Reduces Aortic Valve Calcification In VivoSignificance. *Arterioscler Thromb Vasc Biol*. 2015;35(4):938-947.

187. Dakshanamurthy S, Issa NT, Assefnia S, et al. Predicting new indications for approved drugs using a proteochemometric method. *J Med Chem*. 2012;55(15):6832-6848.

188. Chrousos GP. Stress and Sex Versus Immunity and Inflammation. *Sci Signal*. 2010;3(143):pe36-pe36.

189. Yang Y, Kozloski M. Sex Differences in Age Trajectories of Physiological Dysregulation: Inflammation, Metabolic Syndrome, and Allostatic Load. *Journals Gerontol Ser A*. 2011;66A(5):493-500.

190. Lakoski SG, Cushman M, Criqui M, et al. Gender and C-reactive protein: Data from the Multiethnic Study of Atherosclerosis (MESA) cohort. *Am Heart J*. 2006;152(3):593-598.

191. Duma D, Collins JB, Chou JW, Cidlowski JA. Sexually Dimorphic Actions of Glucocorticoids Provide a Link to Inflammatory Diseases with Gender Differences in Prevalence. *Sci Signal*. 2010;3(143):ra74-ra74.

192. Thorand B, Baumert J, Döring A, et al. Sex differences in the relation of body composition to markers of inflammation. *Atherosclerosis*. 2006;184(1):216-224.

193. Medrikova D, Jilkova ZM, Bardova K, Janovska P, Rossmeisl M, Kopecky J. Sex differences during the course of diet-induced obesity in mice: adipose tissue expandability and glycemic control. *Int J Obes*. 2012;36(2):262-272.

194. Nickelson KJ, Stromsdorfer KL, Pickering RT, et al. A Comparison of Inflammatory and Oxidative Stress Markers in Adipose Tissue from Weight-Matched Obese Male and Female Mice. *Exp Diabetes Res*. 2012;2012:1-8.

195. Griffin C, Lanzetta N, Eter L, Singer K. Sexually dimorphic myeloid inflammatory and metabolic responses to diet-induced obesity. *Am J Physiol Integr Comp Physiol*. 2016;311(2):R211-R216.

196. Singer K, Maley N, Mergian T, et al. Differences in Hematopoietic Stem Cells Contribute to Sexually Dimorphic Inflammatory Responses to High Fat Diet-induced Obesity. *J Biol Chem*. 2015;290(21):13250-13262.

197. Stewart BF, Siscovick D, Lind BK, et al. Clinical factors associated with calcific aortic valve disease. *J Am Coll Cardiol*. 1997;29(3):630-634.

198. Annabi MS, Touboul E, Dahou A, et al. Dobutamine Stress Echocardiography for Management of Low-Flow, Low-Gradient Aortic Stenosis. *J Am Coll Cardiol*. 2018;71(5):475-485.

199. Clavel MA, Pibarot P, Messika-Zeitoun D, et al. Impact of aortic valve calcification, as measured by MDCT, on survival in patients with aortic stenosis: Results of an international registry study. *J Am Coll Cardiol*. 2014;64(12):1202-1213.

200. Bonow RO, Brown AS, Gillam LD, et al. ACC/AATS/AHA/ASE/EACTS/HVS/SCA/SCAI/SCCT/SCMR/STS 2017 Appropriate Use Criteria for the Treatment of Patients With Severe Aortic Stenosis. *J Am Coll Cardiol*. 2017;70(20):2566-2598.

201. Lloyd JW, Nishimura RA, Borlaug BA, Eleid MF. Hemodynamic Response to Nitroprusside in Patients With Low-Gradient Severe Aortic Stenosis and Preserved Ejection Fraction. *J Am Coll Cardiol*. 2017;70(11):1339-1348.

202. Nishimura RA, Otto CM, Bonow RO, et al. 2014 AHA/ACC guideline for the management of patients with valvular heart disease : A report of the american college of cardiology/american heart association task force on practice guidelines. *Circulation*. 2014;129(23):2440-2492.

203. Malouf J, Le Tourneau T, Pellikka P, et al. Aortic valve stenosis in community medical practice: Determinants of outcome and implications for aortic valve replacement. *J Thorac Cardiovasc Surg*. 2012;144(6):1421-1427.

204. Dayan V, Vignolo G, Magne J, Clavel MA, Mohty D, Pibarot P. Outcome and Impact of Aortic Valve Replacement in Patients with Preserved LVEF and Low-Gradient Aortic Stenosis. *J Am Coll Cardiol*. 2015;66(23):2594-2603.

205. Berthelot-Richer M, Pibarot P, Capoulade R, et al. Discordant Grading of Aortic Stenosis Severity: Echocardiographic Predictors of Survival Benefit Associated With Aortic Valve Replacement. *JACC Cardiovasc Imaging*. 2016;9(7):797-805.

206. Walker GA, Masters KS, Shah DN, Anseth KS, Leinwand LA. Valvular myofibroblast activation by transforming growth factor-β: Implications for pathological extracellular matrix remodeling in heart valve disease. *Circ Res*. 2004;95(3):253-260.

207. Hutcheson JD, Ryzhova LM, Setola V, Merryman WD. 5-HT(2B) antagonism arrests non-canonical TGF-β1-induced valvular myofibroblast differentiation. *J Mol Cell Cardiol*. 2012;53(5):707-14.

208. Blondell RD, Azadfard M, Wisniewski AM. Pharmacologic therapy for acute pain. *Am Fam Physician*. 2013;87(11):766-772.

209. Fosbøl EL, Gislason GH, Jacobsen S, et al. The pattern of use of non-steroidal anti-inflammatory drugs (NSAIDs) from 1997 to 2005: a nationwide study on 4.6 million people. *Pharmacoepidemiol Drug Saf*. 2008;17(8):822-833.

210. Solomon SD, McMurray JJ V, Pfeffer MA, et al. Cardiovascular risk associated with celecoxib in a clinical trial for colorectal adenoma prevention. *N Engl J Med*. 2005;352(11):1071-80.

211. U.S. Food and Drug Administration. COX-2 Selective (Includes Bextra, Celebrex, and Vioxx) and Non-Selective Non-Steroidal Anti-Inflammatory Drugs (NSAIDs). 2018.

212. Tu K, Chen Z, Lipscombe LL. Prevalence and incidence of hypertension from 1995 to 2005: a population-based study. *Cmaj*. 2008;178(11):1429-1435.

213. Tu K, Campbell NR, Chen Z-L, Cauch-Dudek KJ, McAlister FA. Accuracy of administrative databases in identifying patients with hypertension. *Open Med*. 2007;1(1):e18-26.

214. Dumitrescu L, Ritchie MD, Denny JC, et al. Genome-wide study of resistant hypertension identified from electronic health records. *PLoS One*. 2017;12(2):e0171745.

215. Ritchie MD, Denny JC, Crawford DC, et al. Robust Replication of Genotype-Phenotype Associations across Multiple Diseases in an Electronic Medical Record. *Am J Hum Genet*. 2010;86(4):560-572.

216. Denny J, Basford M. Type 2 Diabetes - Demonstration Project. *PheKB*. 2012.

217. Yan AT, Koh M, Chan KK, et al. Association Between Cardiovascular Risk Factors and Aortic Stenosis: The CANHEART Aortic Stenosis Study. *J Am Coll Cardiol*. 2017;69(12):1523-1532.

218. R Development Core Team. *R: A Language and Environment for Statistical Computing*. Vienna, Austria: R Foundation for Statistical Computing; 2018.

219. Gould RA, Butcher JT. Isolation of valvular endothelial cells. *J Vis Exp*. 2010;(46):7-12.

220. Otto CM, Kuusisto J, Reichenbach DD, Gown AM, O'Brien KD. Characterization of the early lesion of "degenerative" valvular aortic stenosis. Histological and immunohistochemical studies. *Circulation*. 1994;90(2):844-53.

221. Huse M. Mechanical forces in the immune system. *Nat Rev Immunol*. 2017;17:679-690.

222. Basu R, Huse M. Mechanical Communication at the Immunological Synapse. *Trends Cell Biol*. 2017;27(4):241-254.

223. Lewis JS, Dolgova N V., Chancellor TJ, et al. The effect of cyclic mechanical strain on activation of dendritic cells cultured on adhesive substrates. *Biomaterials*. 2013;34(36):9063-9070.

224. Ballotta V, Driessen-Mol A, Bouten CVC, Baaijens FPT. Strain-dependent modulation of macrophage polarization within scaffolds. *Biomaterials*. 2014;35(18):4919-4928.

225. Miyazaki H, Hayashi K. Effects of cyclic strain on the morphology and phagocytosis of macrophages. *Biomed Mater Eng*. 2001;11(4):301-309.

226. P. Matheu M, Sen D, Cahalan MD, Parker I. Generation of Bone Marrow Derived Murine Dendritic Cells for Use in 2-photon Imaging. *J Vis Exp*. 2008;(17):4-6.

227. Shutt DC, Daniels KJ, Carolan EJ, Hill AC, Soll DR. Changes in the motility, morphology, and F-actin architecture of human dendritic cells in an in vitro model of dendritic cell development. *Cell Motil Cytoskeleton*. 2000;46(3):200-221.

228. Domínguez PM, Ardavín C. Differentiation and function of mouse monocyte-derived dendritic cells in steady state and inflammation. *Immunol Rev*. 2010;234(1):90-104.

229. Barron L, Wynn TA. Fibrosis is regulated by Th2 and Th17 responses and by dynamic interactions between fibroblasts and macrophages. *Am J Physiol Gastrointest Liver Physiol*. 2011;300(5):G723-8.

230. Yoshizaki A, Yanaba K, Iwata Y, et al. Cell Adhesion Molecules Regulate Fibrotic Process via Th1/Th2/Th17 Cell Balance in a Bleomycin-Induced Scleroderma Model. *J Immunol*. 2010;185(4):2502-2515.

231. Meng X, Ao L, Song Y, et al. Expression of functional Toll-like receptors 2 and 4 in human aortic valve interstitial cells : potential roles in aortic valve inflammation and stenosis Chemicals and reagents . M199 medium and human serum albumin ville , MD). Antibodies against human T. 2008;80262:29-35.

232. Madhur MS, Lob HE, McCann LA, et al. Interleukin 17 Promotes Angiotensin II–Induced Hypertension and Vascular Dysfunction. *Hypertension*. 2010;55(2):500-507.

233. Korn T, Bettelli E, Oukka M, Kuchroo VK. IL-17 and Th17 Cells. *Annu Rev Immunol*. 2009;27(1):485-517.

234. Kortylewski M, Xin H, Kujawski M, et al. Regulation of the IL-23 and IL-12 Balance by Stat3 Signaling in the Tumor Microenvironment. *Cancer Cell*. 2009;15(2):114-123.

235. Aguado BA, Schuetze KB, Grim JC, et al. Transcatheter aortic valve replacements alter circulating serum factors to mediate myofibroblast deactivation. *Sci Transl Med*. 2019;11(509):eaav3233.

236. Chen J-H, Simmons CA. Cell–Matrix Interactions in the Pathobiology of Calcific Aortic Valve Disease. *Circ Res*. 2011;108(12):1510-1524.

237. Merryman WD, Lukoff HD, Long RA, Engelmayr GC, Hopkins RA, Sacks MS. Synergistic effects of cyclic tension and transforming growth factor-β1 on the aortic valve myofibroblast. *Cardiovasc Pathol*. 2007;16(5):268-276.

238. Ohishi K, Katayama N, Shiku H, Varnum-Finney B, Bernstein ID. Notch signalling in hematopoiesis. *Semin Cell Dev Biol*. 2003;14(2):143-150.

239. Stier S, Cheng T, Dombkowski D, Carlesso N, Scadden DT. Notch1 activation increases hematopoietic stem cell self-renewal in vivo and favors lymphoid over myeloid lineage outcome. *Blood*. 2002;99(7):2369-2378.

240. Bigas A, Martin DIK, Milner LA. Notch1 and Notch2 Inhibit Myeloid Differentiation in Response to Different Cytokines. *Mol Cell Biol*. 1998;18(4):2324-2333.

241. Miller LJ, Lincoln J. Isolation of Murine Valve Endothelial Cells. *J Vis Exp*. 2014;(90).

242. Zhang X, Goncalves R, Mosser DM. The isolation and characterization of murine macrophages. *Curr Protoc Immunol*. 2008;(SUPPL. 83):1-14.

243. Justus CR, Leffler N, Ruiz-Echevarria M, Yang L V. In Vitro Cell Migration and Invasion Assays. *J Vis Exp*. 2014;(88):1-8.

244. Trickey WR, Vail TP, Guilak F. The role of the cytoskeleton in the viscoelastic properties of human articular chondrocytes. *J Orthop Res*. 2004;22(1):131-139.

245. Hochmuth RM. Micropipette aspiration of living cells. *J Biomech*. 2000;33(1):15-22.

246. Theret DP, Levesque MJ, Sato M, Nerem RM, Wheeler LT. The Application of a Homogeneous Half-Space Model in the Analysis of Endothelial Cell Micropipette Measurements. *J Biomech Eng*. 1988;110(3):190-199.

247. Wobbrock JO, Findlater L, Gergle D, Higgins JJ. The Aligned Rank Transform for nonparametric factorial analyses using only ANOVA procedures. *Conf Hum Factors Comput Syst - Proc*. 2011;(May):143-146.

248. Lee M, Lee Y, Song J, Lee J, Chang SY. Tissue-specific role of CX3CR1 expressing immune cells and their relationships with human disease. *Immune Netw*. 2018;18(1):1-19.

249. Murray PJ. Macrophage Polarization. *Annu Rev Physiol*. 2017;79(1):541-566.

250. Xuan W, Qu Q, Zheng B, Xiong S, Fan G-H. The chemotaxis of M1 and M2 macrophages is regulated by different chemokines. *J Leukoc Biol*. 2015;97(1):61-69.

251. Maritano D, Sugrue ML, Tininini S, et al. The STAT3 isoforms α and β have unique and specific functions. *Nat Immunol*. 2004;5(4):401-409.

252. Goldberg L, Abutbul-Amitai M, Paret G, Nevo-Caspi Y. Alternative Splicing of STAT3 Is Affected by RNA Editing. *DNA Cell Biol*. 2017;36(5):367-376.

253. Lamers MM, van den Hoogen BG, Haagmans BL. ADAR1: "Editor-in-Chief" of Cytoplasmic Innate Immunity. *Front Immunol*. 2019;10(July):1-11.

254. Anstine LJ, Horne TE, Horwitz EM, Lincoln J. Contribution of extra-cardiac cells in murine heart valves is age-dependent. *J Am Heart Assoc*. 2017;6(10):1-13.

255. Li X, Wang Y, Zheng D, et al. M1 macrophages promote aortic valve calcification mediated by microRNA-214/TWIST1 pathway in valvular interstitial cells. *Am J Transl Res*. 2016;8(12):5773-5783.

256. Wynn TA, Chawla A, Pollard JW. Macrophage biology in development, homeostasis and disease. *Nature*. 2013;496(7446):445-455.

257. Geissmann F, Manz MG, Jung S, Sieweke MH, Merad M, Ley K. Development of monocytes, macrophages, and dendritic cells. *Science (80-)*. 2010;327(5966):656-661.

258. Tsou C-L, Peters W, Si Y, et al. Critical roles for CCR2 and MCP-3 in monocyte mobilization from bone marrow and recruitment to inflammatory sites. *J Clin Invest*. 2007;117(4):902-909.

259. Geissmann F, Jung S, Littman DR. Blood Monocytes Consist of Two Principal Subsets with Distinct Migratory Properties. *Immunity*. 2003;19(1):71-82.

260. Crane MJ, Daley JM, Van Houtte O, Brancato SK, Henry WL, Albina JE. The monocyte to macrophage transition in the murine sterile wound. *PLoS One*. 2014;9(1).

261. Boniakowski AE, Kimball AS, Joshi A, et al. Murine macrophage chemokine receptor CCR2 plays a crucial role in macrophage recruitment and regulated inflammation in wound healing. *Eur J Immunol*. 2018;48(9):1445-1455.

262. Yang J, Zhang L, Yu C, Yang XF, Wang H. Monocyte and macrophage differentiation: Circulation inflammatory monocyte as biomarker for inflammatory diseases. *Biomark Res*. 2014;2(1):1-9.

263. Wang J, Shelly L, Miele L, Boykins R, Norcross MA, Guan E. Human Notch-1 Inhibits NF-κB Activity in the Nucleus Through a Direct Interaction Involving a Novel Domain. *J Immunol*. 2001;167(1):289-295.

264. Zhang Q, Wang C, Liu Z, et al. Notch signal suppresses toll-like receptor-triggered inflammatory responses in macrophages by inhibiting extracellular signal-regulated kinase 1/2-mediated nuclear factor κB activation. *J Biol Chem*. 2012;287(9):6208-6217.

265. Blaser MC, Aikawa E. Roles and Regulation of Extracellular Vesicles in Cardiovascular Mineral Metabolism. *Front Cardiovasc Med*. 2018;5(December).

266. Cui L, Rashdan NA, Zhu D, et al. End stage renal disease-induced hypercalcemia may promote aortic valve calcification via Annexin VI enrichment of valve interstitial cell derived-matrix vesicles. *J Cell Physiol*. 2017;232(11):2985-2995.

267. Perrotta I, Moraca FM, Sciangula A, Aquila S, Mazzulla S. HIF-1α and VEGF: Immunohistochemical Profile and Possible Function in Human Aortic Valve Stenosis. *Ultrastruct Pathol*. 2015;39(3):198-206.

268. Zeng Q, Jin C, Ao L, et al. Cross-talk between the toll-like receptor 4 and notch1 pathways augments the inflammatory response in the interstitial cells of stenotic human aortic valves. *Circulation*. 2012;126(11 SUPPL.1):1-20.

269. Baumgartner H, Hung J, Bermejo J, et al. Echocardiographic assessment of valve stenosis: EAE/ASE recommendations for clinical practice. *Eur J Echocardiogr*. 2009;10(1):1-25.

270. Hachicha Z, Dumesnil JG, Bogaty P, Pibarot P. Paradoxical Low-Flow, Low-Gradient Severe Aortic Stenosis Despite Preserved Ejection Fraction Is Associated With Higher Afterload and Reduced Survival. *Circulation*. 2007;115(22):2856-2864.

271. Minners J, Allgeier M, Gohlke-Baerwolf C, Kienzle RP, Neumann FJ, Jander N. Inconsistencies of echocardiographic criteria for the grading of aortic valve stenosis. *Eur Heart J*. 2008;29(8):1043-1048.

272. Minners J, Allgeier M, Gohlke-Baerwolf C, Kienzle RP, Neumann FJ, Jander N. Inconsistent grading of aortic valve stenosis by current guidelines: Haemodynamic studies in patients with apparently normal left ventricular function. *Heart*. 2010;96(18):1463-1468.

273. Roden DM, Pulley JM, Basford MA, et al. Development of a large-scale de-identified DNA biobank to enable personalized medicine. *Clin Pharmacol Ther*. 2008;84(3):362-369.

274. Mosley JD, Levinson RT, Brittain EL, et al. Clinical Features Associated With Nascent Left Ventricular Diastolic Dysfunction in a Population Aged 40 to 55 Years. *Am J Cardiol*. 2018;121(12):1552-1557.

275. Wells QS, Farber-Eger E, Crawford DC. Extraction of echocardiographic data from the electronic medical record is a rapid and efficient method for study of cardiac structure and function. *J Clin Bioinforma*. 2014;4(1):6-11.

276. Fuchs C, Mascherbauer J, Rosenhek R, et al. Gender differences in clinical presentation and surgical outcome of aortic stenosis. *Heart*. 2010;96(7):539-545.

277. Clavel M-A, Magne J, Pibarot P. Low-gradient aortic stenosis. *Eur Heart J*. 2016;37(34):2645-2657.

278. Bonow RO, Carabello BA, Chatterjee K, et al. ACC/AHA 2006 Guidelines for the Management of Patients With Valvular Heart Disease. *Circulation*. 2006;114(5):e84-231.

279. Baumgartner H, Falk V, Bax JJ, et al. *2017 ESC/EACTS Guidelines for the Management of Valvular Heart Disease*. Vol 38.; 2017.

280. Otto CM, Pearlman AS. Doppler echocardiography in adults with symptomatic aortic stenosis. Diagnostic utility and cost-effectiveness. *Arch Intern Med*. 1988;148(12):2553-60.

281. Otto CM, Burwash IG, Legget ME, et al. Prospective Study of Asymptomatic Valvular Aortic Stenosis. *Circulation*. 1997;95(9):2262-2270.

282. Delgado V, Clavel MA, Hahn RT, et al. How Do We Reconcile Echocardiography, Computed Tomography, and Hybrid Imaging in Assessing Discordant Grading of Aortic Stenosis Severity? *JACC Cardiovasc Imaging*. 2019;12(2):267-282.

283. Vaidya KA, Donnelly MP, Gee TW, Ibrahim Aibo M-A, Byers S, Butcher JT. Induction of aortic valve calcification by celecoxib and its COX-2 independent derivatives is glucocorticoid-dependent. *Cardiovasc Pathol*. 2020;46:107194.

284. Cruz-Topete D, Cidlowski JA. One hormone, two actions: Anti- And pro-inflammatory effects of glucocorticoids. *Neuroimmunomodulation*. 2014;22:20-32.

285. Fiorentino DF, Zlotnik A, Mosmann TR, Howard M, O'Garra A. IL-10 inhibits cytokine production by activated macrophages. *J Immunol*. 1991;147(11):3815-22.

286. Ip WKE, Hoshi N, Shouval DS, Snapper S, Medzhitov R. Anti-inflammatory effect of IL-10 mediated by metabolic reprogramming of macrophages. *Science (80-)*. 2017;356(6337):513-519.

287. Huang Y, Qiu J, Dong S, et al. Stat3 isoforms, α and β, demonstrate distinct intracellular dynamics with prolonged nuclear retention of Stat3β mapping to its unique C-terminal end. *J Biol Chem*. 2007;282(48):34958-34967.

288. Aigner P, Mizutani T, Horvath J, et al. STAT3β is a tumor suppressor in acute myeloid leukemia. *Blood Adv*. 2019;3(13):1989-2002.

289. Marino F, Orecchia V, Regis G, et al. STAT3β controls inflammatory responses and early tumor onset in skin and colon experimental cancer models. *Am J Cancer Res*. 2014;4(5):484-94.

290. Zammarchi F, de Stanchina E, Bournazou E, et al. Antitumorigenic potential of STAT3 alternative splicing modulation. *Proc Natl Acad Sci*. 2011;108(43):17779-17784.

291. Zhang HF, Chen Y, Wu C, et al. The Opposing Function of STAT3 as an Oncoprotein and Tumor Suppressor Is Dictated by the Expression Status of STAT3β in Esophageal Squamous Cell Carcinoma. *Clin Cancer Res*. 2016;22(3):691-703.

292. Xu G, Zhang C, Zhang J. Dominant negative STAT3 suppresses the growth and invasion capability of human lung cancer cells. *Mol Med Rep*. 2009;2(5):667-671.

293. Hilfiker-Kleiner D, Hilfiker A, Drexler H. Many good reasons to have STAT3 in the heart. *Pharmacol Ther*. 2005;107(1):131-137.

294. Vaccarino V, Parsons L, Every NR, Barron H V., Krumholz HM. Sex-Based Differences in Early Mortality after Myocardial Infarction. *N Engl J Med*. 1999;341(4):217-225.

295. Vaccarino V, Rathore SS, Wenger NK, et al. Sex and racial differences in the management of acute myocardial infarction, 1994 through 2002. *N Engl J Med*. 2005;353(7):671-682.

296. Wilkinson C, Bebb O, Dondo TB, et al. Sex differences in quality indicator attainment for myocardial infarction: A nationwide cohort study. *Heart*. 2019;105(7):516-523.

297. Brush JE, Krumholz HM, Greene EJ, Dreyer RP. Sex Differences in Symptom Phenotypes Among Patients With Acute Myocardial Infarction. *Circ Cardiovasc Qual Outcomes*. 2020;13(2):e005948.

298. Krishnamurthy P, Rajasingh J, Lambers E, Qin G, Losordo DW, Kishore R. IL-10 Inhibits Inflammation and Attenuates Left Ventricular Remodeling After Myocardial Infarction via Activation of STAT3 and Suppression of HuR. *Circ Res*. 2009;104(2):9-18.

299. Haghikia A, Stapel B, Hoch M, Hilfiker-Kleiner D. STAT3 and cardiac remodeling. *Heart Fail Rev*. 2011;16(1):35-47.

300. de Koning JP, Ward AC, Caldenhoven E, de Groot RP, Löwenberg B, Touw IP. STAT3β does not interfere with granulocyte colony-stimulating factor-induced neutrophilic differentiation. *Hematol J*. 2000;1(4):220-225.

301. Sasse J, Hemmann U, Schwartz C, et al. Mutational analysis of acute-phase response factor/Stat3 activation and dimerization. *Mol Cell Biol*. 1997;17(8):4677-4686.

302. Yoo JY, Huso DL, Nathans D, Desiderio S. Specific ablation of Stat3β distorts the pattern of stat3-responsive gene expression and impairs recovery from endotoxic shock. *Cell*. 2002;108(3):331-344.

303. Schaefer TS, Sanders LK, Nathans D. Cooperative transcriptional activity of Jun and Stat3 beta, a short form of Stat3. *Proc Natl Acad Sci*. 1995;92(20):9097-9101.

304. Lee J, Baldwin WM, Lee CY, Desiderio S. Stat3β mitigates development of atherosclerosis in apolipoprotein E-deficient mice. *J Mol Med*. 2013;91(8):965-976.

305. Yang J, Liao X, Agarwal MK, Barnes L, Auron PE, Stark GR. Unphosphorylated STAT3 accumulates in response to IL-6 and activates transcription by binding to NF B. *Genes Dev*. 2007;21(11):1396-1408.

306. YU Z, ZHANG W, KONE BC. Signal transducers and activators of transcription 3 (STAT3) inhibits transcription of the inducible nitric oxide synthase gene by interacting with nuclear factor κB. *Biochem J*. 2002;367(1):97-105.

307. Yoshida Y, Kumar A, Koyama Y, et al. Interleukin 1 Activates STAT3/Nuclear Factor-κB Cross-talk via a Unique TRAF6- and p65-dependent Mechanism. *J Biol Chem*. 2004;279(3):1768-1776.

308. Lee H, Herrmann A, Deng J-H, et al. Persistently Activated Stat3 Maintains Constitutive NF-κB Activity in Tumors. *Cancer Cell*. 2009;15(4):283-293.

309. Lagerqvist B, James SK, Stenestrand U, Lindbäck J, Nilsson T, Wallentin L. Long-term outcomes with drug-eluting stents versus bare-metal stents in Sweden. *N Engl J Med*. 2007;356(10):1009-1019.

310. Bønaa KH, Mannsverk J, Wiseth R, et al. Drug-eluting or bare-metal stents for coronary artery disease. *N Engl J Med*. 2016;375(13):1242-1252.

311. Cannarile MA, Weisser M, Jacob W, Jegg A-M, Ries CH, Rüttinger D. Colony-stimulating factor 1 receptor (CSF1R) inhibitors in cancer therapy. *J Immunother Cancer*. 2017;5(1):53.

312. Katsume A, Saito H, Yamada Y, et al. Anti-Interleukin 6 (IL-6) Receptor Antibody Suppresses Castelman's Disease Like Symptoms Emerged in IL-6 Transgenic Mice. *Cytokine*. 2002;20(6):304-311.

313. Honda S, Miyamoto T, Watanabe T, et al. A novel mouse model of aortic valve stenosis induced by direct wire injury. *Arterioscler Thromb Vasc Biol*. 2014;34(2):270-278.

314. Natorska J, Marek G, Sadowski J, Undas A. Presence of B cells within aortic valves in patients with aortic stenosis: Relation to severity of the disease. *J Cardiol*. 2016;67(1):80-85.

315. Kirabo A, Fontana V, de Faria APC, et al. DC isoketal-modified proteins activate T cells and promote hypertension. *J Clin Invest*. 2014;124(10):4642-4656.

316. Haniffa MA, Wang X-N, Holtick U, et al. Adult Human Fibroblasts Are Potent Immunoregulatory Cells and Functionally Equivalent to Mesenchymal Stem Cells. *J Immunol*. 2007;179(3):1595-1604.

317. Joglekar A V., Leonard MT, Jeppson JD, et al. T cell antigen discovery via signaling and antigen-presenting bifunctional receptors. *Nat Methods*. 2019;16(2):191-198.

318. Li G, Bethune MT, Wong S, et al. T cell antigen discovery via trogocytosis. *Nat Methods*. 2019;16(2):183-190.

319. Zvyagin I V., Tsvetkov VO, Chudakov DM, Shugay M. An overview of immunoinformatics approaches and databases linking T cell receptor repertoires to their antigen specificity. *Immunogenetics*. 2020;72(1-2):77-84.

320. Barbaro NR, Foss JD, Kryshtal DO, et al. Dendritic Cell Amiloride-Sensitive Channels Mediate Sodium-Induced Inflammation and Hypertension. *Cell Rep*. 2017;21(4):1009-1020.

321. Salomon RG, Bi W. Isolevuglandin Adducts in Disease. *Antioxid Redox Signal*. 2015;22(18):1703-1718.

322. Mohty D, Pibarot P, Després J-P, et al. Association Between Plasma LDL Particle Size, Valvular Accumulation of Oxidized LDL, and Inflammation in Patients With Aortic Stenosis. *Arterioscler Thromb Vasc Biol*. 2008;28(1):187-193.

323. Tastet L, Capoulade R, Clavel MA, et al. Systolic hypertension and progression of aortic valve calcification in patients with aortic stenosis: Results from the PROGRESSA study. *Eur Heart J Cardiovasc Imaging*. 2017;18(1):70-78.

324. Noll NA, Lal H, Merryman WD. Mouse Models of Heart Failure with Preserved or Reduced Ejection Fraction. *Am J Pathol*. April 2020.

Appendix

A: Electronic Medical Record Algorithms and Tables

Electronic Medical Record Diagnostic Algorithms

OVERALL PATIENT POOL

Subject has ≥ 3 visits to VUMC after January 1, 2005 (see Table A.1 for specific criteria).

AND

Subject has ≥ 1 echocardiogram at VUMC after January 1, 2005.

AND

Subject has BMI recorded within one year of January 1, 2005.

AORTIC STENOSIS CASE DEFINITION

Subject has ≥ 2 ICD9 or ICD10 codes for aortic valve disease after January 1, 2005 (see Table A.1 for specific criteria).

AND

Subject has keyword "aortic stenosis" in problem lists, inpatient notes, outpatient notes, radiology reports, or pathology reports after January 1, 2005.

AND NOT (

Subject has keyword "rheumatic" in problem lists, inpatient notes, outpatient notes, radiology reports, or pathology reports at any time.

OR

Subject has ICD9 or ICD10 codes for aortic valve disease prior to January 1, 2005.

OR

Subject has keyword "aortic stenosis" in problem lists, inpatient notes, outpatient notes, radiology reports, or pathology reports prior to January 1, 2005.

)

AORTIC STENOSIS CONTROL DEFINITION

Subject has BMI recorded ≥ 2 years after January 1, 2005.

AND NOT (

Subject has keyword "rheumatic" in problem lists, inpatient notes, outpatient notes, radiology reports, or pathology reports at any time.

OR

Subject has ICD9 or ICD10 codes for aortic valve disease at any time.

OR

Subject has keyword "aortic stenosis" in problem lists, inpatient notes, outpatient notes, radiology reports, or pathology reports at any time.

)

MYOCARDIAL INFARCTION/ISCHEMIC STROKE CASE DEFINITIONS

Subject has ≥ 2 ICD9 or ICD10 codes for the respective condition after January 1, 2005 (see Table A.1 for specific criteria).

AND NOT (

Subject has ICD9 or ICD10 codes for the respective condition prior to January 1, 2005.

)

MYOCARDIAL INFARCTION/ISCHEMIC STROKE CONTROL DEFINITIONS

Subject has BMI recorded ≥ 2 years after January 1, 2005.

AND NOT (

Subject has ICD9 or ICD10 codes for the respective condition.

)

HYPERTENSION CASE DEFINITION

Adapted from Tu, et al.[212]

Subject has ≥ 2 ICD9 or ICD10 codes for hypertension or hypertensive sequelae prior to January 1, 2005 (see Table A.2 for specific criteria).

AND

Subject has systolic blood pressure ≥ 140.

OR

Subject has diastolic blood pressure ≥ 90.

DIABETES CASE DEFINITION

Adapted from Denny, et al.[216]

Subject has ≥ 2 ICD9 or ICD10 codes for diabetes prior to January 1, 2005 (see Table A.3 for specific criteria).

AND

Subject has non-insulin diabetes medications (any of the below).

chlorpropamide, glipizide (Glucotrol, Glucotrol XL), glyburide (Micronase, Glynase, Diabeta), glimepiride (Amaryl), repaglinide (Prandin), nateglinide (Starlix), metformin (Glucophage, Glucophage XR), rosiglitazone (Avandia), pioglitazone (ACTOS), acarbose (Precose), miglitol (Glyset), sitagliptin (Januvia), exenatide (Byetta), tolazamide, troglitazone, tolbutamide, Metaglip, Glucovance, Avandamet, Janumet, Fortamet, Glumetza, Riomet

Table A.1. Patient cohort definition criteria.
Search criteria for identification of patients in the study population are shown. A combination of CPT codes, ICD9 and ICD10 codes, keyword search, and BMI gating was used. CPT = current procedural terminology, ICD = international classification of diseases.

Criterion	Codes
Routine Patient Care Visit CPT codes (≥ 3 of any)	992*
Echocardiogram CPT Codes (≥ 1 of any)	933*
Aortic Stenosis ICD9 Codes	
Mitral valve stenosis and aortic valve stenosis	396.0
Mitral valve insufficiency and aortic valve stenosis	396.2
Aortic valve disorders	424.1
Aortic Stenosis ICD10 Codes	
Nonrheumatic aortic (valve) stenosis	I35.0
Nonrheumatic aortic (valve) stenosis with insufficiency	I35.2
Other nonrheumatic aortic valve disorders	I35.8
Nonrheumatic aortic valve disorders	I35.9
Myocardial Infarction ICD9 Codes	
Acute myocardial infarction	410
Old myocardial infarction	412
Myocardial Infarction ICD10 Codes	
ST elevation (STEMI) and non-STE elevation (NSTEMI) myocardial infarction	I21
Subsequent ST elevation (STEMI) and non-ST elevation (NSTEMI) myocardial	I22
Ischemic Stroke ICD9 Codes	
Occlusion and stenosis of basilar artery with cerebral infarction	433.01
Occlusion and stenosis of carotid artery with cerebral infarction	433.11
Occlusion and stenosis of vertebral artery with cerebral infarction	433.21
Occlusion and stenosis of multiple and bilateral precerebral arteries with cerebral	433.31
Occlusion and stenosis of other specified precerebral artery with cerebral infarction	433.81
Occlusion and stenosis of unspecified precerebral artery with cerebral infarction	433.91
Cerebral thrombosis with cerebral infarction	434.01
Cerebral embolism with cerebral infarction	434.11
Cerebral artery occlusion, unspecified with cerebral infarction	434.91
Ischemic Stroke ICD10 Codes	
Cerebral infarction	I63

Table A.2. Hypertension case definition criteria.
ICD search criteria for identification of patients with hypertension are shown. A combination of ICD9 and ICD10 codes and blood pressure gating was used. ICD = international classification of diseases.

Criterion	Codes
Hypertension ICD9 Codes	
Essential hypertension	401
Hypertensive heart disease	402
Hypertensive chronic kidney disease	403
Hypertensive heart and chronic kidney disease	404
Secondary hypertension	405
Hypertension ICD10 Codes	
Essential (primary) hypertension	I10
Hypertensive heart disease	I11
Hypertensive chronic kidney disease	I12
Hypertensive heart and chronic kidney disease	I13
Secondary hypertension	I15

Table A.3. Diabetes case definition criteria.
ICD search criteria for identification of patients with diabetes are shown. A combination of ICD9 and ICD10 codes and medication list keyword search was used. ICD = international classification of diseases.

| Criterion	Codes
Diabetes ICD9 Codes	
Diabetes mellitus without mention of complication, type II or unspecified type	250.00. 250.02
Diabetes with hyperosmolarity, type II or unspecified type	250.20. 250.22
Diabetes with other coma, type II or unspecified type	250.30. 250.32
Diabetes with renal manifestations, type II or unspecified type	250.40. 250.42
Diabetes with ophthalmic manifestations, type II or unspecified type	250.50. 250.52
Diabetes with neurological manifestations, type II or unspecified type	250.60. 250.62
Diabetes with peripheral circulatory disorders, type II or unspecified type	250.70. 250.72
Diabetes with other specified manifestations, type II or unspecified type	250.80. 250.82
Diabetes with unspecified complication, type II or unspecified type	250.90. 250.92
Diabetes ICD10 Codes	
Type 2 diabetes mellitus with hyperosmolarity	E11.0
Type 2 diabetes mellitus with kidney complications	E11.2
Type 2 diabetes mellitus with ophthalmic complications	E11.3
Type 2 diabetes mellitus with neurological complications	E11.4
Type 2 diabetes mellitus with circulatory complications	E11.5
Type 2 diabetes mellitus with other specified complications	E11.6
Type 2 diabetes mellitus with unspecified complications	E11.8
Type 2 diabetes mellitus without complications	E11.9

B: Immunofluorescence Control Images
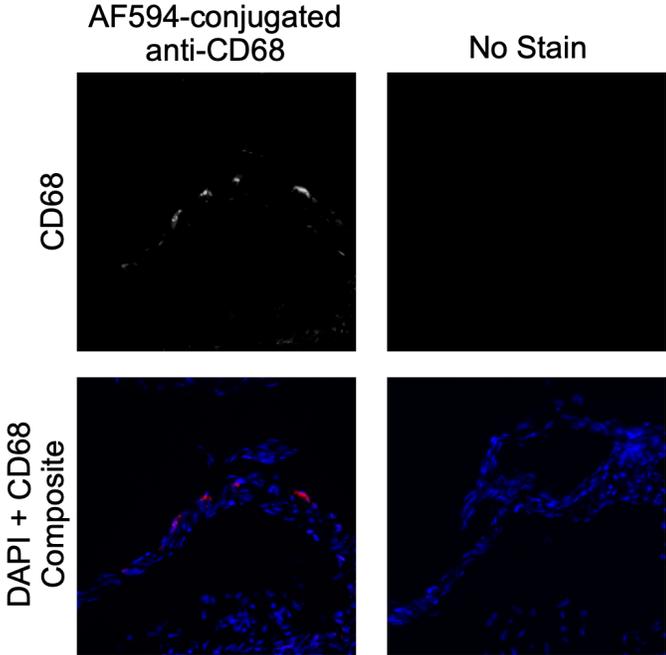
Figure A.1. CD68 control immunofluorescence images.
Negative control images for the anti-CD68 antibody are shown. In CD68 only images, CD68 is in white. In composite images, CD68 is in red and DAPI (nuclei) is in blue.
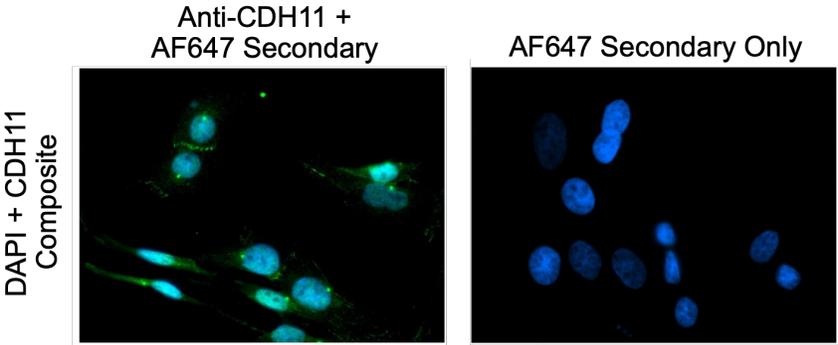

Figure A.2. CDH11 control immunofluorescence images.
Negative control images for the anti-CDH11 antibody are shown. CDH11 is in green and DAPI (nuclei) is in blue.
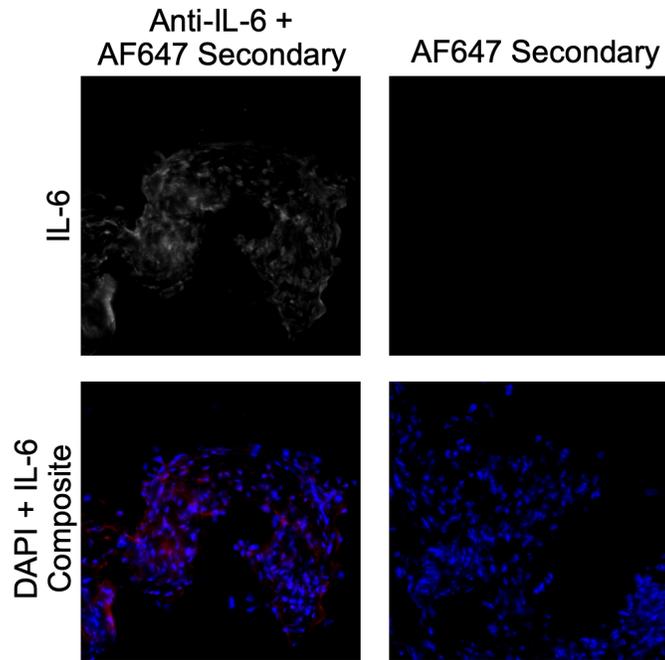
Figure A.3. IL-6 control immunofluorescence images.
Negative control images for the anti-CD68 antibody are shown. In IL-6 only images, IL-6 is in white. In composite images, IL-6 is in red and DAPI (nuclei) is in blue.
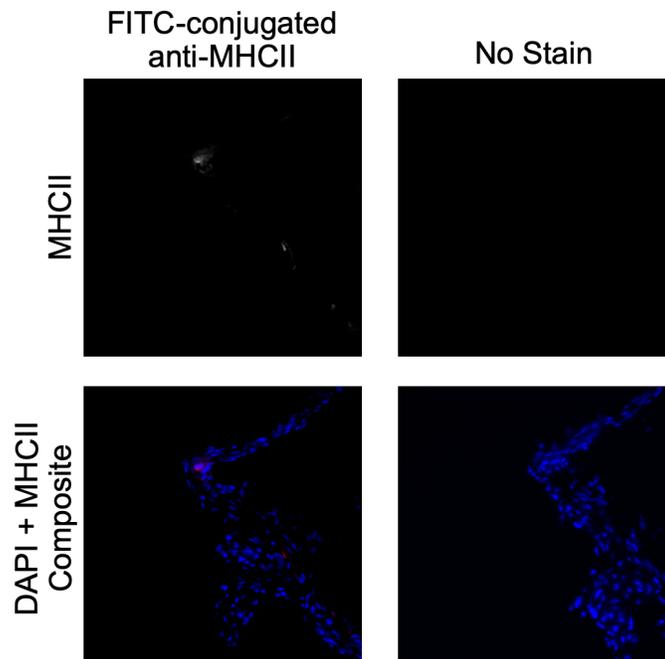

Figure A.4. MHCII control immunofluorescence images.
Negative control images for the anti-MHCII antibody are shown. In MHCII only images, MHCII is in white. In composite images, MHCII is in red and DAPI (nuclei) is in blue.
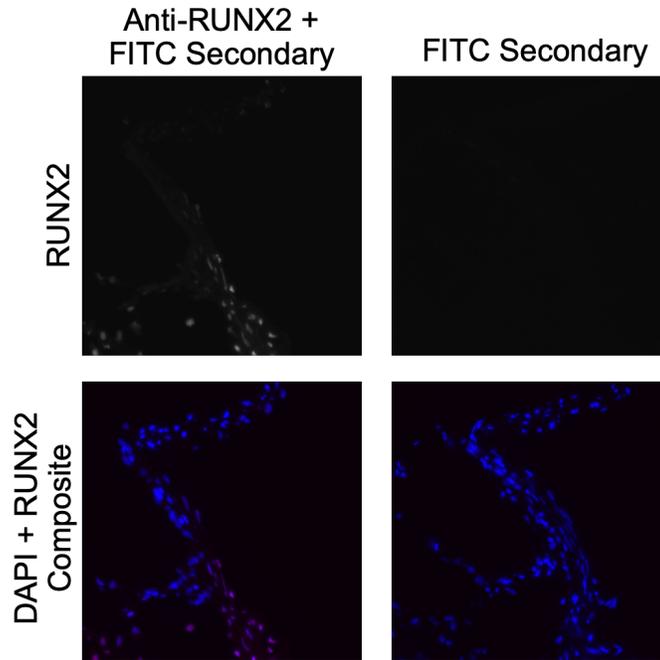
Figure A.5. RUNX2 control immunofluorescence images.
Negative control images for the anti-RUNX2 antibody are shown. In RUNX2 only images, RUNX2 is in white. In composite images, RUNX2 is in red and DAPI (nuclei) is in blue.
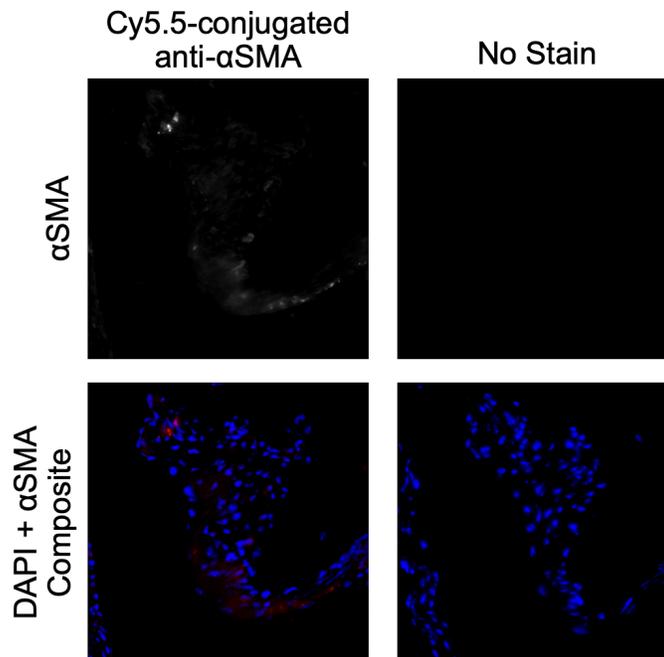
Figure A.6. αSMA control immunofluorescence images.
Negative control images for the anti-αSMA antibody are shown. In αSMA only images, αSMA is in white. In composite images, αSMA is in red and DAPI (nuclei) is in blue.

C: Image Processing Analysis Code

The following R code was used in Chapter 5 to test the hypothesis that the distances between alpha smooth muscle actin-positive (αSMA^+) aortic valve interstitial cells (AVICs) and CD68-positive macrophages did not fall into a null distribution, but instead were skewed towards zero. This process is shown as written for αSMA^+, but was replicated for $RUNX2^+$ AVICs, therefore applying the process to both myofibroblast-like and osteoblast-like calcifying AVICs.

```r
#Print initial time stamp.
Sys.time()

#Specify file path.
path = "/Users/Michael/ImageProcessing/08.09.19/"

#Specify which type of stain will be used to identify either
myofibroblast-like (aSMA) or osteoblast-like (RUNX2) AVICs.
These two datasets are tested independently, in sequence. Use
either "aSMA.tif" or "runx.tif".
file.names <- dir(path, pattern ="aSMA.tif")

#Establish data frames for data collection.
ImageData <- data.frame(matrix(ncol = 17))
CellData <- data.frame(matrix(ncol = 7))

set.seed(33)

setwd(path)

print(length(file.names))

#Initiate for loop to iterate through every image set.
for(i in 1:length(file.names)){

    #Read in, blur, and threshold images with AVIC stain of
    interest, then identify continuous shapes in the black and
    white mask. This outputs 'realMyos' (for real myofibroblasts
    here), which is a data frame holding positional and
    geometric data about each aSMA-positive AVIC.
    img <- readImage(file.names[1])
    img.blur <- gblur(img*4, sigma = 4)
```

```r
img.thres <- img.blur > otsu(img.blur, c(0, 5))
img.thres.cnt <- bwlabel(img.thres)
Myos <- data.frame(computeFeatures.shape(img.thres.cnt))
realMyos <- subset(Myos, Myos$s.area >1500)

#Read in, blur, and threshold corresponding DAPI images,
then identify continuous shapes in the black and white mask.
This stores the total cell count in an image, and can be
used as a denominator to calculate the percent of total
cells that are calcifying, the percent of total cells that
are CD68-positive macrophages, or other summary data.
dapi <- readImage(paste0(substr(file.names[i], 1, 9), "-
     dapi.tif"))
dapi.blur <- gblur(dapi*5, sigma = 1.5)
dapi.thres <- dapi.blur > 1.195*otsu(dapi.blur, c(0, 5))
dapi.thres.cnt <- bwlabel(dapi.thres)
Cells <- data.frame(computeFeatures.shape(dapi.thres.cnt))
realCells <- subset(Cells, Cells$s.area >50)

#Store summary information about the image and cell counts.
ImageData[i,1] <- file.names[i] #filename
ImageData[i,2] <- substr(file.names[i], 1,3) #mouse
ImageData[i,3] <- substr(file.names[i], 5,7) #treatment
ImageData[i,4] <- length(realCells[,1]) #number of cells
ImageData[i,5] <- length(realMyos[,1]) #number of myoFBs
ImageData[i,11] <- sum(unlist(img)) #aSMA stain intensity

#If a corresponding CD68 images exists, this reads in,
blurs, and thresholds the image. It then identifies
continuous shapes in the black and white mask. This outputs
'realMacs' (for real macrophages), which is a data frame
holding positional and geometric data about each CD68-
positive macrophage.
if (file.exists(paste0(substr(file.names[i], 1, 9), "-
          mac.tif"))){
     cd68 <- readImage(paste0(substr(file.names[i], 1, 9),
          "-mac.tif"))
     cd68.blur <- gblur(cd68*13, sigma = 2)
     cd68.thres <- cd68.blur > otsu(cd68.blur, c(0, 10))
     cd68.thres.cnt <- bwlabel(cd68.thres)
     Macs <-
          data.frame(computeFeatures.shape(cd68.thres.cnt))
     realMacs <- subset(Macs, Macs$s.area >50)
```

```r
#Store updated summary information about the image and
cell counts.
ImageData[i,4] <- length(realCells[,1]) -
    length(realMacs[,1]) #Number of AVICs
ImageData[i,6] <- length(realMacs[,1]) #Number of Macs

#Calculate the positions of all activated AVICs.
imgpos <- computeFeatures.moment(img.thres.cnt)
imgpos <- imgpos[which(Myos$s.area > 1500),]

#Calculate the positions of all macrophages.
cd68pos <- computeFeatures.moment(cd68.thres.cnt)
cd68pos <- cd68pos[which(Macs$s.area > 50),]

#Clear lists for the following for loop.
celldist <- list(NULL)
fakecelldist <-list(NULL)
fakecelldistmin <- list(NULL)
fakecelldistmax <- list(NULL)

#Cycle through all activated cells. Store the position
of the activated AVIC, and cycle through the position
of every macrophage and calculate the distance between
the two.
for(j in 1:length(imgpos[,1])){
    macdist <- list(NULL)
    montelist <- list(NULL)
    myo.x <- imgpos[j,1]
    myo.y <- imgpos[j,2]

    for(k in 1:length(cd68pos[,1])) {
        mac.x <- cd68pos[k,1]
        mac.y <- cd68pos[k,2]
        macdist[k] <- sqrt((myo.x-mac.x)^2 + (myo.y-
        mac.y)^2)
    }

    #Monte Carlo simulation: (1) Calculate the
    distance from the AVIC of interest to a random
    macrophage. Repeat this process for the number of
    macrophages in the real distribution. (2) Store
    the smallest distance as the distance to the
    nearest "fake" macrophage. (3) Repeat this
    process 500 times to account for randomness.
    for(m in 1:500){
        fakedist <- list(NULL)
```

```r
        #Create a random macrophage and calculate
        distance for the amount of times that there
        are real macrophages.
        for (l in 1:length(cd68pos[,1])) {
              fakedist[l] <- sqrt((myo.x-
              runif(1,0,1940))^2 + (myo.y-
              runif(1,0,1460))^2)
        }

        #Store closest random macrophage for this
        iteration of Monte Carlo.
        montelist[m] <- min(unlist(fakedist))
    }

    #Store all of the data for this cell including
    (1) cell line, (2) any treatments, (3) real
    distance to closest macrophage, (4) including the
    median distance to the nearest macrophage in
    Monte Carlo simulation, (5) and (6) quantile data
    from the Monte Carlo simulation.
    CellData[length(CellData$X1)+1, 1] <-
          ImageData[i,2] <- substr(file.names[i], 1,3)
    CellData[length(CellData$X1), 2] <-
          ImageData[i,3] <- substr(file.names[i], 5,7)
    CellData[length(CellData$X1), 3] <-
          min(unlist(macdist))
    CellData[length(CellData$X1), 4] <-
          quantile(unlist(montelist), 0.5)
    CellData[length(CellData$X1), 5] <-
          quantile(unlist(montelist), 0.25)
    CellData[length(CellData$X1), 6] <-
          quantile(unlist(montelist), 0.75)
}

#Store summary data about this image and all of the
activated AVICs within.
ImageData[i,8] <- mean(unlist(celldist))
ImageData[i,17] <- median(unlist(celldist))
ImageData[i,9] <- sd(unlist(celldist))
ImageData[i,10] <-
    sd(unlist(celldist))/sqrt(length(imgpos[,1]))
ImageData[i,13] <- median(unlist(fakecelldist))
ImageData[i,14] <- median(unlist(fakecelldistmin))
```

```r
        ImageData[i,15] <- median(unlist(fakecelldistmax))


    }


    #Print time stamp to monitor progress.
    print(i)
    print(Sys.time())
}

#Perform simple calculations to output (1) percent of AVICs that
are calcifying (2) total aSMA stain normalized to cell count (3)
image-level difference between real and expected distances.
ImageData[,7] <- ImageData[,5]/ImageData[,4]*100
ImageData[,12] <- ImageData[,11]/ImageData[,4]
ImageData[,16] <- ImageData[,8] / ImageData[,13]

#Calculate Distance Index
CellData[,7] <- CellData[,3] / CellData[,4]

#Name all columns/variables.
colnames(CellData) <- c("Cell", "Tx", "RealDist", "medDist",
    "minDist", "maxDist", "DistIndex")
colnames(ImageData) <-
    c("File", "CellLine", "Tx", "TotalCells", "myoFBs", "Macs",
    "percentMyo", "DistAvg", "DistSD", "DistSEM", "aSMA",
    "aSMAperCell", "randomDist", "random25", "random75",
    "DistIndex", "medRealDist")

#Print final time stamp.
print(Sys.time())
```

D: Raw Protein Blot Images.
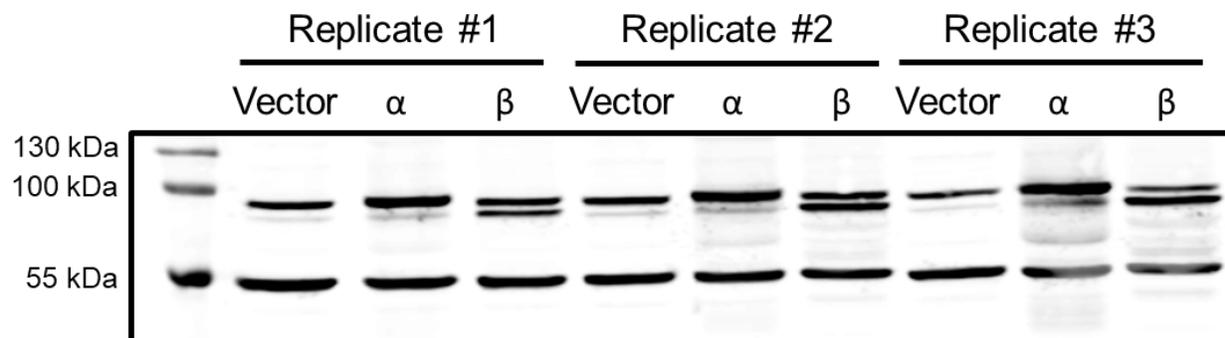
Figure A.7. Western blot confirmation of STAT3 plasmid transfection.
Representative raw Western blot data for STAT3 expression in samples transfected with empty vector plasmid (Vector), STAT3α overexpression plasmid (α), or STAT3β overexpression plasmid (β). STAT3α is stained at ~88 kDa with STAT3β just below. Loading control is α-Tubulin stained at ~50 kDa. STAT3 is visualized with anti-mouse IgG2a secondary antibody and α-Tubulin is visualized with anti-mouse IgG1 secondary antibody: both in the 700 channel. Reprinted, with permission, from Raddatz, et al.[28]
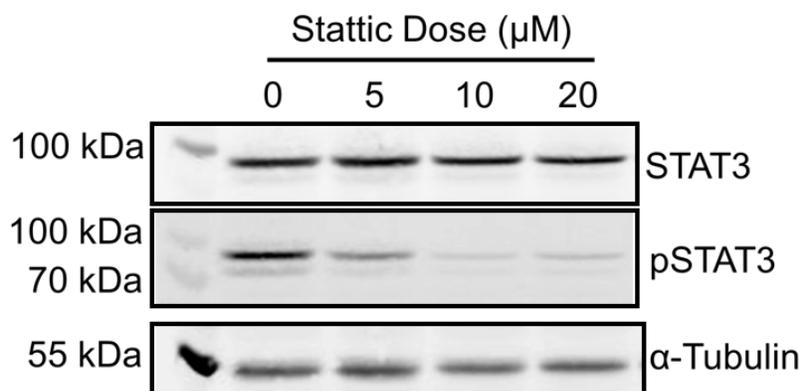

Figure A.8. Western blot confirmation of STAT3 phosphorylation blockade with Stattic.
Representative raw Western blot data for STAT3 phosphorylation in samples treated with increasing doses of Stattic. STAT3 and pSTAT3 are stained at ~88 kDa. Loading control is α-Tubulin stained at ~50 kDa. STAT3 is visualized with anti-mouse IgG2a secondary antibody, pSTAT3 with anti-rabbit IgG secondary antibody in the 800 channel, and α-Tubulin with anti-mouse IgG1 secondary antibody in the 700 channel.
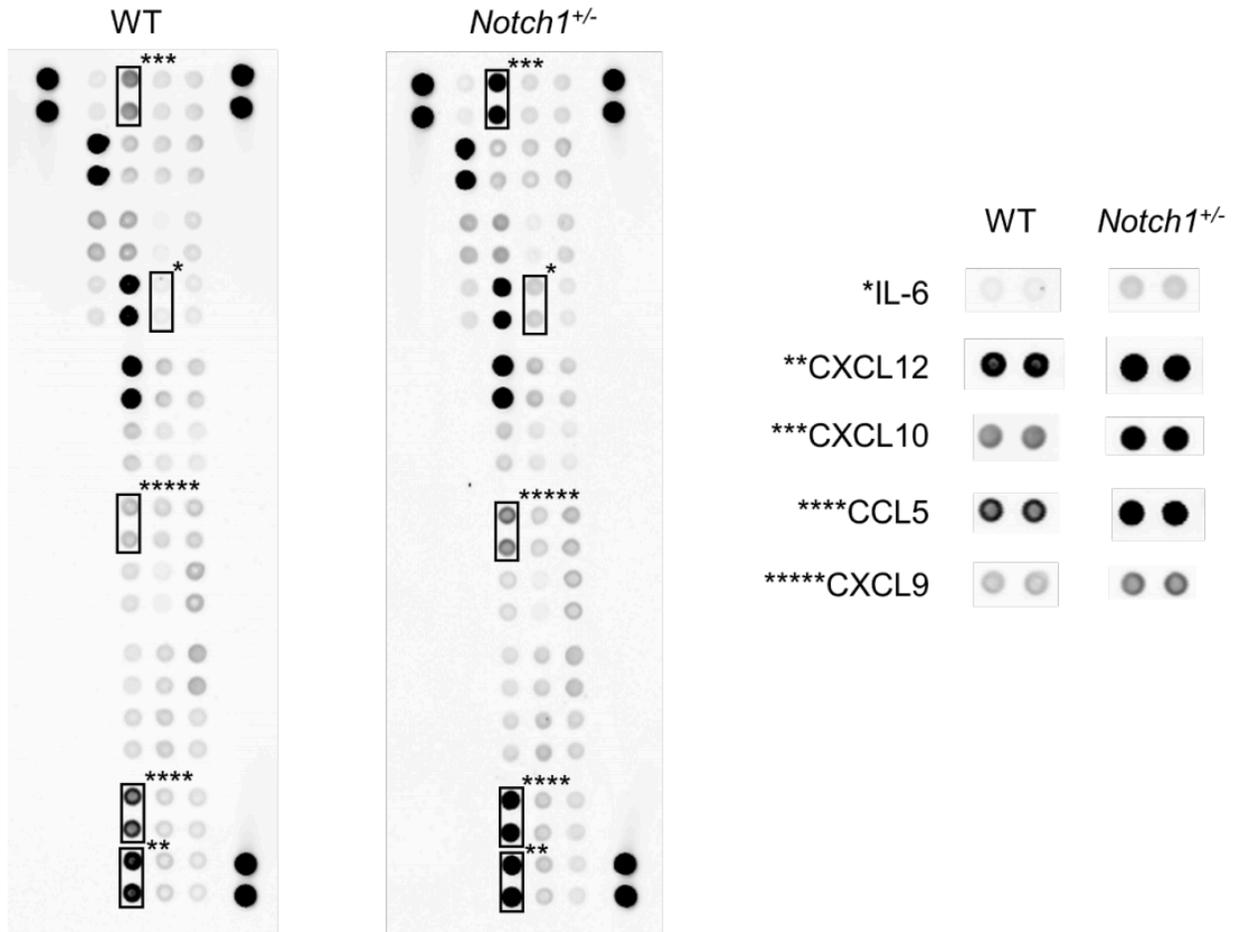
Figure A.9. Raw Proteome Profiler microarray results.
Microarray of secreted factors from wild-type (WT) and Notch1+/- AVICs. *Denotes corresponding microarray spots cropped for comparison.
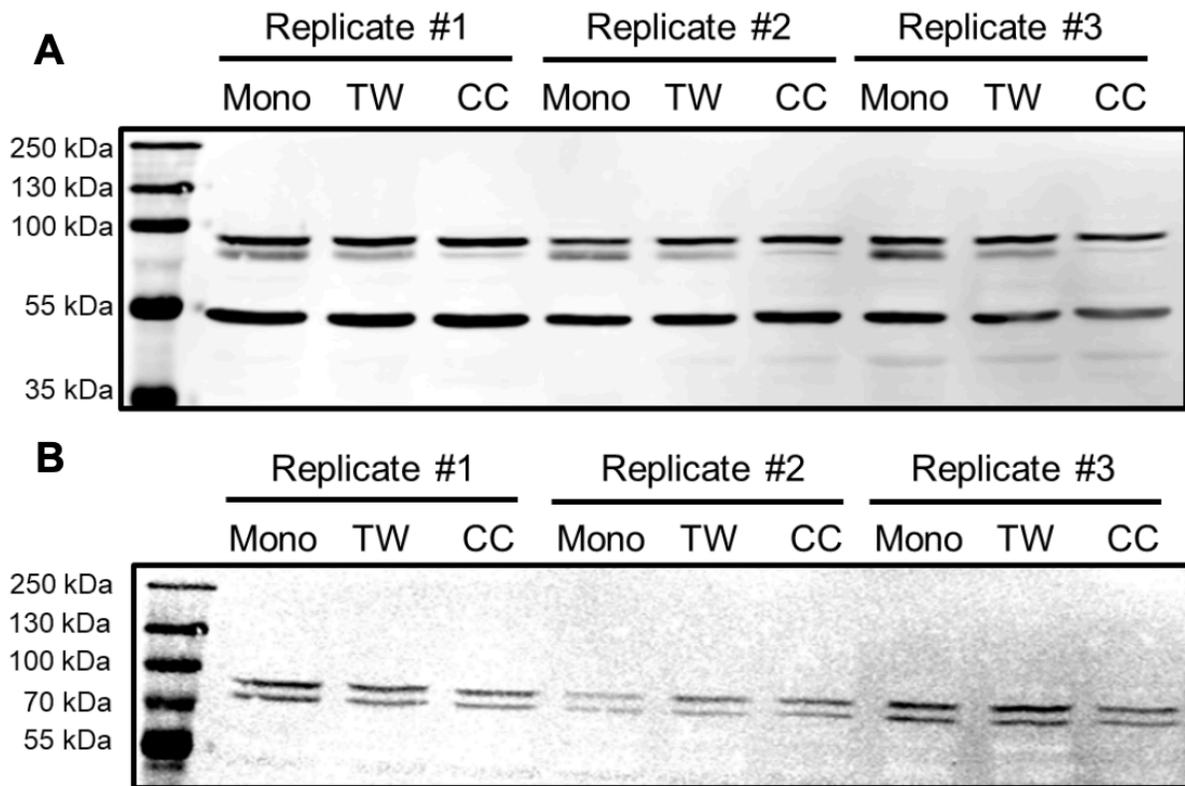
Figure A.10. STAT3 splicing in AVICs exposed to macrophages.
Raw Western blot data for STAT3 splicing (A) and phosphorylation (B) in AVICs in monoculture (Mono), Transwell culture (TW), or direct coculture (CC) with macrophages. p/STAT3α is stained at ~88 kDa with p/STAT3β just below. Loading control is α-Tubulin stained at ~50 kDa (A). STAT3 is visualized with anti-mouse IgG2a secondary antibody in the 700 channel, pSTAT3 with antirabbit IgG secondary antibody in the 800 channel, and α-Tubulin with anti-mouse IgG1 secondary antibody in the 700 channel.
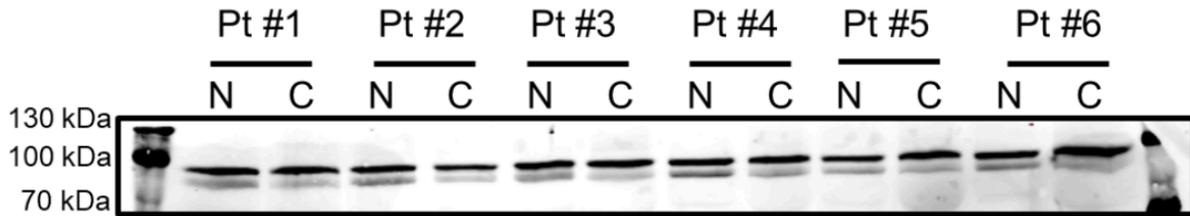
Figure A.11. STAT3 splicing in human calcific aortic valve disease.
Representative raw Western blot data for STAT3 splicing in non-calcified (N) and calcified (C) tissue from patients with calcific aortic valve disease. STAT3α is stained at ~88 kDa with STAT3β just below. Total STAT3 quantified from previous Western blot was used as loading control in order to normalize STAT3β to total STAT3. STAT3 is visualized with anti-mouse IgG2a secondary antibody in the 700 channel.
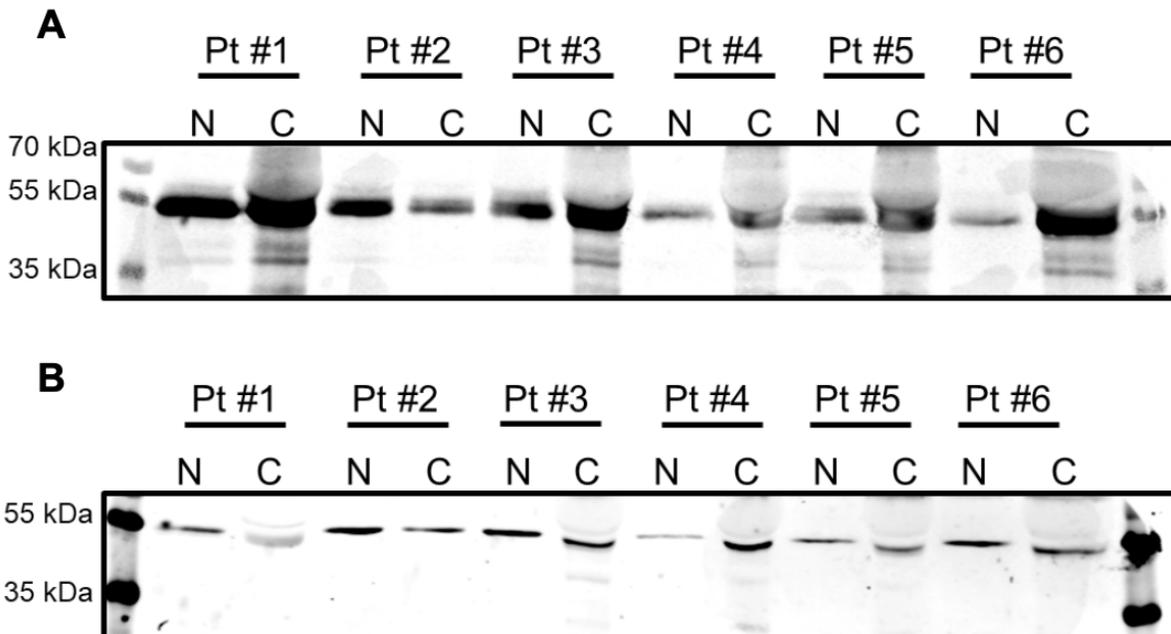
Figure A.12. RUNX2 in human calcific aortic valve disease.
Representative raw Western blot data for RUNX2 expression in non-calcified (N) and calcified (C) tissue from patients with calcific aortic valve disease. RUNX2 is stained at ~56 kDa (A). Loading control is α-Tubulin stained at ~50 kDa (B). RUNX2 is visualized with anti-rabbit IgG1 secondary antibody in the 800 channel and α-Tubulin is visualized with anti-mouse IgG1 secondary antibody in the 700 channel. Although they are in separate channels, RUNX2 was stained first followed by αTubulin to prevent any bleed over of α-Tubulin signal into RUNX2 densitometry quantification.